

EFFECT OF FIBER TYPE AND CONCRETE STRENGTH ON THE ENERGY
ABSORPTION CAPACITY OF FIBER REINFORCED CONCRETE PLATES
UNDER QUASI-STATIC BENDING

A THESIS SUBMITTED TO
THE GRADUATE SCHOOL OF NATURAL AND APPLIED SCIENCES
OF
MIDDLE EAST TECHNICAL UNIVERSITY

BY

ALİ MACİT MERCAN

IN PARTIAL FULFILLMENT OF THE REQUIREMENTS
FOR
THE DEGREE OF MASTER OF SCIENCE
IN
CIVIL ENGINEERING

SEPTEMBER 2019

Approval of the thesis:

**EFFECT OF FIBER TYPE AND CONCRETE STRENGTH ON THE
ENERGY ABSORPTION CAPACITY OF FIBER REINFORCED
CONCRETE PLATES UNDER QUASI-STATIC BENDING**

submitted by **ALİ MACİT MERCAN** in partial fulfillment of the requirements for the degree of **Master of Science in Civil Engineering Department, Middle East Technical University** by,

Prof. Dr. Halil Kalıpçılar
Dean, Graduate School of **Natural and Applied Sciences**

Prof. Dr. Ahmet Türer
Head of Department, **Civil Engineering**

Prof. Dr. İsmail Özgür Yaman
Supervisor, **Civil Engineering, METU**

Dr. Burhan Aleessa Alam
Co-Supervisor, **Civil Engineering, METU**

Examining Committee Members:

Assoc. Prof. Dr. Serdar Göktepe
Civil Engineering, METU

Prof. Dr. İsmail Özgür Yaman
Civil Engineering, METU

Prof. Dr. Mustafa Şahmaran
Civil Engineering, Hacettepe University

Assist. Prof. Dr. Can Baran Aktaş
Civil Engineering, TED University

Assist. Prof. Dr. Hande Işık Öztürk
Civil Engineering, METU

Date: 04.09.2019

I hereby declare that all information in this document has been obtained and presented in accordance with academic rules and ethical conduct. I also declare that, as required by these rules and conduct, I have fully cited and referenced all material and results that are not original to this work.

Name, Surname: Ali Macit Mercan

Signature:

ABSTRACT

EFFECT OF FIBER TYPE AND CONCRETE STRENGTH ON THE ENERGY ABSORPTION CAPACITY OF FIBER REINFORCED CONCRETE PLATES UNDER QUASI-STATIC BENDING

Mercan, Ali Macit
Master of Science, Civil Engineering
Supervisor: Prof. Dr. İsmail Özgür Yaman
Co-Supervisor: Dr. Burhan Aleessa Alam

September 2019, 92 pages

With all the known solid advantages of concrete, it has also limitations in its mechanical properties, such as low ductility, tensile strength and energy absorption capacity/toughness. In order to eliminate or minimize these limitations, some developments have been worked up by introducing natural or artificial fibers into the concrete mixture.

The main scope of this thesis is to observe the effect of different fiber types and dosages on the performance of two different concrete grades. Two steel fibers with lengths of 30 and 60 mm and dosages of 30, 60, and 90 kg/m³ were used along with one synthetic fiber with a length of 54 mm and dosages of 3, 6 and 9 kg/m³. The performance of the prepared concrete mixtures was measured by the mean of load carrying capacities and toughness through centrally loaded square plates. Three plate specimens were tested for each mixture to obtain the load-displacement data up to a 25 mm displacement deflection. Then, the energy absorption capacity/toughness was determined for each specimen. As a result, it was observed that the addition of fibers increased the ultimate load and energy absorption capacity of the concrete. The test results showed that the increase in fiber dosage leads to increase in crack lengths.

Specifically, concrete specimens with steel fibers showed better performance than the ones with synthetic fibers.

Keywords: Fiber Reinforced Concrete, High and Normal Performance Concrete, Steel Fibers, Synthetic Fibers, Square Plate Test

ÖZ

LİF TİPİNİN VE BETON DAYANIMININ YARI STATİK YÜK ALTINDAKİ LİFLİ BETON PLAKALARIN ENERJİ YUTMA KAPASİTESİNE ETKİSİ

Mercan, Ali Macit
Yüksek Lisans, İnşaat Mühendisliği
Tez Danışmanı: Prof. Dr. İsmail Özgür Yaman
Ortak Tez Danışmanı: Dr. Burhan Aleessa Alam

Eylül 2019, 92 sayfa

Bilinen üstün özelliklerine rağmen beton; süneklik, çekme dayanımı ve enerji absorpsiyon kapasitesi gibi bazı mekanik özelliklerinde kısıtlamalara sahiptir. Betonun, anılan kısıtlı mekanik özelliklerini geliştirebilmek için, son zamanlarda, doğal ve yapay fiberlerin beton karışımına eklenmesine yönelik bazı yenilikler üzerinde çalışılmaktadır.

Bu çalışmanın başlıca amacı, iki farklı beton türü (normal ve yüksek performanslı beton) için fiber dozajları 30, 60 ve 90 kg/m³ ve uzunlukları 30 ve 60 mm olan çelik liflerin, ve fiber dozajları 3, 6 ve 9 kg/m³ olan sentetik liflerin eklenmesi ile elde edilen beton numunelerinin kare plaka testi ile yük taşıma ve enerji absorpsiyon kapasitelerinin araştırılmasıdır. Sonuçların tutarlı elde edilebilmesi için, her bir beton türü için üç numune hazırlanarak nokta yükleme test methodu uygulanmış ve neticesinde yük deplasman davranışlarına ulaşılmıştır. 25 mm'ye kadar deplasman davranışının belirlenmesi ile enerji yutma kapasitelerine ulaşılmıştır. Sonuç olarak, beton karışımına liflerin eklenmesi ile, hem kritik yükte hem de enerji yutma kapasitesinde artış gözlenmiştir. Çalışma sonucunda, numunelerdeki fiber dozajının artırılmasının, numuneler üzerindeki çatlak uzunluklarının da artmasını sağladığı

görülmüştür. Özellikle, çelik lifli beton numuneler, sentetik lifli numunelere göre daha iyi performans göstermiştir.

Anahtar Kelimeler: Lif Donatılı Beton, Yüksek ve Normal Performanslı Beton, Çelik Lif, Sentetik Lif, Kare Plaka Deneyi

To my family

ACKNOWLEDGEMENTS

I would like to express my gratefulness to my supervisor Prof. Dr. İsmail Özgür Yaman for his great support, perfect guidance and supervision during the preparation of this thesis.

I would also like to express my sincere thanks to my co-supervisor Dr. Burhan Aleessa Alam, for his endless guidance and support for all stages of the preparation of this thesis.

Special thanks go to my friends Aydınç Güzelce and Emin Şengün for their wonderful support during the stages of this thesis.

Finally, I would like to thank my family for their endless encouragement and support.

TABLE OF CONTENTS

ABSTRACT	v
ÖZ	vii
ACKNOWLEDGEMENTS	x
TABLE OF CONTENTS	xi
LIST OF TABLES	xiii
LIST OF FIGURES	xv
CHAPTERS	
1. INTRODUCTION	1
1.1. General	1
1.2. Objective and Scope	1
2. LITERATURE REVIEW	3
2.2. Fibers	4
2.2.1. Introduction.....	4
2.2.2. Steel Fibers	5
2.2.3. Synthetic Fibers	6
2.3. Fiber Reinforced Concrete (FRC)	8
2.3.1. Historical Development of FRC	8
2.3.2. Properties of FRC	9
2.3.2.1. Effects of Fibers on Concrete.....	9
2.3.2.2. Panel Testing of FRC	11
2.3.3. Applications of FRC	17
3. EXPERIMENTAL PROCEDURE	19
3.1. General	19

3.2. Materials.....	19
3.3. Testing Procedure	23
3.4. Interpreting Test Data	25
4. RESULTS AND DISCUSSIONS	27
4.1. General.....	27
4.2. Steel Fibers.....	27
4.2.1. NPC with Steel Fibers	27
4.2.2. HPC with Steel Fibers	29
4.3. Synthetic Fibers.....	31
4.3.1. NPC with Synthetic Fibers	31
4.3.2. HPC with Synthetic Fibers	33
4.4. Effect of Fiber Type and Dosage on Energy Absorption Capacity	35
4.4.1. Effect of Fiber Type and Dosage on NPC.....	35
4.4.2. Effect of Fiber Type and Dosage on HPC.....	36
4.5. Effect of Concrete Strength on Energy Absorption Capacity.....	36
4.6. Comparison of FRC with RC and ECC	38
4.7. Crack Patterns	39
5. CONCLUSIONS & RECOMMENDATIONS	45
REFERENCES	47
APPENDICES	
A. FORCE-DISPLACEMENT TEST RESULTS	51
B. ENERGY-DISPLACEMENT TEST RESULTS	67
C. CRACK PATTERNS	83

LIST OF TABLES

TABLES

Table 2.1. Mechanical Properties of Fibers	4
Table 2.2. Tensile Strength Values of Some Types of Steel Fibers.....	6
Table 2.3. Mechanical Properties of Fibers	8
Table 2.4. Physical Properties of Synthetic Fibers	8
Table 2.5. Concrete Mix Design used in the Experiment	13
Table 2.6. Fiber Parameters used in the Experiment	13
Table 3.1. Properties of the Fibers used in the Experiments.....	20
Table 3.2. Mix Proportions of the Concrete Specimens	21
Table 3.3. Fresh and Hardened Properties of the Mixtures.....	22
Table 3.4. Standard of mixture proportion for ECC specimen	23
Table 4.1. Force-displacement values of NPC with Steel Fibers.....	29
Table 4.2. Energy-displacement values of NPC with Steel Fibers	29
Table 4.3. Force-displacement values of HPC with Steel Fibers.....	31
Table 4.4. Energy-displacement values of HPC with Steel Fibers	31
Table 4.5. Force-displacement values of NPC with Synthetic Fibers.....	32
Table 4.6. Energy-displacement values of NPC with Synthetic Fibers	33
Table 4.7. Force-displacement values of HPC with Synthetic Fibers.....	34
Table 4.8. Energy-displacement values of HPC with Synthetic Fibers	34
Table A.1. Force Displacement Test Results of NPC Steel.....	55
Table A.2. Force Displacement Test Results of HPC Steel.....	60
Table A.3. Force Displacement Test Values of NPC Synthetic	63
Table A.4. Force Displacement Test Values of HPC Synthetic	66
Table B.5. Energy Displacement Test Values of NPC Steel	71
Table B.6. Energy Displacement Values of HPC Steel	76
Table B.7. Energy Displacement Values of NPC Synthetic	79

Table B.8. Energy Displacement Test Values of HPC Synthetic 82

LIST OF FIGURES

FIGURES

Figure 2.1. Main Shapes of Steel Fibers	5
Figure 2.2. Working Mechanism of the Fibers	10
Figure 2.3. Test Results of Energy Absorption Capacities	14
Figure 3.1. The Fibers used in the Experiments	20
Figure 3.2. Concrete Batching Mixer	23
Figure 3.3. Fresh Concrete in Steel Mold	24
Figure 3.4. Plate Testing	25
Figure 3.5. Sample Graph	26
Figure 4.1. Average Force Displacement Graphs of NPC with 30 mm Steel Fibers.	28
Figure 4.2. Average Force Displacement Graphs of NPC with 60 mm Steel Fibers.	28
Figure 4.3. Average Force Displacement Graphs of HPC with 30 mm Steel Fibers.	30
Figure 4.4. Average Force Displacement Graphs of HPC with 60 mm Steel Fibers.	30
Figure 4.5. Average Force Displacement Graphs of NPC Synthetic.....	32
Figure 4.6. Average Force Displacement Graphs of HPC Synthetic.....	33
Figure 4.7. Average Energy Displacement Graphs of NPC	35
Figure 4.8. Average Energy Displacement Graphs of HPC	36
Figure 4.9. Comparison of Energy Displacement Graphs of NPC and HPC.....	37
Figure 4.10. Load-Displacement Graph of HPC 60/90, RC and ECC.....	38
Figure 4.11. Average Energy Displacement Graphs of HPC 60/90, RC and PVA ...	39
Figure 4.12. Average Crack Lengths for HPC and NPC	40
Figure 4.13. Crack Lengths of NPC with $V_f = 0.3\%$	41
Figure 4.14. Crack Lengths of NPC with $V_f = 0.6\%$	41
Figure 4.15. Crack Lengths of NPC with $V_f = 0.9\%$	42
Figure 4.16. Crack Lengths of HPC with $V_f = 0.3\%$	42
Figure 4.17. Crack Lengths of HPC with $V_f = 0.6\%$	43

Figure 4.18. Crack Lengths of HPC with $V_f = 0.9\%$	43
Figure A.1. Force Displacement Graphs of NPC Control.....	51
Figure A.2. Force Displacement Graphs of NPC Steel 30/30.....	51
Figure A.3. Force Displacement Graphs of NPC Steel 30/60.....	52
Figure A.4. Force Displacement Graphs of NPC Steel 30/90.....	52
Figure A.5. Force Displacement Graphs of NPC Steel 60/30.....	53
Figure A.6. Force Displacement Graphs of NPC Steel 60/60.....	53
Figure A.7. Force Displacement Graphs of NPC Steel 60/90.....	54
Figure A.8. Force Displacement Graphs of HPC Control.....	56
Figure A.9. Force Displacement Graphs of HPC Steel 30/30.....	56
Figure A.10. Force Displacement Graphs of HPC Steel 30/60.....	57
Figure A.11. Force Displacement Graphs of HPC Steel 30/90.....	57
Figure A.12. Force Displacement Graphs of HPC Steel 60/30.....	58
Figure A.13. Force Displacement Graphs of HPC Steel 60/60.....	58
Figure A.14. Force Displacement Graphs of HPC Steel 60/90.....	59
Figure A.15. Force Displacement Graphs of NPC Synthetic Control.....	61
Figure A.16. Force Displacement Graphs of NPC Synthetic 3 kg.....	61
Figure A.17. Average Force Displacement Graphs of NPC Synthetic 6 kg.....	62
Figure A.18. Average Force Displacement Graphs of NPC Synthetic 9 kg.....	62
Figure A.19. Force Displacement Graphs of HPC Synthetic Control.....	64
Figure A.20. Force Displacement Graphs of HPC Synthetic 3 kg.....	64
Figure A.21. Force Displacement Graphs of HPC Synthetic 6 kg.....	65
Figure A.22. Force Displacement Graphs of HPC Synthetic 9 kg.....	65
Figure B.23. Energy Displacement Graphs of NPC Control.....	67
Figure B.24. Energy Displacement Graphs of NPC Steel 30/30.....	67
Figure B.25. Energy Displacement Graphs of NPC Steel 30/60.....	68
Figure B.26. Energy Displacement Graphs of NPC Steel 30/90.....	68
Figure B.27. Energy Displacement Graphs of NPC Steel 60/30.....	69
Figure B.28. Energy Displacement Graphs of NPC Steel 60/60.....	69
Figure B.29. Energy Displacement Graphs of NPC Steel 60/90.....	70

Figure B.30. Energy Displacement Graphs of HPC Control	72
Figure B.31. Energy Displacement Graphs of HPC Steel 30/30	72
Figure B.32. Energy Displacement Graphs of HPC Steel 30/60	73
Figure B.33. Energy Displacement Graphs of HPC Steel 30/90	73
Figure B.34. Energy Displacement Graphs of HPC Steel 60/30	74
Figure B.35. Energy Displacement Graphs of HPC Steel 60/60	74
Figure B.36. Energy Displacement Graphs of HPC Steel 60/90	75
Figure B.37. Energy Displacement Graph of NPC Control.....	77
Figure B.38. Energy Displacement Graphs of NPC Synthetic 3 kg	77
Figure B.39. Energy Displacement Graphs of NPC Synthetic 6 kg	78
Figure B.40. Energy Displacement Graphs of NPC Synthetic 9 kg	78
Figure B.41. Energy Displacement Graphs of HPC Control	80
Figure B.42. Energy Displacement Graphs of HPC Synthetic 3 kg	80
Figure B.43. Energy Displacement Graphs of HPC Synthetic 6 kg	81
Figure B.44. Energy Displacement Graphs of HPC Synthetic 9 kg	81
Figure C.45. Crack Patterns of NPC Control #1, #2 and #3	83
Figure C.46. Crack Patterns of NPC 30/30 #1, #2 and #3	83
Figure C.47. Crack Patterns of NPC 30/60 #1, #2 and #3	84
Figure C.48. Crack Patterns of NPC 30/90 #1, #2 and #3	84
Figure C.49. Crack Patterns of NPC 60/30 #2 and #3	85
Figure C.50. Crack Patterns of NPC 60/60 #1, #2 and #3	85
Figure C.51. Crack Patterns of NPC 60/90 #1, #2 and #3	86
Figure C.52. Crack Patterns of NPC 3 kg #1, #2 and #3	86
Figure C.53. Crack Patterns of NPC 6 kg #1, #2 and #3	87
Figure C.54. Crack Patterns of NPC 9 kg #1, #2 and #3	87
Figure C.55. Crack Patterns of HPC Control #1, #2 and #3	88
Figure C.56. Crack Patterns of HPC 30/30 #1, #2 and #3	88
Figure C.57. Crack Patterns of HPC 30/60 #1, #2 and #3	89
Figure C.58. Crack Patterns of HPC 30/90 #1, #2 and #3	89
Figure C.59. Crack Patterns of HPC 60/30 #1, #2 and #3	90

Figure C.60. Crack Patterns of HPC 60/60 #1, #2 and #3	90
Figure C.61. Crack Patterns of HPC 60/90 #1, #2 and #3	91
Figure C.62. Crack Patterns of HPC 3 kg #1, #2 and #3	91
Figure C.63. Crack Patterns of HPC 6 kg #1, #2 and #3	92
Figure C.64. Crack Patterns of HPC 9 kg #1, #2 and #3	92

CHAPTER 1

INTRODUCTION

1.1. General

Despite many advantages; concrete has also limitations in its mechanical properties, such as low ductility, tensile strength and energy absorption capacity/toughness. In order to eliminate or minimize these limitations; recently, some developments have been achieved by introducing natural or artificial fibers into the concrete mixture.

With the inclusion of the fibers into the concrete mixture, some mechanical properties can be enhanced, thus stronger and more durable material can be formed. Mechanically, the fibers can control the cracking on the concrete and change the behavior of the concrete against cracking. The degree of enhancement on these properties depends on the type, form, geometry as well as the amount of the fibers.

One of the main purposes of fiber addition is to improve the tensile and flexural strength along with the energy absorption capacity of concrete. The increase in the tensile strength and the enhancement of the toughness with the inclusion of the fibers is directly related to the interaction between the fibers and concrete matrix.

There are many standards that define the use of fibers in concrete, like ASTM C1116, TS 10514, etc.). On the other hand, there are many test methods developed in order to measure the effects of fibers on the concrete. One of the most commonly used test methods is the point loading plate test which is described under many standards, i.e. ASTM C 1550 and EN 14488-5.

1.2. Objective and Scope

Although increasing the amount of fiber is expected to be proportional with the energy absorption capacity and the tensile strength of the concrete, an optimal amount should

be determined in order to achieve a workable concrete as well as fulfil the economic concerns.

The main scope of this thesis is to observe the effect of different fiber types and dosages on the performance of two different concrete grades, normal and high-performance concrete. Two steel fibers with lengths of 30 and 60 mm and dosages of 30, 60, and 90 kg/m³ were used along with one macro synthetic fiber made from polypropylene with a length of 54 mm and dosages of 3, 6 and 9 kg/m³. The performance of the prepared concrete mixtures was measured by the mean of centrally loaded square plates. In order to provide consistency, three plate specimens were used for each concrete mixture, and the load and displacement values were recorded up to a deflection of 25 mm. Then, the energy absorption capacity/toughness was measured. Moreover, the crack patterns of the concrete specimens were also examined.

This thesis is consisted of five chapters including this one. Literature review and detailed information about concrete and fibers are separately presented in the Chapter 2. Moreover, historical background and the properties of fiber reinforced concrete (FRC) are explained in detail in the same chapter. In Chapter 3, the experimental procedures including the material properties, mixture designs, and the testing methods are explained. In Chapter 4, the discussions of the obtained test results are presented with numbers and graphs. Finally, the conclusions are made in Chapter 5 by remarking the results of the research and giving recommendations for the future studies in this area.

CHAPTER 2

LITERATURE REVIEW

2.1. General

Concrete is an artificial conglomerate construction material made mainly of portland cement, water, and aggregates. In the daily lives of human beings, there is almost no structure or infrastructure that does not depend on concrete. With the production of approximately 12 billion tons, concrete is the most widely used construction material all around the world. The reason of its popularity mainly comes from its advantages over the other construction materials. Those advantages can be listed as follows:

- ✓ Durability, especially the resistance to water,
- ✓ The ability to be formed into almost any shape,
- ✓ Worldwide availability

When cement and water are first mixed, the output paste is a plastic material. Due to the chemical reactions between cement and water, this paste gains rigidity and hardness as time passes (Erdogan, 2005). When aggregates are added to this equation, this process results in gaining strength, thus, rock-like mass named concrete forms.

Although the compressive strength of concrete is quite high, the traditional concrete has some shortcomings, i.e. shrinkage and cracking, low tensile and flexural strength, poor toughness, high brittleness, and low shock resistance, which restrict its applications. To overcome these deficiencies, additional materials are added to improve the performance of concrete. Therefore, the idea of reinforcement in the concrete comes to the forefront in order to provide higher tensile strength as well. The common practice is to use steel reinforcing bars. However, this method has some drawbacks in terms of long-term usage. The main concern is the corrosion of the reinforcing steel, since this can directly affect durability, thus the performance of the

reinforced concrete especially in the marine and underground environment (MacDonald, Clifford, Ballou, & Biddle, 2009). Moreover, the requirement of heavy workmanship and relatively higher costs could also be disadvantages of common steel reinforcement practices. To eliminate those drawbacks of traditional steel reinforcement, the introduction of fiber was brought in as an alternative to enhance the tensile and shear strengths as well as improving the ductility of concrete.

2.2. Fibers

2.2.1. Introduction

Fibers, by definition, are fibrous materials that enhance concrete in terms of mainly strength and durability. The source of fibers can both be natural or artificial. Considering its raw material, the fibers can be grouped into two: organic fibers and inorganic fibers. The former could be made of natural and synthetic fibers, while the latter could be metallic (Sarzalajo, Rossi, Perri, Winterberg, & Aristeguieta, 2014). Although there are various types of fibers in terms of the usage purposes in concrete applications, the mostly used fiber types are steel and synthetic fibers. The mechanical properties of some fibers can be seen in Table 2.1 (Johnston & Colin, 1982).

Table 2.1. Mechanical Properties of Fibers

Fiber	Diameter (μm)	Density (10 ³ kg/m ³)	Modulus of Elasticity (GPa)	Tensile strength (GPa)	Elongation at break (%)
Steel	5-500	7.84	200	1-3	3-4
Stainless Steel	5-500	7.84	160	2.1	3
Fibrillated Polypropylene	20-200	0.91	5	0.5	20
Carbon- Type I	3	1.90	380	1.80	0.5
Carbon	9	1.90	230	2.60	1

2.2.2. Steel Fibers

Steel fibers are discrete, short lengths of steel sticks, having an aspect ratio of length/diameter in the range of 20 to 100 with any of the several cross-sections which are sufficiently small to be easily and randomly dispersed in fresh concrete mix using conventional mixing procedures (ACI Committee 544, 2002). The concept of introducing steel fiber reinforcement into concrete has been utilized for many years. It was the early 1960s that steel fibers were first used in concrete to improve its characteristics (ACI Committee 544, 2002). Steel fibers have a typical length and diameter ranges of 6 to 64 mm and 0.5 to 1.00 mm, respectively (Hasan, Afroz, & Mahmud, 2011).

Each fiber is characterized by its length L , and diameter D . The fiber is often described by a convenient parameter called “aspect ratio”, which is the ratio of L/D (Sarzialejo et al., 2014). This ratio indicates the slenderness of the fiber i.e. for the same fiber length, the higher aspect ratio shows that the diameter of the fiber is smaller, thus the fiber is thinner. This means a larger number and surface of fibers for the same weight. The shape of the steel fibers may be straight or shaped, transversely, and the cross section of the fiber may be round, rectangular or irregular (Sarzialejo et al., 2014). Recently, many studies have been carried out on the shape and size of the steel fibers to obtain better improved fiber-concrete mix bond characteristics and fiber dispersability (Nemati, 2015). The main shapes of steel fibers are shown in Figure 2.1.

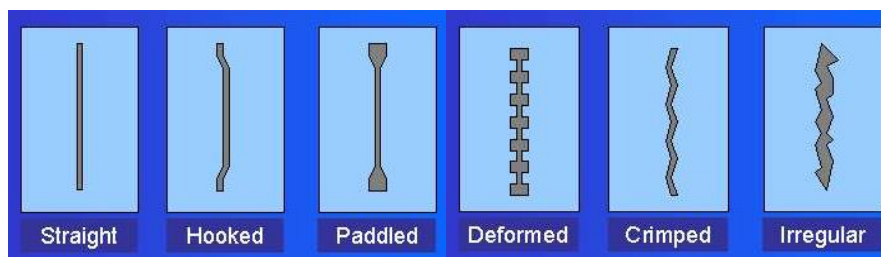


Figure 2.1. Main Shapes of Steel Fibers

As per the studies, it was found that hook-ended stainless-steel wires have physical properties better than the straight ones. This is definitely resulted from the better

anchorage and the higher effective aspect ratio of the hook-ended steel wires. The purpose of inclusion of the steel fibers is mainly to improve the post cracking tensile resistance. For that, steel FRC is generally regarded more economical than the conventional reinforced concrete. Other advantages of using steel fibers in terms of mechanical properties are the higher stiffness and ductility, and better dynamic behavior (Al-lami, 2015). In most of the applications, the steel fibers are mostly utilized as secondary reinforcement along with the conventional reinforcing steel bars or prestressing strands as the main reinforcement. However, for high volume fractions of steel fibers, these fibers can provide better mechanical properties, thus can be used without main reinforcement (Behbahani, Nematollahi, & Farasatpour, 2011). In order to compensate the high tensile stresses that form the cracks, a high tensile strength is required for the steel fibers. Typical steel fiber tensile strengths vary from 1100 to 1700 MPa (Kavitha & Kala, 2018). A comparison table that shows the change in tensile strength of the steel fibers with respect to equivalent diameter and type of the fiber is given in Table 2.2 (Sarzialejo et al., 2014).

Table 2.2. Tensile Strength Values of Some Types of Steel Fibers

Equivalent Diameter (mm)	Tensile Strength (N/mm ²)					
	R1		R2		R3	
	SF	PF	SF	PF	SF	PF
0.15≤D<0.50	400	480	900	1080	1700	2040
0.50≤D<0.80	350	450	800	1040	1550	2015
0.80≤D<1.20	300	390	700	910	1400	1820

NOTE:1) Straight fibers. 2) Profiled fibers. R1, R2, R3 indicates three tensile strength classes.

2.2.3. Synthetic Fibers

The concept of introducing synthetic fiber reinforcement was first realized in 1978. These fibers were used in relatively low dosages to reduce the plastic shrinkage cracking (MacDonald et al., 2009). Synthetic fibers are usually obtained from polymer-based materials such as polypropylene, polyethylene or nylon (NRMCA, 2014). Yet other materials, like carbon, glass, and basalt can be used. These fibers can also be produced in different shapes, which increase the bonding properties between

the concrete (Wang, Backer, & Li, 1987). They can be circular, triangular or flat in cross section. Synthetic fibers can be classed into two: micro-fibers and macro-fibers. The fibers in each class can have different properties and capabilities. In order to reduce the plastic shrinkage in concrete, micro-fibers are introduced, whereas macro-fibers are designed to control cracks in hardened concrete.

Micro-fibers are generally produced with diameter less than 0.1 mm. These fibers should be added at low ratios in order to maintain a good workability. Because of this, their effects on the properties of hardened concrete are insignificant. Polypropylene fiber is one of the most common materials used for micro-fibers. Macro-fibers, on the other hand, have a length more than 30 mm and a diameter more than 0.1mm. These fibers could be used at higher ratios, thus an improvement in the flexural toughness can be achieved. Macro-fibers could be a better solution for enhanced performance, such as facilitate light weight concrete structure, high corrosion resistance; better residual (post-cracking) flexural strength, smaller crack width, and improved performance under impact and abrasion along with a better leveled surface compared to traditional steel FRC.

Synthetic fibers made of polypropylene are commonly used in concrete industry. Due to their hydrophobic property; these fibers do not absorb water; thus, they have minimum effect on water requirements of the concrete. These fibers could be formed as either fibrillated bundles or monofilaments (Laning, 1992). Polyester fibers, like polypropylene ones, are also hydrophobic. The main difference of these fibers from polypropylene fibers is their tendency to disintegrate in the alkaline environment. Therefore, the polyester fibers should be coated in order to have resistance to alkali attack (Laning, 1992). Polyester fibers are made of in monofilament form only. Unlike polypropylene and polyester fibers, nylon fibers have hydrophilic nature. This provides chemical bond to the concrete matrix as well, while polypropylene and polyester fibers bond only mechanically (Laning, 1992). The nylon fibers, unlike the polypropylene fibers, can only be produced in monofilament form. However, nylon fibers show weak properties against heat and light. The mechanical properties of the

mainly used fibers can be seen in Table 2.3 (Sarzialejo et al., 2014). On the other hand, for specific polymer-based synthetic fiber materials, typical physical properties are given in Table 2.4 (Laning, 1992).

Table 2.3. Mechanical Properties of Fibers

Fiber	Diameter (μm)	Density (10^3 kg/m^3)	Young's modulus (kN/mm^2)	Tensile strength (kN/mm^2)	Elongation at break (%)
Steel	5-500	7.84	200	0.5-2	0.5-3.5
Glass	9-15	2.60	70-80	2-4	2-3.5
Asbestos	0.02-0.04	3.00	180	3.30	2-3
Polypropylene	20-200	0.90	5-7	0.5-0.75	8
Nylon	-	1.10	4	0.90	13-15
Polyethylene	-	0.95	0.30	0.0007	10
Carbon	9	1.90	230	2.60	1
Kevlar	10	1.45	65-133	3.60	2.1-4
Acrylic	18	1.18	14-19.5	0.4-1	3

Table 2.4. Physical Properties of Synthetic Fibers

Fiber	Type	Specific Gravity	Length (mm)
Polypropylene	Fibrillated	0.91	6.35- 63.5
Polypropylene	Monofilament	0.91	12.7- 19.05
Polyester	Monofilament	1.34	19.05- 50.8
Nylon	Monofilament	1.16	19.05- 50.8

2.3. Fiber Reinforced Concrete (FRC)

2.3.1. Historical Development of FRC

Concrete is considered a relatively brittle material, which means when it is subjected to tensile stresses; it will crack and fail under small deformations. Therefore, to overcome this problem, initiatives to use steel reinforcement in the concrete were begun in mid 1800s (Brown, Shukla, & Natarajan, 2002). The mechanism of reinforced concrete under stresses assumes the concrete to carry the compressive loads, whereas the steel reinforcement to carry the tensile ones. However, it was realized that long-term durability of reinforced concrete is low, since the steel

reinforcement faces corrosion problems. In order to avoid such problems and their consequences, researches have been made to find a replacement for the steel reinforcement. Thus, the idea of introducing fibers into the concrete mixtures was first arisen in the 1940s (Brown et al., 2002). The addition of fibers leads to the formation of a new material, which characteristics of these material are different from the normal concrete (Sarzalajo et al., 2014). In the early 1960s; Romualdi, Batson, and Mandel published a paper about this issue, that brought FRC to the attention of academic and industry researchers around the world (Zollo, 1997). In the early stages, steel and synthetic fibers were not readily available to use. The fibers were provided from different industries including the automobile tire manufacturing and textile industries. The diameters of the first fibers tested varied from 0.15 to 0.25 mm, and they were relatively stiff. This inevitably resulted in mixing and casting problems. However, within time, suitable mixtures had been reached in laboratory, thus significant improvement in strength was achieved in both the pre and post-cracking behavior of FRC. New fiber types and geometries have been started to be introduced to concrete since the mid-1980s. These new technologies have undoubtedly affected the strength and toughness performance measures of FRC (Zollo, 1997).

2.3.2. Properties of FRC

2.3.2.1. Effects of Fibers on Concrete

Due to durability concerns, it is becoming a common approach to use small, randomly distributed fibers in many applications in order to reinforce the concrete. Yet, fibers can also be used to increase the energy absorption capacity and toughness of the concrete, as well as providing strength characteristics (Nemati, 2015). As a result of shrinkage, tensile stresses develop and cracks may occur, if the shrinkage is restrained. Plastic shrinkage occurs at early age i.e. when concrete still has not enough tensile strength (Eren & Marar, 2010). Adding fibers can minimize these cracks. As mentioned above, inclusion of micro-fibers reducing the plastic shrinkage in concrete, whereas macro-fibers are designed to control cracks in hardened concrete. The

working mechanism of the fibers in the case of cracking is shown in Figure 2.2 (Sinha, 2012).

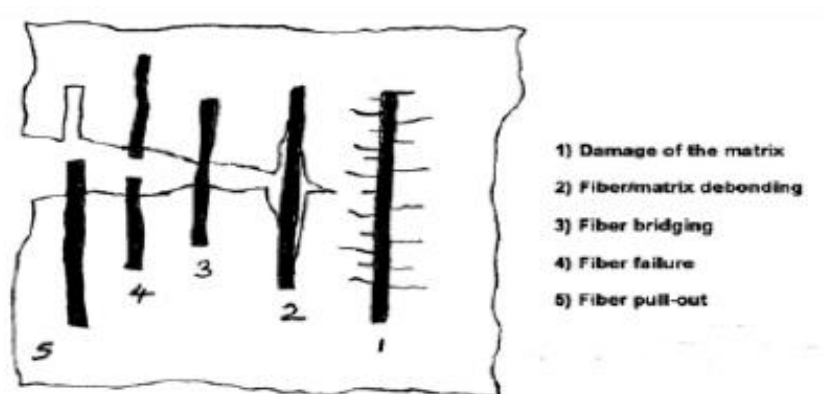


Figure 2.2. Working Mechanism of the Fibers

As can be seen in Figure 2.2, the role of fiber is to minimize the propagation of cracking in concrete. In other words, when fibers are properly bonded, the interaction of these fibers and the concrete matrix is at the level of micro cracks, thus these fibers effectively bridge these cracks. This prevents the cracks to have an unstable growth (Ahmad & Kshipra Kapoor, 2016). The investigations on the fractured FRC specimens demonstrate that the failure could be resulted from two cases: debonding and fiber pull-out (Nemati, 2015). The fiber pull-out scenario is more desirable since it shows more ductility, thus higher energy absorption capacity (Al-lami, 2015).

It is obvious that the advantages provided by fibers in the fresh state of concrete also contribute to the properties of the hardened concrete. In plain concrete, the cracks occurred in the fresh state can propagate in the hardened state as well. Thus, preventing these cracks from the beginning also precludes further cracks in the hardened concrete (NRMCA, 2014). The main drawback of the utilizing fibers in concrete is on the possible decrease in workability (Mohod, 2012). As a result of inadequate workability, non-uniform distribution of fibers occurs in the concrete mix. However, to overcome this problem, superplasticizers have been used not only

enhance the workability but also to maintain the plasticity of the mix for a longer time (Behbahani et al., 2011).

The factors affecting the hardened properties of FRC are listed below:

- The fibers properties, like geometry, aspect ratio, contents, orientation, and distribution,
- The properties of concrete matrix, resistance and maximum dimension of the aggregates,
- The interface bond between the fibers and the concrete matrix,
- The testing procedures in hardened state: dimensions, geometry and methodology (Sarzialejo et al., 2014).

2.3.2.2. Panel Testing of FRC

Recently, many experiments have been carried out on the energy absorption capacity of FRC in order to compare its performance with the plain or reinforced concrete.

In a study, the energy absorption and load capacities of shotcrete panels with polypropylene fiber (PF), steel mesh (SM) and PF+SM reinforcement were evaluated (Kahraman, 2015).

The study was carried out on the 600×600×100 mm square test panel by applying load at the center of the panel by 100 kN testing machine at 1.5 mm/min deformation rate. Then, the load and displacement values are recorded up to 25 mm deformation. As a result, the ultimate load values were recorded as 24.1, 29.2, 63.1 and 47.9 kN for plain concrete, concrete specimen with 4 kg/m³ synthetic fiber, concrete specimen with 4 kg/m³ synthetic fiber and steel mesh, and concrete with steel mesh, respectively. On the other hand, the energy absorption capacities were recorded as 36.7, 275.4, 683.5 and 541.2 Joule for plain concrete, concrete specimen with 4 kg/m³ synthetic fiber, concrete specimen with 4 kg/m³ synthetic fiber and steel mesh, and concrete with steel mesh, respectively.

According to these test results, it was seen that although the dosage of fibers has little effect on the ultimate load, the energy absorption capacities have been considerably developed with the increased amount of fibers.

In another experiment, the effect of test methods on the performance of fiber reinforced concrete with different dosages and matrices was investigated (Hetemoğlu, 2018). In this study, plain concrete control mixture and macro-synthetic fibers with volume fractions of 0.32, 0.65 and 0.98% were used for both high performance and pervious concrete. Then, round panel and square panel tests were conducted on these mixtures in accordance with ASTM 1550 and EFNARC Panel Test, respectively. At the end of the experiment, for high performance concrete specimens, the average energy values at 25 mm deflection were recorded as 85.5, 616.1, 1095.8 and 1503.0 Joule for control, specimen with 0.32%, specimen with 0.65% and specimen with 0.98% fiber, respectively. In addition, for the pervious concrete specimens, the average energy values at 25 mm deflection were recorded as 29.5, 173.0, 304.2 and 506.7 Joule for control, specimen with 0.32%, specimen with 0.65% and specimen with 0.98% fiber, respectively. Thus, it was concluded that the fiber addition was increased the energy absorption capacities for both strong (high performance) and weak (pervious) matrices substantially.

In a study, the effect of different dosages of fibers on the performance of normal and high performance concrete was investigated as well (Öztürk, 2018). In this experiment, macro-synthetic fibers with volume fractions of 0.3, 0.6 and 0.9% were used for normal performance concrete square specimens. For comparison, macro-synthetic fibers with volume fractions of 1.32, 1.67 and 2.64% were used for high performance concrete square specimens. At the end of the tests, the energy absorption capacities were recorded as 625.7, 1009.7, 1386.7 Joule for normal concrete with fiber volume fraction of 0.3, 0.6 and 0.9%, respectively. Moreover, the energy absorption capacities were found as 2107.9, 2518.4 and 2429.8 Joule for high performance concrete with fiber volume fraction of 1.32, 1.67 and 2.64%, respectively. Thus, it was concluded that for normal concrete, with the increased fiber amount, the toughness

was also increased significantly. For high performance, on the other hand, with the increased amount of fiber, the energy absorption capacity of the concrete was also increased although in the concrete specimen with the fiber volume fraction of 2.64% show less performance than the one with the 1.67%.

In another experiment, the steel and macro synthetic fiber reinforced square concrete panel specimens were tested in order to observe the performance of different FRC specimen types with increasing age (Juhász & Schaul, 2019). The concrete mix design was identical in all specimens except for fiber types and dosages, and is given in Table 2.5.

Table 2.5. Concrete Mix Design used in the Experiment

Mix ID	Cement (kg/m ³)	Water (kg/m ³)	Admixture (kg/m ³)	Synthetic Fiber (kg/m ³)	Steel Fiber (kg/m ³)	Fine Agg. (kg/m ³)
1	480	216	4	6	-	1620
2	480	216	4	8	-	1620
3	480	216	4	-	55	1620

To observe the performance of the fibers in detail, one type of steel and three types of synthetic fibers were used in the experiments with different dosages and the parameters of these fibers are given in Table 2.6.

Table 2.6. Fiber Parameters used in the Experiment

Mix ID	Fiber Type	Fiber Dosage (kg/m ³)	Fiber Length (mm)
BC48-6kg	Macro Synthetic	6	48
BC48-8kg	Macro Synthetic	8	48
BC54-6kg	Macro Synthetic	6	54
BC54-8kg	Macro Synthetic	8	54
DT57-6kg	Macro Synthetic	6	57
DT57-8kg	Macro Synthetic	8	57
SF35-55kg	Steel	55	35

The test results of energy absorption capacities of the square panel specimens were given in Figure 2.3.

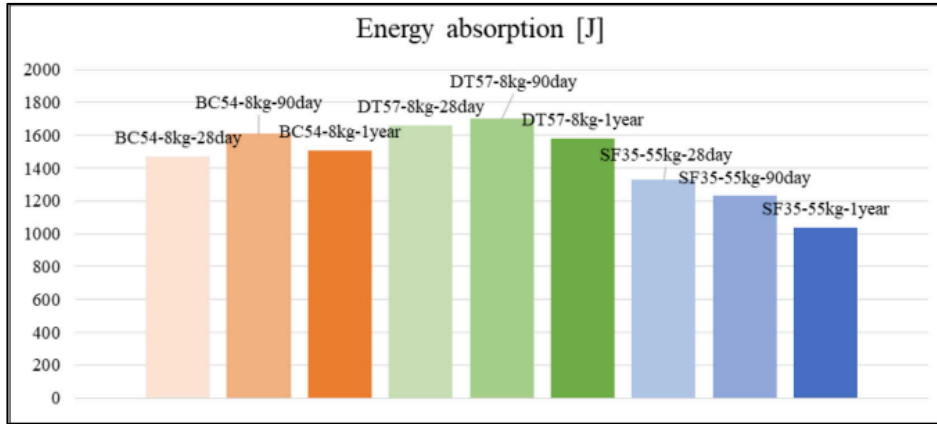


Figure 2.3. Test Results of Energy Absorption Capacities

From this experiment, it is clearly inferred that inclusion of fibers to the plain concrete increased the post-crack performance of the concrete. Moreover, it was observed that during the test period, the ductility of steel fibers decreased while the ductility of the synthetic fibers remained almost constant.

The effect of inclusion of the fibers to other main mechanical properties of the concrete are presented below.

Compressive Strength:

Experiments show that the compressive strength of the concrete is not changed significantly with the addition of the fibers. In order to observe the performance of the FRC under compression, there are many investigations carried out with mainly steel fibers. A moderate increase for certain inclusion rates of steel fibers (no less than 1.5% in volume) could be observed (Sarzialejo et al., 2014). Similarly, it was reported that the effect of steel fibers on the compressive strength of concrete is variable (ACI Committee 544, 2010). Inclusion of 2% volumetric ratio of steel fiber with an aspect ratio of 100 increases the compressive strength in a range between 0 to 23%. Another

experiment reports that using 1.5% volumetric ratio of steel fiber could increase the compressive strength by 37% (Khaloo & Kim, 1996).

In another research about the use of micro synthetic fibers in concrete, the test results demonstrate that although the strength increase percentage increased when more fibers are used, this effect is not that significant (Hasan et al., 2011).

Flexural Strength:

Researches show that adding fibers mainly steel ones, contributes to the development of flexural strength of the concrete. In an experiment with regards to the flexural strength, compared to the ones with the macro synthetic fibers, the concrete specimens with the steel fibers steel fibers show better performance (Buratti, Mazzotti, & Savoia, 2011).

It was reported by the ACI that two types of flexural strength for steel FRC are existed (ACI Committee 544, 2002). The first one is first-crack flexural strength, which shows a linear behavior. This strength can be increased by almost 100% for concrete reinforced with 1% of straight steel fibers (Shah & Rangan, 1971). Another experiment carried out by Song and Hwang shows that 2% of hooked steel fibers with aspect ratio of 64 could increase the first-crack flexural strength of high strength concrete up to 127% (Song & Hwang, 2004). A similar result was found by Thomas and Ramaswamy when hooked fibers with aspect ratio of 60 were used in a range between 0.5% to 1.5% , which resulted in an increases in the first-crack flexural strength up to about 145% (Thomas & Ramaswamy, 2007).

The second type of flexural strength is the ultimate flexural strength, which is related to the maximum load achieved. Hooked-end fibers, for example, can increase ultimate flexural strength by 100% (Erdogan, 2005).

Tensile Strength:

Normal concrete loses the tensile load carrying capacity after crack widths of about 0.3 mm. However, in FRC, the new cracks will keep propagate in the brittle matrix of

normal concrete, because the fibers across the cracks are able to carry more loading (Lofgren, 2005). There are many studies done to show the importance of introducing fibers to the concrete with regards to tensile strength. In one of them, an indirect tensile test was carried out cube specimens with variable volume fractions of macro synthetic fibers. The results show that with the addition of macro synthetic fibers, the indirect tensile strength of the concrete was significantly increased. This increase in the tensile strength is due to the fiber bridging properties in the concrete. The plain concrete specimen failed suddenly when the cracking occurred, on the other hand, FRC specimens did not fully separate, although cracking was observed. Thus, it is inferred that the FRC can absorb energy in the post-cracking stage as well (Hasan et al., 2011).

Flexural Toughness:

Considering the studies on both the compressive and the tensile strength of FRC, it could be concluded that although fibers increase the strength of concrete, their main contribution is to the flexural toughness of the material, which is the total absorbed energy when a specimen breaks under flexure. Since plain concrete is a brittle material, it possesses no toughness. In other words, it has no residual strength or post-crack strength after failure (Jiabiao, 2011). An experiment was carried out on average residual strength of different volume fractions of fibers introduced to the concrete (MacDonald et al., 2009). As a result of this experiment, it was observed that the average residual strength of the concrete specimens significantly improved with the increased fiber volume.

Flexural toughness is defined in ACI 544 as the area under load-deflection curve under static loading (ACI Committee 544, 2002). In other words, it is the total energy achieved until the complete separation of the specimen. The toughness can be measured by various tests, including static, impact, and fatigue tests. However, static loading test is mostly applied since the variations in the results are not that high and the test equipment are more available (Al-Ghamdy, Wight, & Tons, 1994). Utilizing fibers in concrete can improve the post-peak compressive strength of concrete. In other

words, using fiber increases the toughness and energy observation. Thus, it prevents a sudden failure of concrete and provides high strength concrete (Al-lami, 2015).

2.3.3. Applications of FRC

The addition of fibers to concrete has gained importance especially in concrete structures with a relatively large surface area that are exposed to threats regarding the plastic shrinkage cracking. Examples for these structures are walls, bridge decks, slabs and overlays (ACI Committee 544, 2010). There are examples of steel FRC used in shotcrete applications, which could be seen in slope stabilization, tunnel lining and bridge repair (Behbahani et al., 2011). There are also examples of introducing macro synthetic fibers to shotcrete, which is used to repair marine structures in very severe climates. These examples show how the fibers successfully work in the concrete that is exposed to aggressive environments including impacts, alkali reactivity and freezing- thawing cycles.

FRC have been used in tunnel linings as well (Jiabiao, 2011). Since there are many cases regarding the corrosion of the reinforcing bars in the tunnel lining due to the water filtration, the fibers have been introduced to these types of structures in order to improve durability characteristics. There are also various examples of FRC in airport, road and industrial floor areas as well as precast concrete industry (Behbahani et al., 2011).

FRC can be used in the construction of new pavements or for the repair of existing pavements. Thanks to its higher flexural strength, the thickness of the pavement could be decreased. Moreover, the resistance to impact and repeated loading will be increased (Behbahani et al., 2011).

It was also reported that the use of FRC in concrete overlays on asphalt or composite pavement has been significantly increased in the past ten years. The main benefits of FRC for pavements are providing additional structural capacity, reducing crack widths and as a result, extending serviceability of the pavements (Roesler, Bordelon, Brand, & Amirkhanian, 2019).

CHAPTER 3

EXPERIMENTAL PROCEDURE

3.1. General

The main aim of this experimental study is to investigate the effects of different fibers on the energy absorption capacity of normal and high-performance concrete. Within this regard, two types of steel fibers with different lengths (30 and 60 mm) and one type of macro synthetic fiber in bundle form with a length of 54 mm were added in three different dosages for each type (30, 60, and 90 kg/m³ for the steel fibers, and 3, 6, and 9 kg/m³ for the synthetic one) to two different concrete grades, normal and high performance concrete. The tests are conducted over square plate specimens with dimensions of 600×600×100 mm. Along with that, plain concrete specimens and steel rebar reinforced specimens were also prepared for comparison purposes. The square plate specimens were loaded on the center point in line with the EN 14488 standard, in order to determine the energy absorption capacity of the different concrete mixtures. The tests were carried out upon the completion of 28-days curing period using a displacement-controlled loading scheme. All the experimental studies were conducted in the Materials of Construction Laboratory, Department of Civil Engineering, Middle East Technical University.

3.2. Materials

In all the concrete mixtures, CEM I 42.5 R portland cement, Class F fly ash and crushed limestone aggregates were used. The fly ash was used to provide additional binder material, and improve the workability of the mixtures.

Moreover, in order to enhance the workability of the mixtures, normal range water reducer was added to normal performance concrete, while a polycarboxylic ether based high range superplasticizer was used in high performance concrete to enhance

the workability of the fresh concrete. The crushed limestone aggregates were used in three different sizes that are 0-4 mm for fine aggregate, 4-12 mm and 12-25 mm for the coarse aggregates with a ratio of 50%, 25%, and 25% respectively. To enhance the strength of high performance FRC, silica fume was also used in those mixtures.

The pictures of the fibers used in this study are presented in Figure 3.1, while their properties are presented in Table 3.1.



Figure 3.1. The Fibers used in the Experiments

Table 3.1. Properties of the Fibers used in the Experiments

	Macro-synthetic fiber	Steel Fiber
Commercial Name	Forta-Ferro	Dramix 3D
Base Material	Pure Copolymer PP/PE	Steel
Shape/Surface Texture	Twisted Bundles	Curved 3 Times in Both Ends
Length (mm)	54	60
Diameter (mm)	0.34	0.75
Aspect Ratio	158.82	80
Number of Fibers per kg	220,000	4,690
Tensile Strength (MPa)	550-750	1,225
Young's Modulus (GPa)	5.75	200

The mix proportions are given in Table 3.2. In addition, fresh and hardened properties were presented in Table 3.3. It should be noted that the low slump values are related to the addition of the fibers. However, when a mechanical vibrator was used, placing the mixtures in the molds was done properly. The average compressive strength and the average modulus of elasticity of the concrete batches were about 38.9 MPa with Coefficient of Variation (CoV) of 11% and 33.4 GPa, respectively for NPC batches and 63.0 MPa with CoV of 6% and 37.4 GPa, respectively for HPC batches.

Table 3.2. Mix Proportions of the Concrete Specimens

Concrete Matrix		Type of Mixture	Cement (kg/m ³)	Silica Fume (kg/m ³)	Fly Ash (kg/m ³)	W/B (%)	SP (%)	Fiber (kg/m ³)	Fine Agg. (kg/m ³)	Coarse Agg.1 (kg/m ³)	Coarse Agg.2 (kg/m ³)	Density (kg/m ³)					
NPC	Control	Steel Fibers	250	0	63	50	1	0	890	461	2342						
								30	936	484	2406						
								60	931	481	2426						
								90	926	479	2446						
	Synt. Fibers	Steel Fibers						3 kg	936	484	2380						
								6 kg	932	482	2375						
								9 kg	928	480	2369						
								Control	0	819	423	2370					
	HPC	Control						Steel Fibers	400	30	100	32	1	30	816	422	2396
														60	811	420	2416
														90	806	417	2436
														3 kg	817	423	2370
Synt. Fibers		Steel Fibers	6 kg	811	420	2362											
			9 kg	808	418	2358											
			Control	0	819	423	2370										
			30	816	422	2396											

Table 3.3. Fresh and Hardened Properties of the Mixtures

Matrix	Mixture Type	Fiber Amount (kg/m³)	Volume Fraction %	Slump or Flow* (cm)	Compressive Strength (MPa)
HPC	Control	-	-	70*	56.4
	30 mm Steel	30	0.38	75*	59.4
		60	0.75	57*	68.6
		90	1.13	62*	74.1
	60 mm Steel	30	0.38	56*	71.6
		60	0.75	18	58.6
		90	1.13	0	69.2
	Synthetic	3	0.34	20	53.6
		6	0.68	18	56.2
		9	1.02	5	62.7
NPC	Control	-	-	23	40.6
	30 mm Steel	30	0.38	17	37.5
		60	0.75	18	38.5
		90	1.13	18	39.4
	60 mm Steel	30	0.38	12	39.4
		60	0.75	0	38.4
		90	1.13	0	35.2
	Synthetic	3	0.34	0	40.5
		6	0.68	0	43.2
		9	1.02	0	36.3

*Flow test was applied.

For comparison reasons, two types of plate specimens were also produced, one made of Engineered Cementitious Concrete (ECC), a widely known cementitious composite prepared using 6 mm polyvinyl alcohol (PVA) fibers with a volume of 2%, and the second made of steel rebar reinforced concrete. The ECC mixture used is known as M45 (Table 3.4). As for the rebar reinforcement panels, NPC Control mix, which contains no fibers, was used along with steel reinforcements on both directions of the panel with a ratio of $\phi 12@100$ mm and length of 550 mm.

Table 3.4. Standard of mixture proportion for ECC specimen

	ECC (M45)
Cement (C), kg/m ³	570
Fly Ash (FA), kg/m ³	684
Sand (S), kg/m ³	455
Water (W), kg/m ³	331
Fiber (PVA), kg/m ³	26
HRWR, kg/m ³	4.9
FA/C	1.2
W/CM*	0.26
S/C	0.8

*CM: Cementitious Materials (cement + fly ash)

3.3. Testing Procedure

Upon determining the mix proportions of each concrete group, the materials were mixed in a rotary mixer to obtain the required concrete (Figure 3.2). The fresh concrete was then placed into the steel molds and waited for 24 hours before it was removed from the molds (Figure 3.3).



Figure 3.2. Concrete Batching Mixer

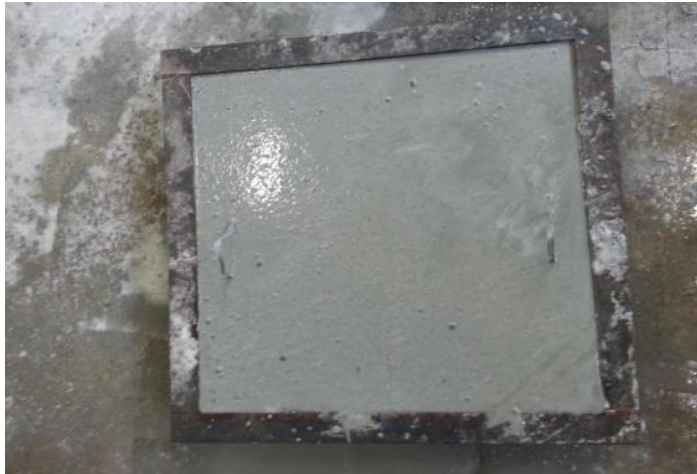


Figure 3.3. Fresh Concrete in Steel Mold

Three plates were tested for each mixture. The tests were done after holding the specimens for the 28-days in wet condition under room temperature

Energy absorption capacity tests were conducted on 600×600×100 mm plates in accordance with EN 14488. These tests were performed with using a 250 kN MTS Landmark testing device (Figure 3.4).

During the tests, the plates edges were first placed over an open square frame, with an outer length of 60 cm from the outside and 50 cm from the inside. Then, a center load was applied through a 10 cm square steel plate, at a constant speed of 1 mm/min. During the test, the load-displacement values were recorded up to 25 mm deflections. Based on these values, the energy absorption capacity of each specimen was calculated as the area under the load-displacement curve. At the end of the test, the photo of the bottom surface of each specimen was taken in order to examine the crack pattern.



Figure 3.4. Plate Testing

3.4. Interpreting Test Data

After testing all three specimens, the data, which was transferred from the testing device, was used for computing average force versus displacement of each mixture. A software, MATLAB, was used for converting the raw data of the performed tests into equal interval in terms of displacement. By obtaining arithmetic average of the three specimens, the average force values for the corresponding displacements were calculated. Energy absorption capacity values were also calculated by using force versus displacement data, as the area under this curve was calculated by trapezoidal rule. From the corresponding area, energy values up to 25 mm displacement were obtained (Figure 3.5).

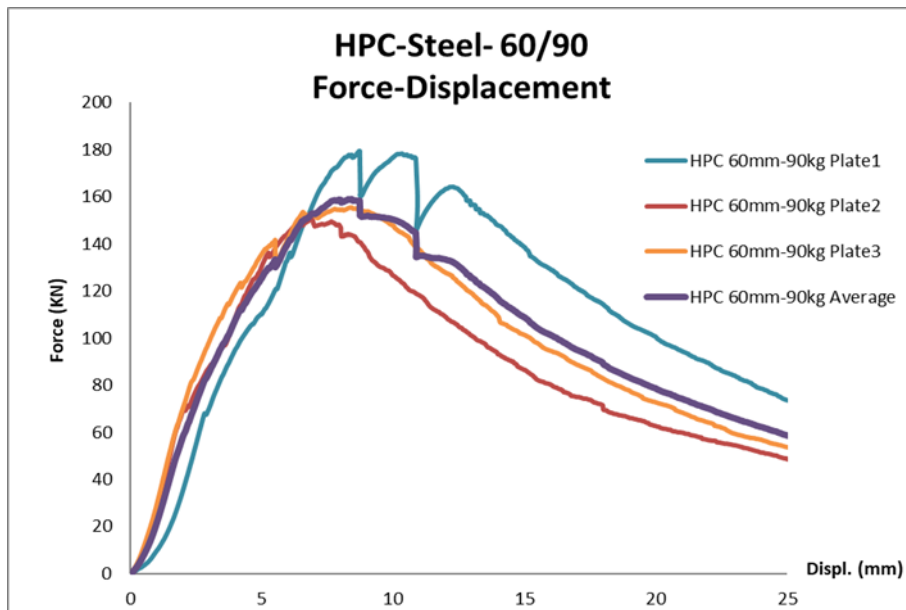


Figure 3.5. Sample Graph

All of the test data for individual specimens and their average were provided in Appendix A and B.

CHAPTER 4

RESULTS AND DISCUSSIONS

4.1. General

From the test results, the force-displacement and energy-displacement graphs for each mixture were obtained in order to examine the effect of fiber type and amount on the performance of FRC. The crack patterns of the specimen were also investigated. Three plates were tested for each mixture. The average results of the three specimens are presented in this chapter, while the results of each specimen are presented in the appendices.

4.2. Steel Fibers

4.2.1. NPC with Steel Fibers

The average force-displacement curves of the normal concrete specimens with 30 mm and 60 mm steel fibers are presented in Figure 4.1 and Figure 4.2. The first crack loads along with the ultimate loads are presented in Table 4.1, whereas the energy values in 5 mm intervals are summarized in Table 4.2.

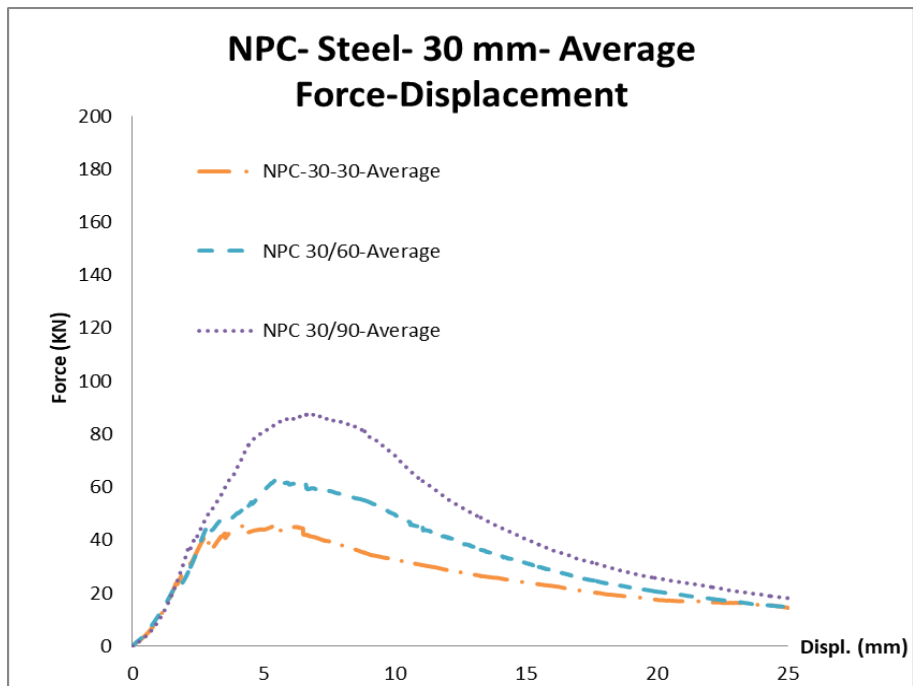


Figure 4.1. Average Force Displacement Graphs of NPC with 30 mm Steel Fibers

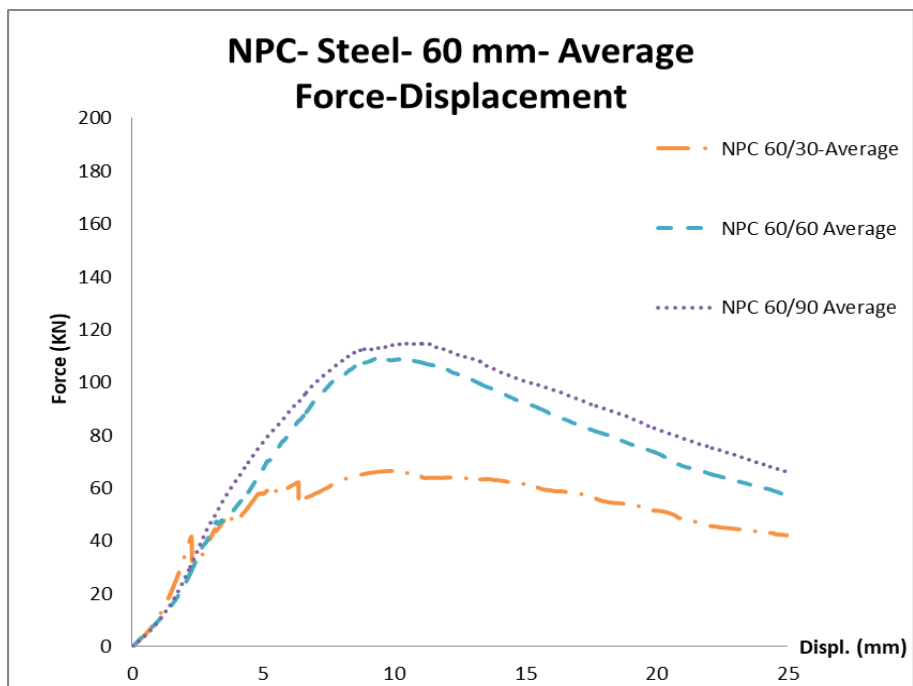


Figure 4.2. Average Force Displacement Graphs of NPC with 60 mm Steel Fibers

Table 4.1. Force-displacement values of NPC with Steel Fibers

	First crack load (kN)	Displacement at first crack (mm)	Ultimate load (kN)	Displacement at ultimate load (mm)	% increase in the ultimate load
NPC Control	48.2	2.5	48.2	2.5	0%
NPC 30-30	41.2	2.5	53.0	5.1	10%
NPC 30-60	53.5	4.1	67.6	5.5	40%
NPC 30-90	46.4	2.5	93.2	6.7	93%
NPC 60-30	41.6	2.6	69.3	9.9	44%
NPC 60-60	52.8	2.6	110.2	9.2	129%
NPC 60-90	77.5	6.0	115.6	10.9	140%

Table 4.2. Energy-displacement values of NPC with Steel Fibers

	Energy (Joule)					% increase in the ultimate load
	at 5 mm	at 10 mm	at 15 mm	at 20 mm	at 25 mm	
NPC Control	47.6	47.6	47.6	47.6	47.6	0%
NPC 30-30	145.2	341.8	481.9	584.6	665.9	1299%
NPC 30-60	162.3	450.6	647.9	774.0	861.0	1709%
NPC 30-90	201.6	616.0	884.7	1044.4	1152.5	2321%
NPC 60-30	152.7	477.4	789.4	1071.4	1300.2	2632%
NPC 60-60	208.0	657.3	1195.4	1612.9	1947.1	3991%
NPC 60-90	184.0	689.8	1236.5	1695.2	2065.0	4238%

4.2.2. HPC with Steel Fibers

The average force-displacement curves of the high-performance concrete specimens with 30 mm and 60 mm steel fibers are presented in Figure 4.3 and Figure 4.4. The first crack loads along with the ultimate loads are presented in Table 4.3, whereas the energy values in 5 mm intervals are summarized in Table 4.4.

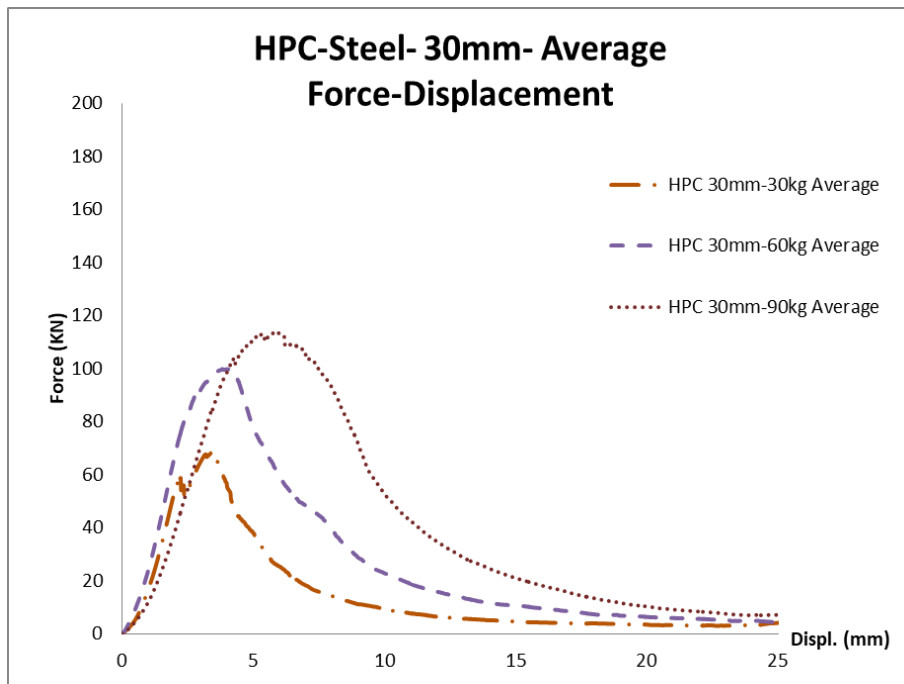


Figure 4.3. Average Force Displacement Graphs of HPC with 30 mm Steel Fibers

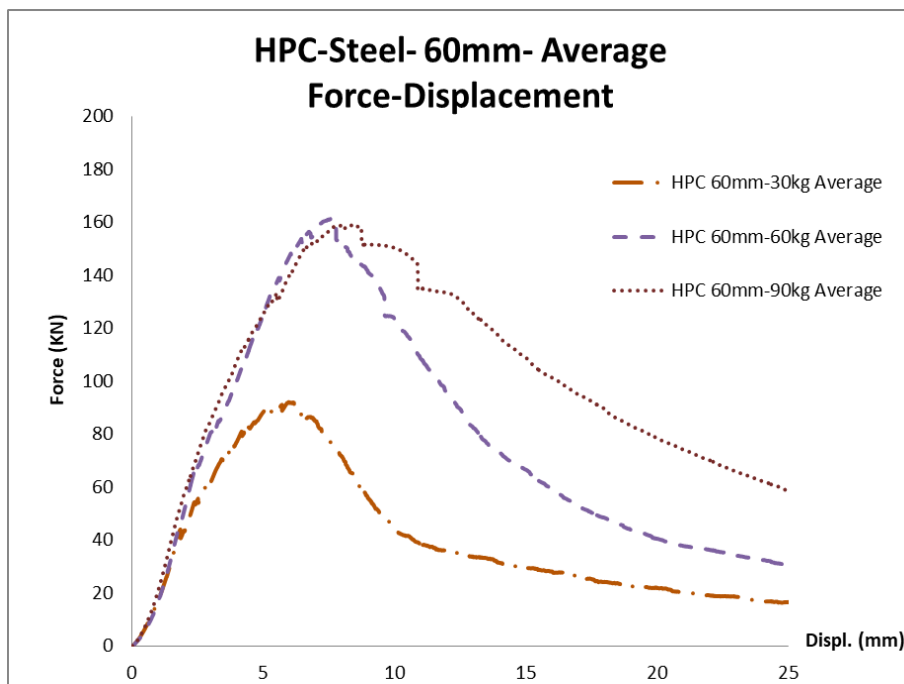


Figure 4.4. Average Force Displacement Graphs of HPC with 60 mm Steel Fibers

Table 4.3. Force-displacement values of HPC with Steel Fibers

	First crack load (kN)	Displacement at first crack (mm)	Ultimate load (kN)	Displacement at ultimate load (mm)	% increase in the ultimate load
HPC Control	75.2	1.9	75.2	1.9	0%
HPC 30-30	49.8	2.1	72.5	3.1	-4%
HPC 30-60	81.5	2.7	100.6	4.1	34%
HPC 30-90	109.1	4.4	120.8	5.6	61%
HPC 60-30	51.0	2.0	95.7	5.8	27%
HPC 60-60	71.1	2.5	163.4	7.3	117%
HPC 60-90	86.9	3.0	161.9	8.0	115%

Table 4.4. Energy-displacement values of HPC with Steel Fibers

	Energy (Joule)					% increase in the ultimate load
	at 5 mm	at 10 mm	at 15 mm	at 20 mm	at 25 mm	
HPC Control	66.4	66.4	66.4	66.4	66.4	0%
HPC 30-30	208.2	299.5	331.8	352.0	368.7	455%
HPC 30-60	327.0	551.9	628.6	669.8	697.0	950%
HPC 30-90	276.1	740.3	907.6	982.2	1023.3	1441%
HPC 60-30	248.1	616.9	793.5	920.5	1014.5	1428%
HPC 60-60	311.4	1038.0	1492.4	1749.8	1926.3	2801%
HPC 60-90	335.1	1079.6	1724.2	2186.3	2527.2	3706%

4.3. Synthetic Fibers

4.3.1. NPC with Synthetic Fibers

The average force-displacement curve of the normal concrete specimens with macro-synthetic fibers is presented in Figure 4.5. The first crack loads along with the ultimate loads are presented in Table 4.5, whereas the energy values in 5 mm intervals are summarized in Table 4.6.

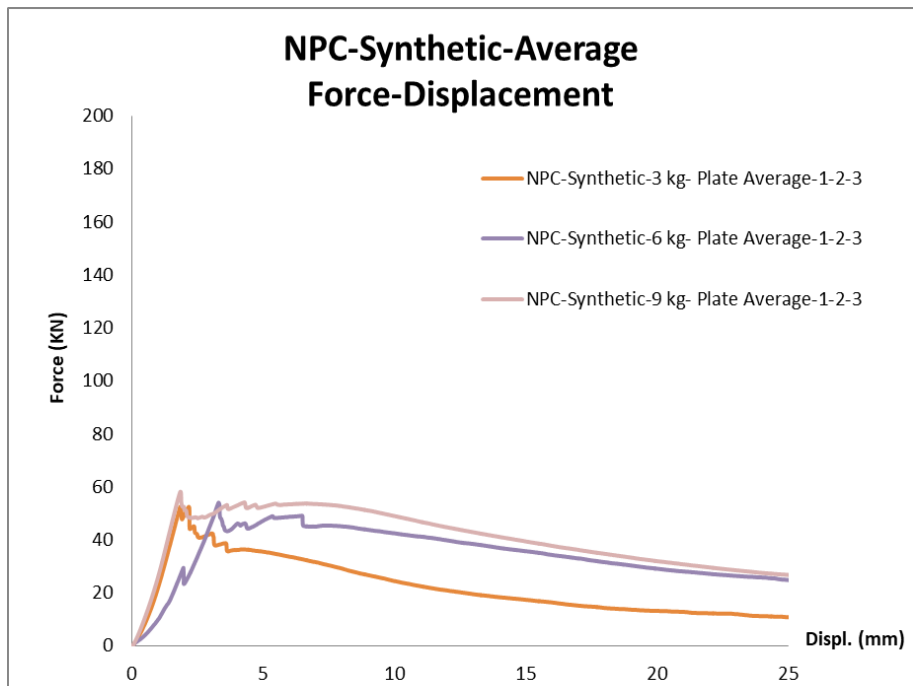


Figure 4.5. Average Force Displacement Graphs of NPC Synthetic

Table 4.5. Force-displacement values of NPC with Synthetic Fibers

	First crack load (kN)	Displacement at first crack (mm)	Ultimate load (kN)	Displacement at ultimate load (mm)	% increase in the ultimate load
NPC Control	48.2	2.5	48.2	2.5	0%
NPC 3 kg	61.0	2.1	61.0	2.1	27%
NPC 6 kg	19.4	1.3	63.8	4.4	32%
NPC 9 kg	64.1	2.7	64.1	2.7	33%

Table 4.6. Energy-displacement values of NPC with Synthetic Fibers

	Energy (Joule)					% increase in the ultimate load
	at 5 mm	at 10 mm	at 15 mm	at 20 mm	at 25 mm	
NPC Control	47.6	47.6	47.6	47.6	47.6	0%
NPC 3 kg	167.0	319.0	421.0	496.0	557.0	1070%
NPC 6 kg	151.0	380.0	575.0	737.0	872.0	1732%
NPC 9 kg	210.0	472.0	692.0	870.0	1016.0	2034%

4.3.2. HPC with Synthetic Fibers

The average force-displacement curve of the normal concrete specimens with macro-synthetic fibers is presented in Figure 4.6. The first crack loads along with the ultimate loads are presented in Table 4.5, whereas the energy values in 5 mm intervals are summarized in Table 4.6.

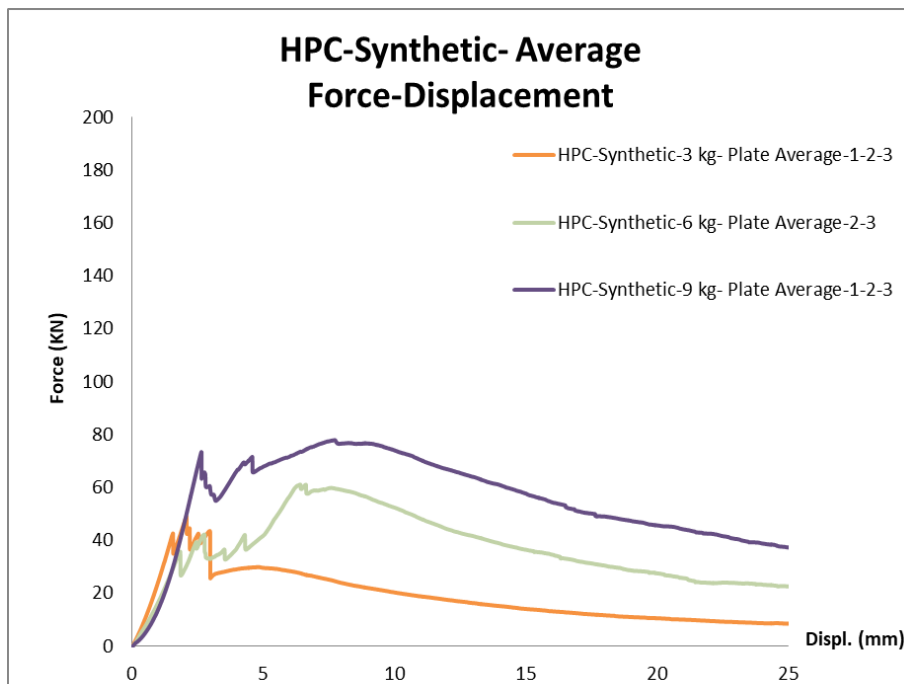


Figure 4.6. Average Force Displacement Graphs of HPC Synthetic

Table 4.7. Force-displacement values of HPC with Synthetic Fibers

	First crack load (kN)	Displacement at first crack (mm)	Ultimate load (kN)	Displacement at ultimate load (mm)	% increase in the ultimate load
HPC Control	75.2	1.9	75.2	1.9	0%
HPC 3 kg	63.2	2.2	63.2	2.2	-16%
HPC 6 kg	48.6	2.3	62.4	6.7	-17%
HPC 9 kg	75.6	2.7	87.0	5.0	16%

Table 4.8. Energy-displacement values of HPC with Synthetic Fibers

	Energy (Joule)					% increase in the ultimate load
	at 5 mm	at 10 mm	at 15 mm	at 20 mm	at 25 mm	
HPC Control	66.4	66.4	66.4	66.4	66.4	0%
HPC 3 kg	147.0	272.0	357.0	417.0	464.0	599%
HPC 6 kg	144.0	424.0	640.0	798.0	919.0	1284%
HPC 9 kg	224.0	596.0	924.0	1177.0	1385.0	1986%

Based on the test results, it can be said that as it was expected, the addition of fibers generally improved the ultimate load of the mixtures. With the increase of the fiber dosage, the ultimate load increased as well for the same fiber type and concrete group. Moreover, the increase in the fiber length has a significant effect on the performance of FRC. For the same amount of steel fiber, the ultimate load increased in an average of 33%. As for the synthetic fiber, although the ultimate loads were improved in most of the cases, this improvement significantly low compared to the one of steel fibers. This shows the clear effect of the fiber type on the performance of FRC. On the other hand, while the use of stronger concrete yielded higher strength of FRC; the percent improvements in the ultimate load were slightly larger for NPC mixtures. Moreover, for the first crack loads, the high-performance mixtures showed better results

compared to the normal performance mixtures, thus improving the concrete strength is crucial for obtaining such values as well as adding fibers to the mixtures.

4.4. Effect of Fiber Type and Dosage on Energy Absorption Capacity

4.4.1. Effect of Fiber Type and Dosage on NPC

In this section, the effects of fiber type and dosage on normal performance concrete specimens were analyzed. The average energy-displacement curves of the normal concrete specimens with 30 and 60 mm steel fibers and the macro synthetic fibers are presented in Figure 4.7 with different amounts.

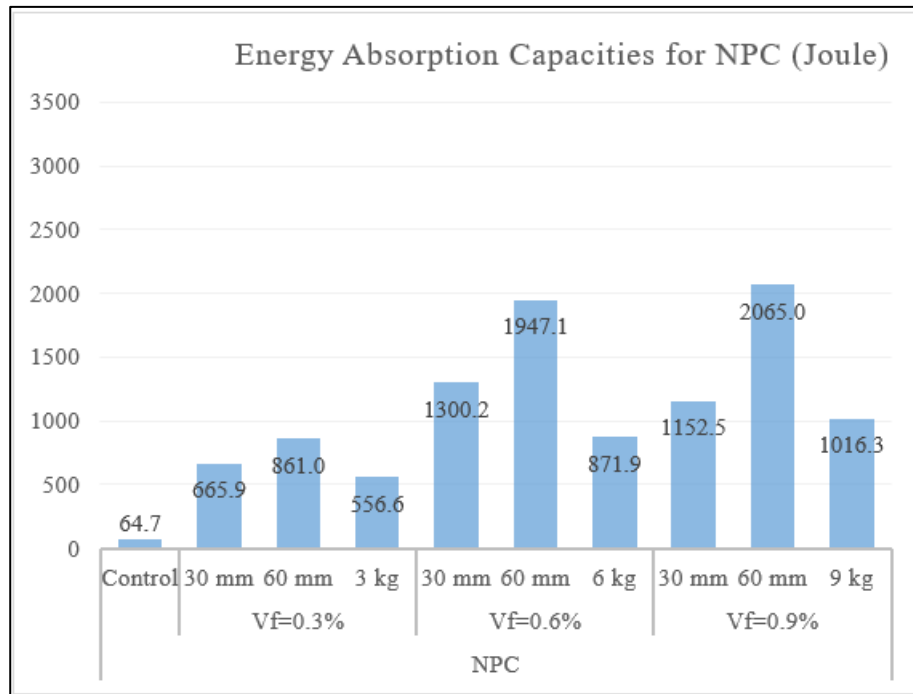


Figure 4.7. Average Energy Displacement Graphs of NPC

As can be seen, the addition of fibers significantly increased energy absorption capacity of the normal performance concrete. Moreover, with the increase of the fiber dosage, the ultimate energy values increased as well for the same fiber type and concrete group.

4.4.2. Effect of Fiber Type and Dosage on HPC

For the high-performance concrete specimens, the effect of fiber type and dosage were also investigated. The average energy-displacement curves of the high-performance concrete specimens with 30 and 60 mm steel fibers and the macro synthetic fibers are presented in Figure 4.8 with different amounts.

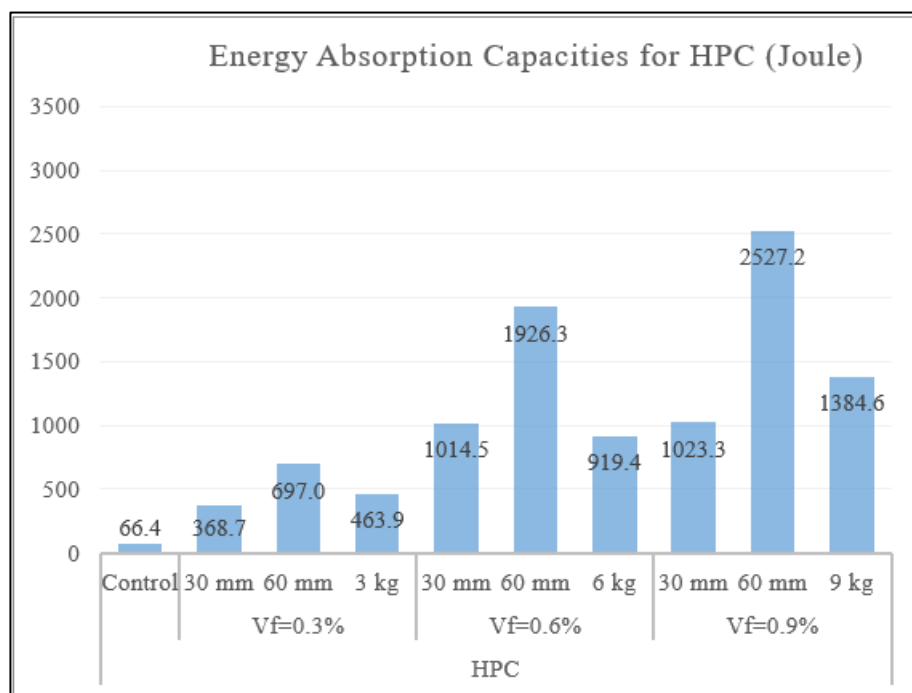


Figure 4.8. Average Energy Displacement Graphs of HPC

Similar to the normal performance concrete results, the addition of fibers significantly increased energy absorption capacity of the high-performance concrete. As for the synthetic fiber, it was observed that the used synthetic fibers were a match for the 30 mm steel fibers. Yet, steel fibers with 60 mm length reached the highest values. Therefore, this shows the effect of fiber type and length on the performance of FRC.

4.5. Effect of Concrete Strength on Energy Absorption Capacity

Since the experiments were conducted both on normal and high performance concrete, the effect of concrete strength on energy absorption capacities was also investigated.

Within this purpose, comparison graph of normal and high performance concrete specimens was presented in Figure 4.9.

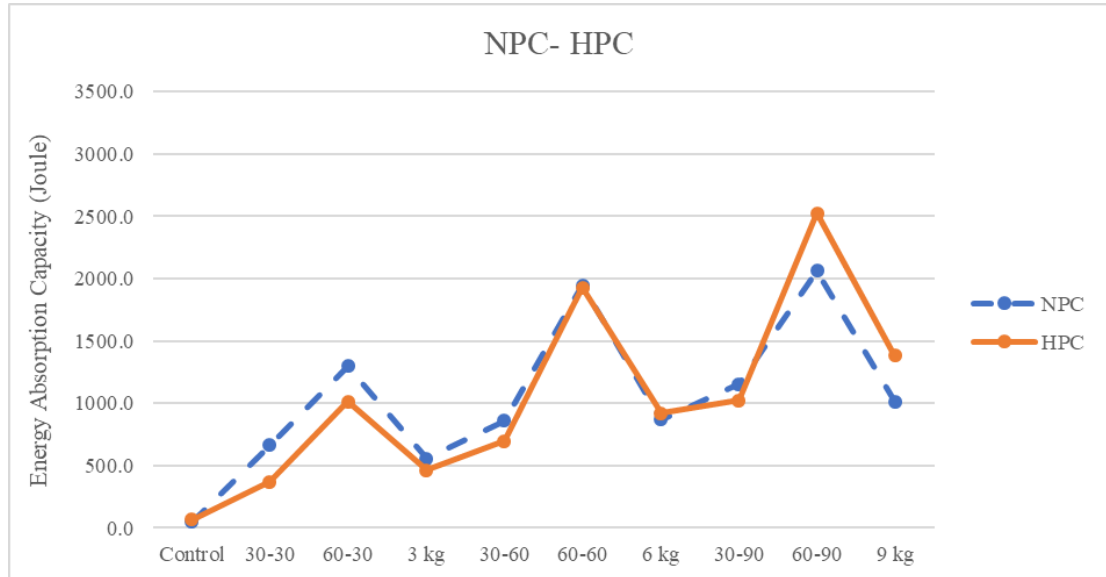


Figure 4.9. Comparison of Energy Displacement Graphs of NPC and HPC

Based on the test results, the conclusions made in the previous section are valid for this section. The addition of fibers has significantly increased the energy absorption values. With the increase of the fiber dosage, the ultimate energy values increased as well for the same fiber type and concrete group. This increase was almost linear for the HPC mixtures. Moreover, the increase in the fiber length almost doubled the energy values for the same amount of steel fiber. As for the synthetic fiber, although the ultimate loads were lower than the ones of steel fibers, from the energy absorption capacities point of view, the used synthetic fibers were a match for the 30 mm steel fibers. Yet, steel fibers with 60 mm length reached the highest values. This shows the effect of fiber type and length on the performance of FRC. On the other hand, when the energy results of NPC and HPC are compared to each other (for the same fiber type and amount), it can be seen that using a high-performance concrete is an over-design when a low amount of fiber is used. However, when the fiber amount is increased, the stronger concrete matrix will start giving a better performance.

4.6. Comparison of FRC with RC and ECC

For comparison reasons, two types of plate specimens were also produced, one made of Engineered Cementitious Concrete (ECC), a widely known cementitious composite prepared using 6 mm polyvinyl alcohol (PVA) fibers with a volume of 2%, and the second made of steel rebar reinforced concrete. As for the rebar reinforcement panels, NPC Control mix, which contains no fibers, was used along with steel reinforcements on both directions of the panel with a ratio of $\phi 12@100$ mm and length of 550 mm.

The load-displacement curves of the mentioned specimens are given in below Figure 4.10.

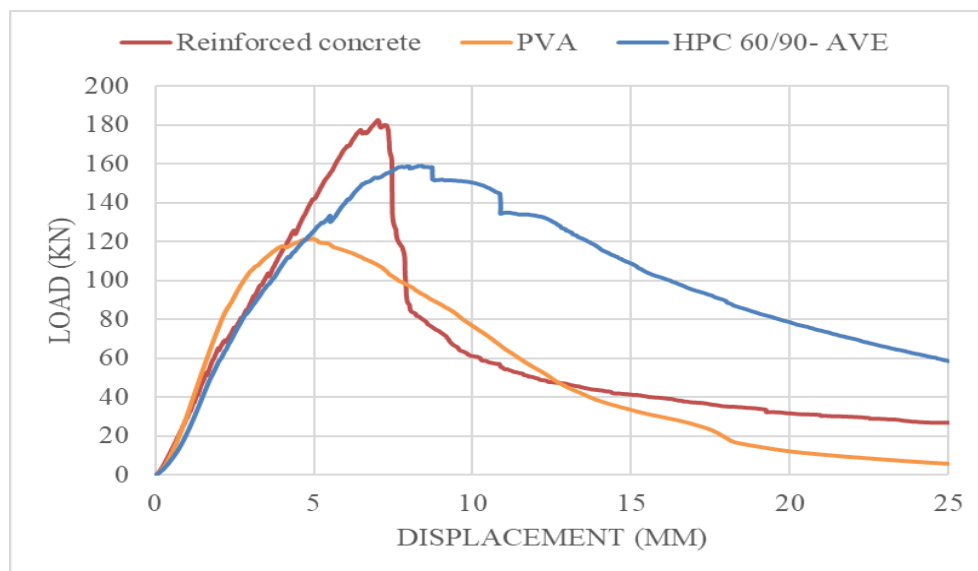


Figure 4.10. Load-Displacement Graph of HPC 60/90, RC and ECC

Although the ultimate load of the HPC 60/90 was lower than RC specimen, the post cracking behavior was greater than both RC and ECC.

In Figure 4.11, the curves of best-result high-performance steel fiber reinforced concrete, RC and ECC were demonstrated.

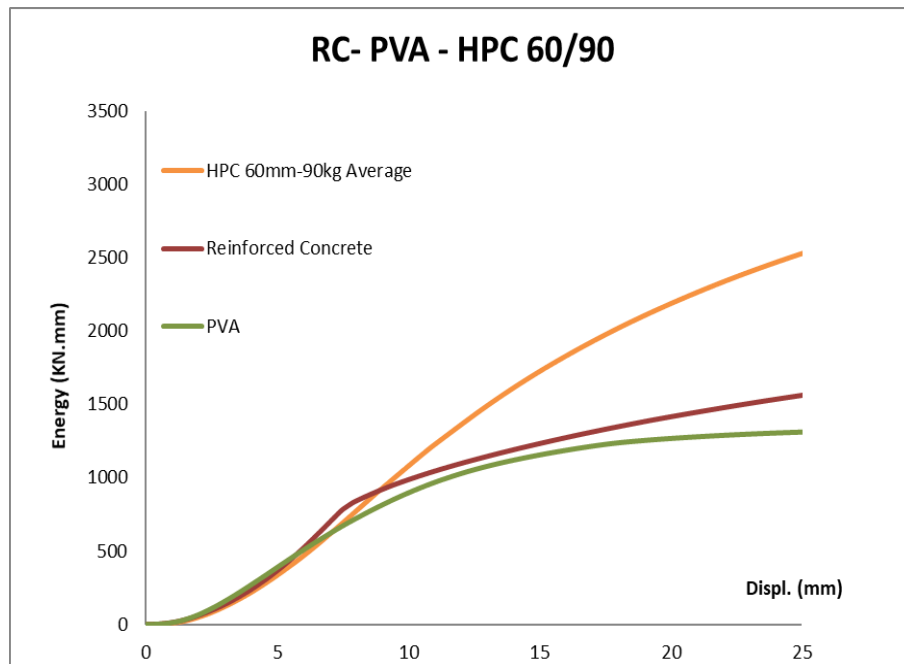


Figure 4.11. Average Energy Displacement Graphs of HPC 60/90, RC and PVA

It was observed that high-performance fiber reinforced concrete with 60 mm steel fibers showed better energy absorption capacity properties than the reinforced normal concrete and ECC.

4.7. Crack Patterns

Upon conducting the plate testing, the photograph of each crack specimen was taken in order to observe the cracking patterns. The photographs and figures of each specimen are given in Appendix C.

The average measured crack lengths of the specimens are shown in the Figure 4.12.

In order to calculate the crack lengths, the photographs of deformed specimens were taken and transferred to the AutoCAD software. Then, total length of the cracks for each specimen was measured with the “Total Spline Length” command on the mentioned software.

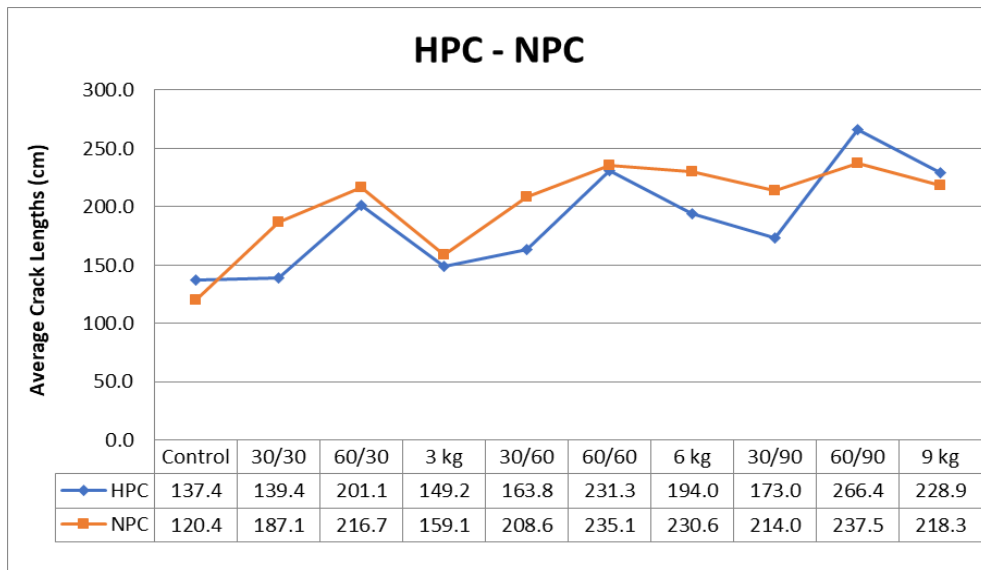


Figure 4.12. Average Crack Lengths for HPC and NPC

As shown in Figure 4.12, the increase in crack length was proportional to the increase in fiber dosage for both normal and high-performance specimens. The crack lengths were almost similar for specimens with 30 mm steel and synthetic fibers, whereas specimens with 60 mm steel showed longer crack lengths.

To observe the effect of fiber type and dosage on the crack lengths of the normal performance specimens, the lengths were measured for each specimen and shown in Figure 4.13, Figure 4.14 and Figure 4.15.

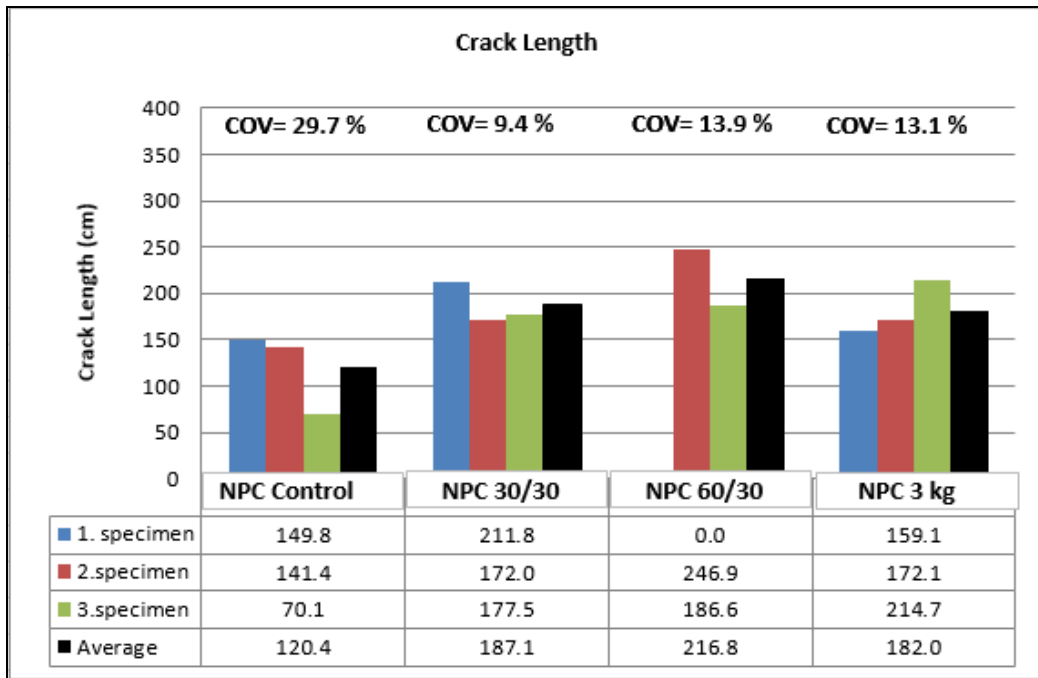


Figure 4.13. Crack Lengths of NPC with $V_f=0.3\%$

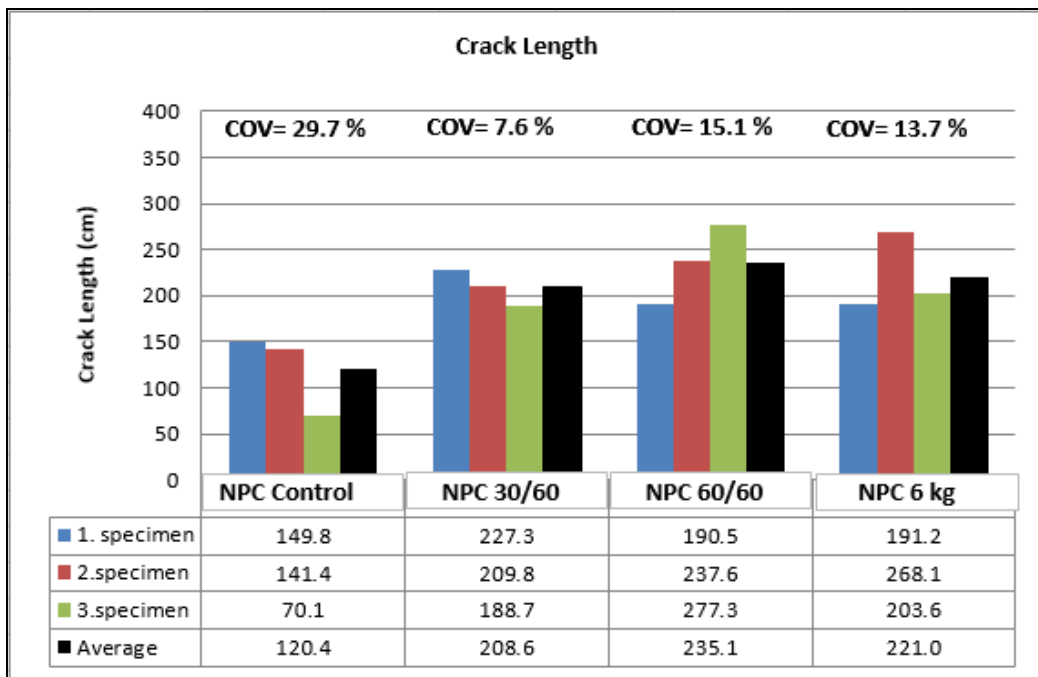


Figure 4.14. Crack Lengths of NPC with $V_f=0.6\%$

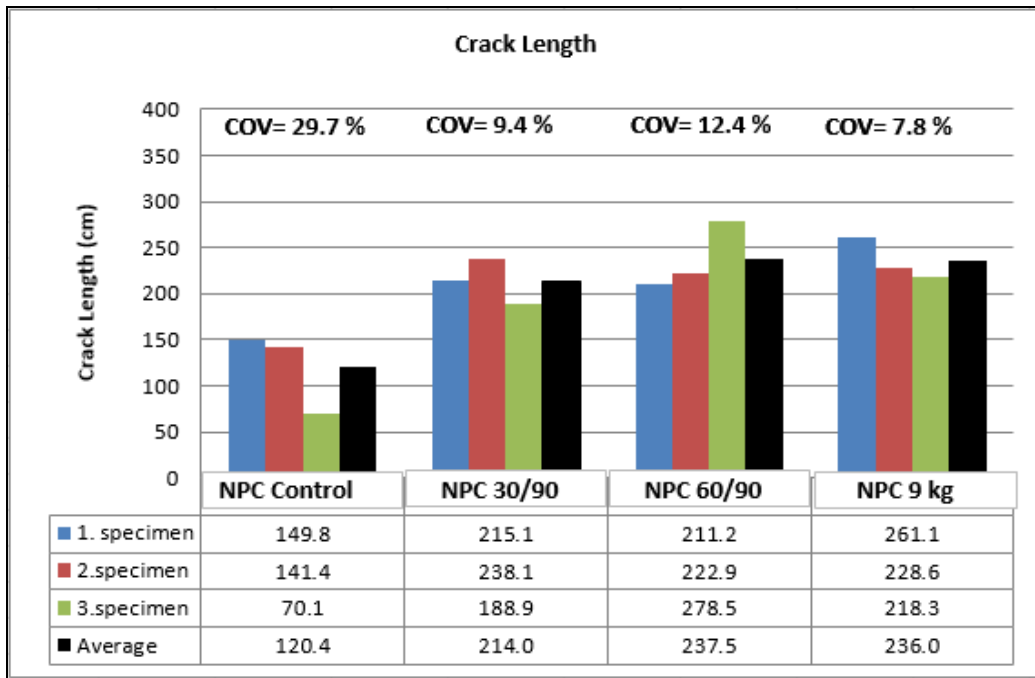


Figure 4.15. Crack Lengths of NPC with $V_f = 0.9\%$

Similarly, the effect of fiber type and dosage on the crack lengths of the high performance specimens is presented in Figure 4.16, Figure 4.17 and Figure 4.18.

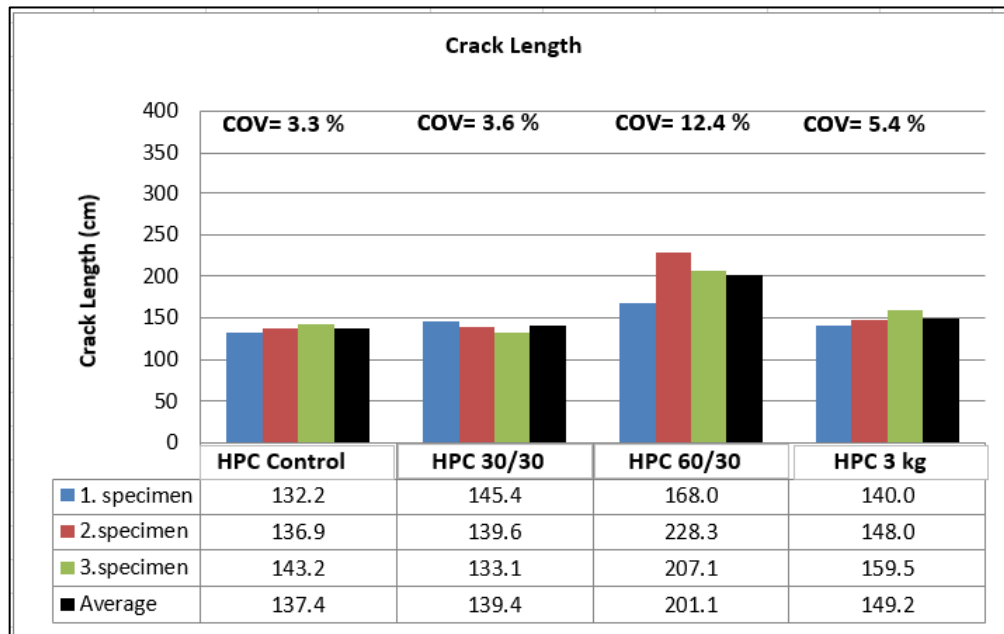


Figure 4.16. Crack Lengths of HPC with $V_f = 0.3\%$

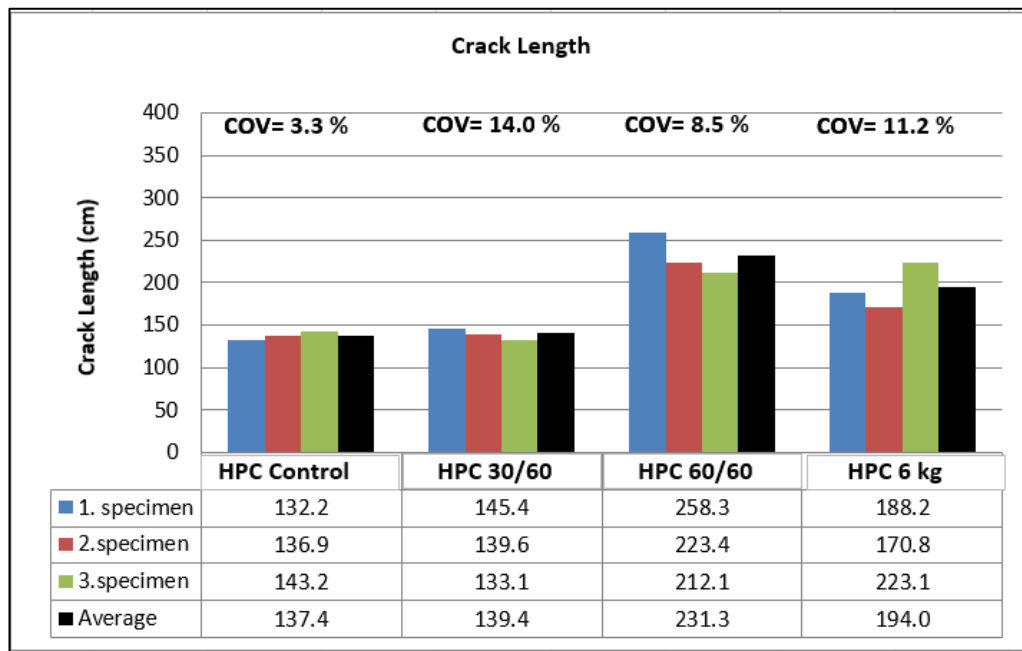


Figure 4.17. Crack Lengths of HPC with $V_f= 0.6\%$

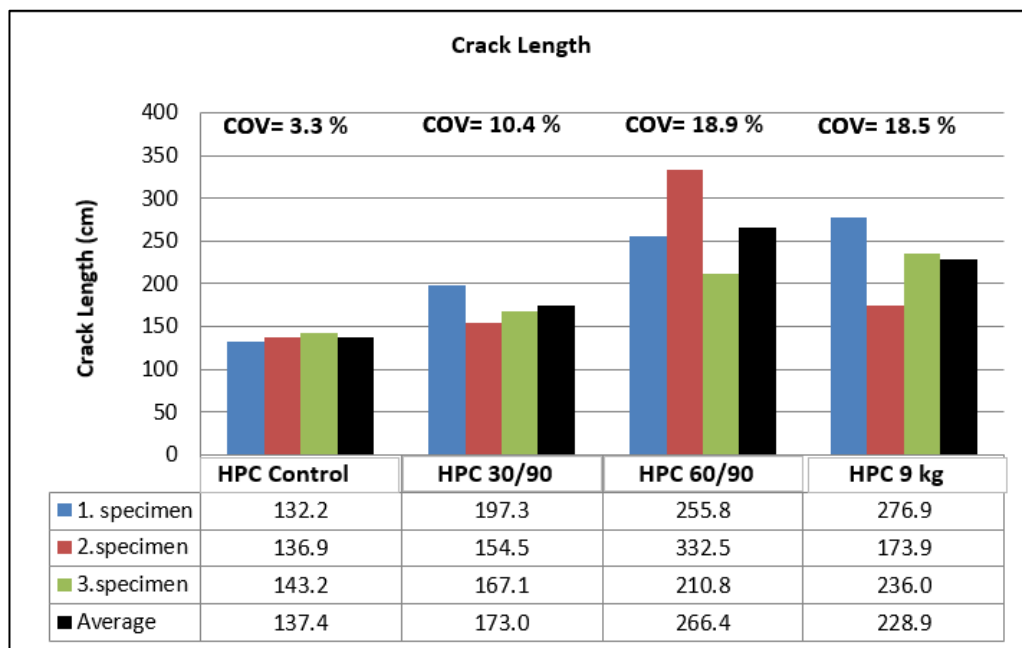


Figure 4.18. Crack Lengths of HPC with $V_f= 0.9\%$

In these experiments, it was observed that the crack patterns in the square plate specimens were not predictable. This may be due to the lack of determinate support conditions used in this test method.

The crack patterns were observed as analogic for both NPC and HPC specimens. It was noted that the increase in the fiber dosage resulted in an increase in the number of cracks. This may be due to the fact that the addition of fibers yielded a stronger concrete matrix by providing crack bridging.

CHAPTER 5

CONCLUSIONS & RECOMMENDATIONS

In this study, the effects of fiber type and amount on the performance of two FRC groups were investigated through centrally loaded plate test. Two types of steel fibers with same properties but different lengths along with one type of synthetic fibers were used. The load-displacement curves along with the energy absorption capacities at different displacement values for each specimen were determined. As per the test results obtained in these experiments, the below conclusions can be made:

1. It was observed that as the amount of fibers was increased, the workability of the concrete mixture was reduced. However, the use of chemical admixtures and silica fume in the high-performance concrete mixtures provided a better workability compared to the normal performance mixtures.
2. The addition of fibers to the concrete matrix increased the ultimate load and the energy absorption capacity (flexural toughness) in a significant way.
3. While this increase can be directly related to the amount of fibers used, the effects of fiber type and properties were crystal clear. The increase in steel fiber length, lead to an increase of 2 to 3 times in the energy absorption at 25 mm. Moreover, while the performance of steel fibers was better than the one of the synthetic fibers in the terms of the ultimate load, the energy absorption capacities of the 30 mm steel fibers and the 54 mm synthetic fibers were very close to each other.
4. Changing the properties of the concrete matrix can highly affect the behavior of the fibers. Surprisingly, using a stronger concrete decreased the energy absorption capacity of the FRC mixtures, especially for low fiber dosage amount. However, when the fiber amount was maximized, the concrete with higher compressive strength performed better. The reason for this might be the

optimum concrete matrix for each fiber dosage. In other words, while NPC matrix was able to put all or most the fibers in work for low fiber dosages, the brittle failure of the stronger HPC matrix prevented the low amount of fibers from acting completely. This mode changes when more fibers are used, thus a ductile behavior is reached for the stronger matrix with a larger amount of fibers.

5. Although the steel fibers showed better performance than synthetic fibers in terms of toughness, the synthetic fibers could also be used due to its economic advantages over the steel ones.
6. The crack patterns were observed as analogic for both NPC and HPC specimens. It was noted that the increase in the fiber dosage resulted in the increase in number of cracks. This may be due to the fact that the addition of fibers yielded a stronger concrete matrix by providing crack bridging.
7. In these experiments, it was observed that the crack patterns in the square plate specimens were not predictable. This may due to the lack of determinate support conditions used in this test method.

In the light of the conclusions reached from this study, for the further research studies, it could be suggested that:

1. The amount of the cementitious materials can be increased to be able to add larger amount of fibers.
2. New FRC batches with hybrid fibers (combinations of fibers of different size, types, or properties) can be produced and tested.
3. The concrete matrix can be modified to ensure getting a better workability.
4. The tests can be conducted on different specimens with different fiber dosages under constant workability conditions.

REFERENCES

- ACI Committee 544. (2002). Report on Fiber Reinforced Concrete. In *ACI Structural Journal* (Vol. 96).
- ACI Committee 544. (2010). ACI 544.5R-10 - Report on the Physical Properties and Durability of Fiber-Reinforced Concrete. In *ACI Structural Journal*.
- Ahmad, E. G., & Kshipra Kapoor, E. (2016). A Review Study on Use of Steel Fiber As Reinforcement Material With Concrete. *International Journal of Latest Research in Science and Technology*, 5(3), 37–39. Retrieved from <http://www.mnkjournals.com/ijlrst.htm>
- Al-Ghamdy, D. O., Wight, J. K., & Tons, E. (1994). Flexural Toughness of Steel Fiber Reinforced Concrete. *JKAU: Eng. Sci*, 6, 81–97. Retrieved from http://www.kau.edu.sa/Files/320/Researches/52581_22887.pdf
- Al-lami, K. A. (2015). *Experimental Investigation of Fiber Reinforced Concrete Beams*. <https://doi.org/10.13140/RG.2.1.1481.2885>
- Behbahani, H. P., Nematollahi, B., & Farasatpour, M. (2011). Steel Fiber Reinforced Concrete : A Review. *ICSECM 2011*. <https://doi.org/10.1007/978-981-10-2507-5>
- Brown, R., Shukla, a., & Natarajan, K. R. (2002). *Fiber Reinforcement of Concrete Structures*. (536101), 1–51.
- Buratti, N., Mazzotti, C., & Savoia, M. (2011). Post-cracking behaviour of steel and macro-synthetic fibre-reinforced concretes. *Construction and Building Materials*. <https://doi.org/10.1016/j.conbuildmat.2010.12.022>
- Erdogan, T. Y. (2005). Materials of Construction. In *ODTÜ GELİŞTİRME VAKFI YAYINCILIK VE İLETİŞİM A.Ş.*

- Eren, Ö., & Marar, K. (2010). Effect of steel fibers on plastic shrinkage cracking of normal and high strength concretes. *Materials Research*, 13(2), 135–141. <https://doi.org/10.1590/S1516-14392010000200004>
- Hasan, M. J., Afroz, M., & Mahmud, H. M. I. (2011). An Experimental Investigation on Mechanical Behavior of Macro Synthetic Fiber Reinforced Concrete. *Environmental Engineering*, 11(June), 18–23.
- Hetemoğlu, Y. O. (2018). *Effect of Test Methods on the Performance of Fiber Reinforced Concrete with Different Dosages and Matrices*. Middle East Technical University.
- Jiabiao, J. (2011). *Synthetic Structure Fibers for Toughness and Crack Control of Concrete*.
- Johnston, C. D., & Colin, D. (1982). Fibre Reinforced Concrete. *Progress in Concrete Technology CANMET, Energy, Mines and Resources*, 88(Reapproved), 215–236. Retrieved from <http://www.concrete.org/Publications/InternationalConcreteAbstractsPortal.aspx?m=details&i=3144>
- Juhász, K. P., & Schaul, P. (2019). The effect of age and testing method on the added fracture energy of fibre reinforced concrete. *Concrete Structures*. <https://doi.org/10.32970/cs.2019.1.4>
- Kahraman, B. (2015). Determining optimal polypropylene fiber dosages in sprayed concrete for mining and civil engineering applications. *Earth Sciences Research Journal*. <https://doi.org/10.15446/esrj.v19n1.40995>
- Kavitha, S., & Kala, T. F. (2018). *Experimental study on stress strain behavior of steel fibre reinforced concrete*. (January 2019), 29–33.
- Khaloo, A., & Kim, N. (1996). Mechanical Properties of Normal to High-Strength Steel Fiber-Reinforced Concrete. *Cement, Concrete and Aggregates*, 18(2), 92–97. <https://doi.org/10.4188/transjtnsj1965a.24.P621>

- Laning, A. (1992). *Synthetic fibers*.
- Lofgren, I. (2005). *Fibre-Reinforced Concrete for Industrial Construction*. Chalmers University of Technology.
- MacDonald, F., Clifford, N., Ballou, M., & Biddle, D. (2009). *Case Histories Using Synthetic Fiber Reinforced Concrete*. Retrieved from <http://dc.engconfintl.org/shotcrete/5/>
- Mohod, M. V. (2012). Performance of Steel Fiber Reinforced Concrete. *International Journal of Engineering and Science*, 1(12), 2278–4721. <https://doi.org/10.3141/2313-18>
- Nemati, K. M. (2015). University of Washington- Lecture Notes. In *CM 425 Concrete Technology- Fiber Reinforced Concrete*. <https://doi.org/10.4188/transjtmsj1965a.24.P621>
- NRMCA. (2014). CIP 24 - Synthetic Fibers for Concrete. *N/A*.
- Öztürk, Ç. (2018). *High Performance Macro Synthetic Fiber Reinforced Concrete*.
- Roesler, J., Bordelon, A., Brand, A. S., & Amirkhanian, A. (2019). *Fiber-Reinforced Concrete for Pavement Overlays: Technical Overview, Report InTrans Project 15-532*. (March).
- Sarzalejo, A. G., Rossi, B., Perri, G., Winterberg, R., & Aristeguieta, R. E. P. (2014). *Fibers as Structural Element for the Reinforcement of Concrete: technical manual*.
- Shah, S., & Rangan, B. (1971). Fiber reinforced concrete properties. *ACI Journal Proceedings*, (68), 126–137. Retrieved from <http://www.concrete.org/Publications/InternationalConcreteAbstractsPortal.aspx?m=details&i=11299>
- Sinha, D. A. (2012). *Engineering Strength Characteristics of hybrid fibre reinforced concrete*. (2277), 71–73.

- Song, P. S., & Hwang, S. (2004). Mechanical properties of high-strength steel fiber-reinforced concrete. *Construction and Building Materials*, 18(9), 669–673. <https://doi.org/10.1016/j.conbuildmat.2004.04.027>
- Thomas, J., & Ramaswamy, A. (2007). Mechanical Properties of Steel Fiber-Reinforced Concrete. *Journal of Materials in Civil Engineering*, 19(5), 385–392. [https://doi.org/10.1061/ASCE0899-1561\(2007\)19:5\(385\)](https://doi.org/10.1061/ASCE0899-1561(2007)19:5(385))
- Wang, Y., Backer, S. J., & Li, V. C. (1987). An experimental study of synthetic fibre reinforced cementitious composites. *Journal of Materials Science*, 22(12), 4281–4291.
- Zollo, R. F. (1997). Fiber-reinforced concrete: an overview after 30 years of development. *Cement and Concrete Composites*, 19(2), 107–122. [https://doi.org/10.1016/S0958-9465\(96\)00046-7](https://doi.org/10.1016/S0958-9465(96)00046-7)

APPENDICES

A. FORCE-DISPLACEMENT TEST RESULTS

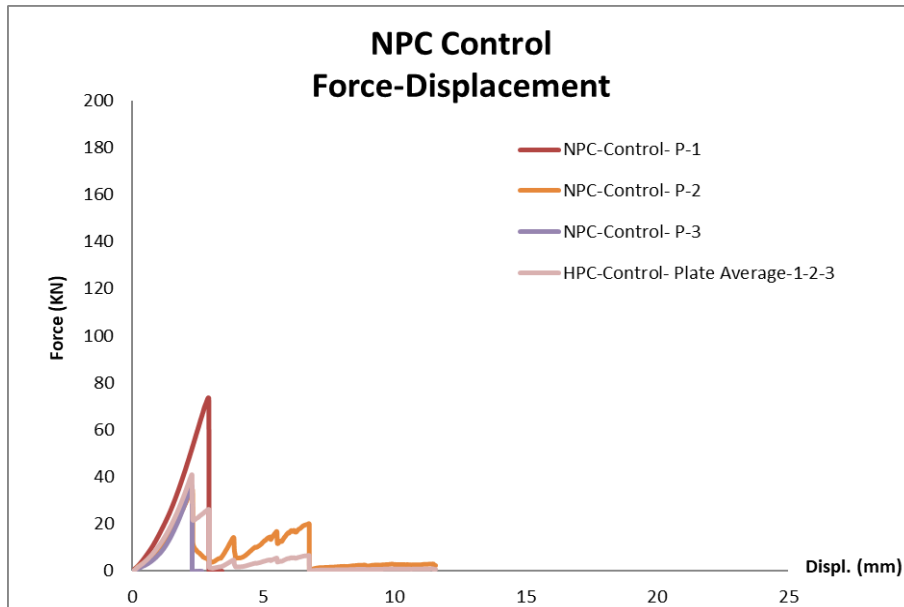


Figure A.1. Force Displacement Graphs of NPC Control

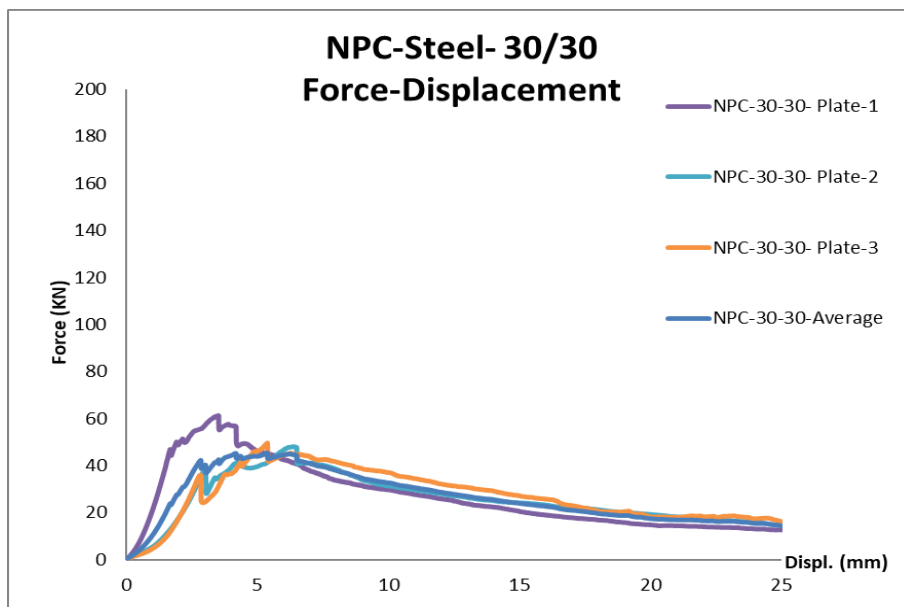


Figure A.2. Force Displacement Graphs of NPC Steel 30/30

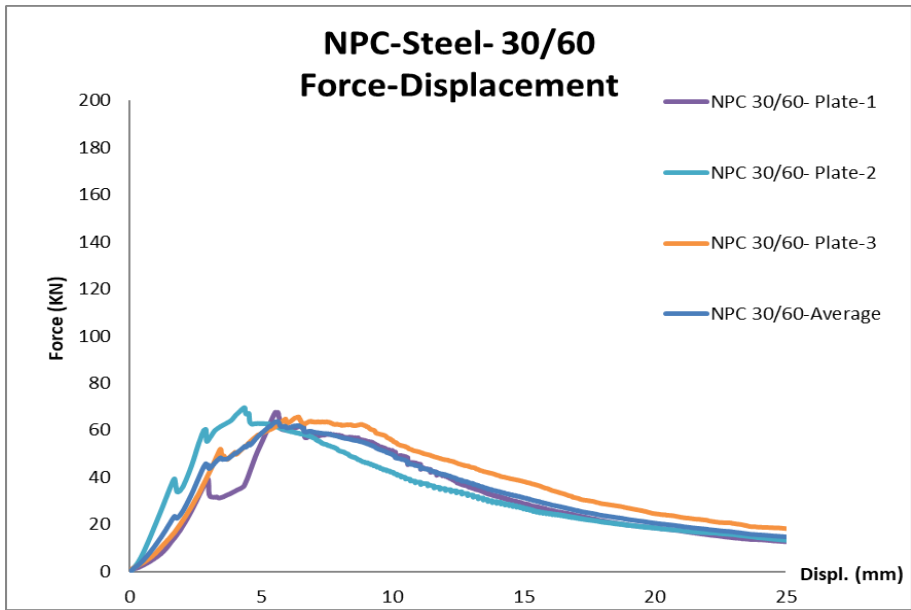


Figure A.3. Force Displacement Graphs of NPC Steel 30/60

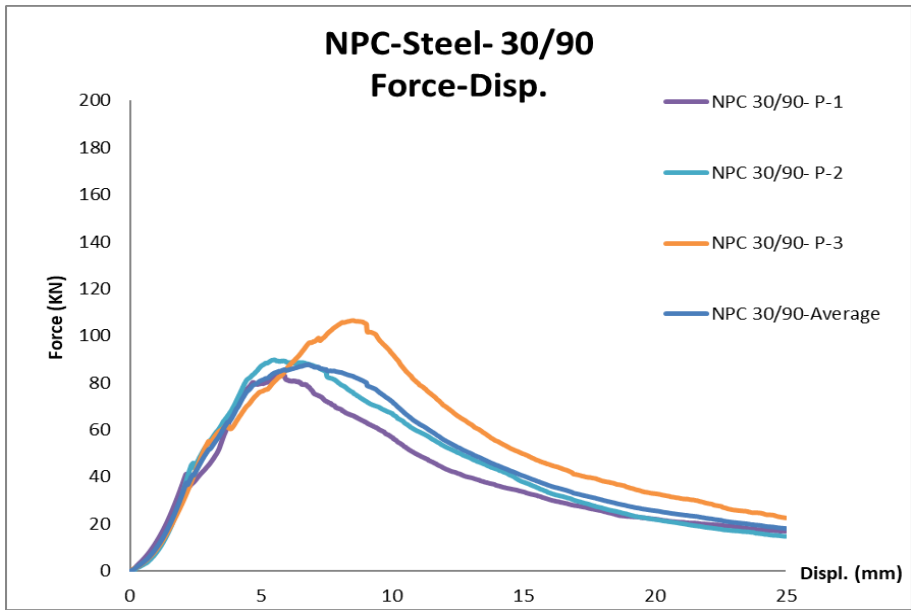


Figure A.4. Force Displacement Graphs of NPC Steel 30/90

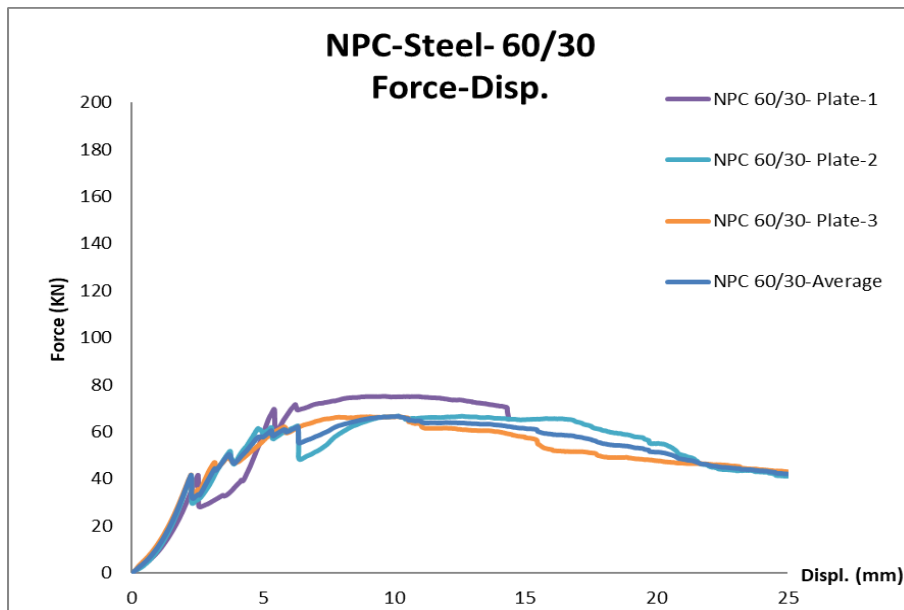


Figure A.5. Force Displacement Graphs of NPC Steel 60/30

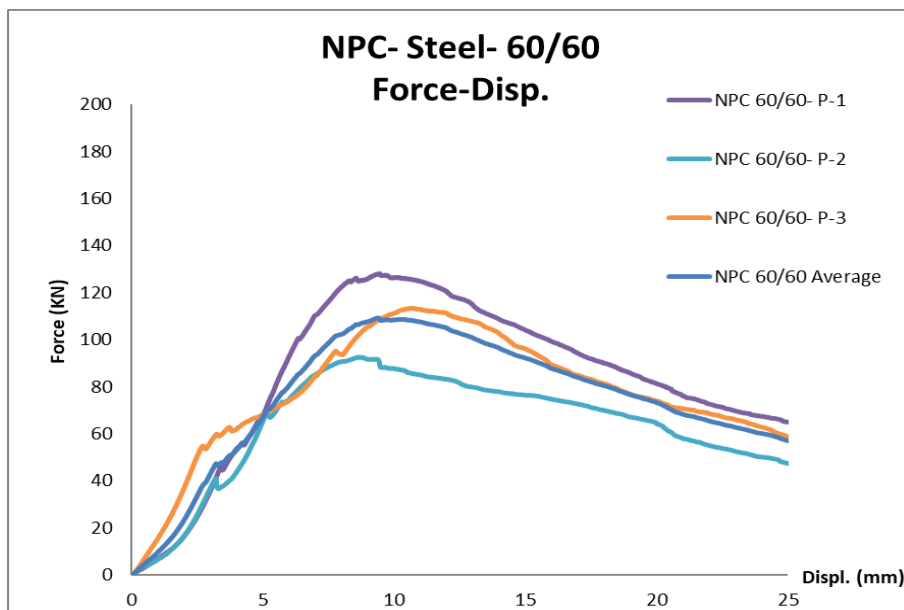


Figure A.6. Force Displacement Graphs of NPC Steel 60/60

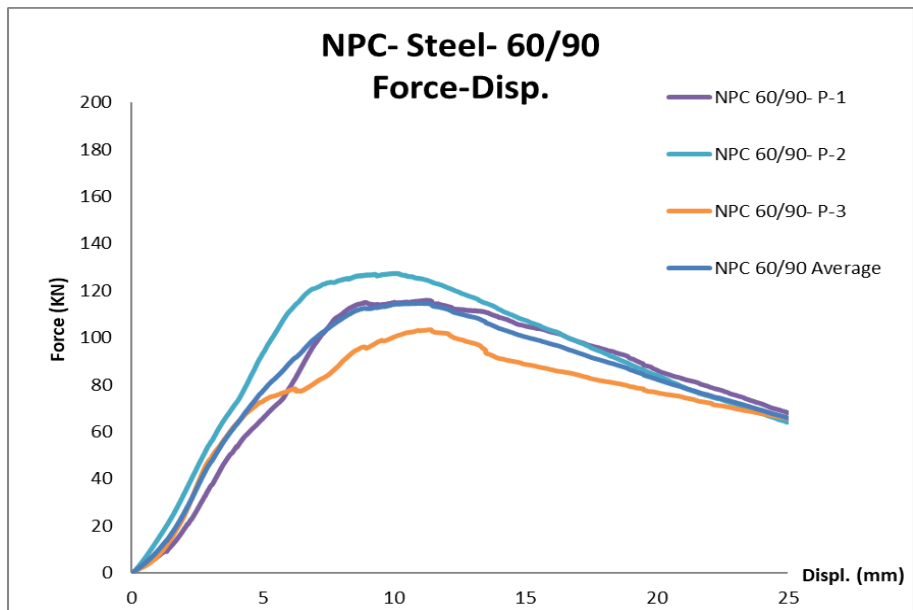


Figure A.7. Force Displacement Graphs of NPC Steel 60/90

Table A.1. Force Displacement Test Results of NPC Steel

		Max Force	Displacement At Max Force	Cracking Force	Displacement At Cracking Force
NPC Control	1	73.6	2.9	73.6	2.9
	2	34.9	2.3	34.9	2.3
	3	36.1	2.3	36.1	2.3
	Ave.	48.2	2.5	48.2	2.5
	St. Dev.	45.7	15.0	45.7	15.0
NPC 30-30	1	61.3	3.5	45.8	1.6
	2	48.1	6.4	38.3	3.0
	3	49.6	5.4	39.4	2.9
	Ave.	53.0	5.1	41.2	2.5
	St. Dev.	13.6	28.6	9.8	30.1
NPC 30-60	1	67.7	5.6	38.2	3.0
	2	69.6	4.4	59.3	2.9
	3	65.6	6.4	63.0	6.5
	Ave.	67.6	5.5	53.5	4.1
	St. Dev.	2.9	19.0	25.0	50.1
NPC 30-90	1	83.2	5.8	40.7	2.2
	2	89.8	5.8	44.7	2.3
	3	106.5	8.5	53.8	2.9
	Ave.	93.2	6.7	46.4	2.5
	St. Dev.	12.9	23.3	14.5	16.4
NPC 60-30	1	75.1	9.7	39.3	2.5
	2	66.5	10.0	39.9	2.2
	3	66.3	10.0	45.8	3.2
	Ave.	69.3	9.9	41.6	2.6
	St. Dev.	7.2	2.0	8.6	18.9
NPC 60-60	1	128.1	9.5	44.8	3.3
	2	90.7	8.1	40.0	3.2
	3	111.9	10.1	51.1	2.5
	Ave.	110.2	9.2	52.8	2.6
	St. Dev.	17.0	11.2	10.5	17.2
NPC 60-90	1	116.0	11.3	-	-
	2	127.4	10.1	-	-
	3	103.4	11.4	77.5	6.0
	Ave.	115.6	10.9	77.5	6.0
	St. Dev.	10.4	6.8	-	-

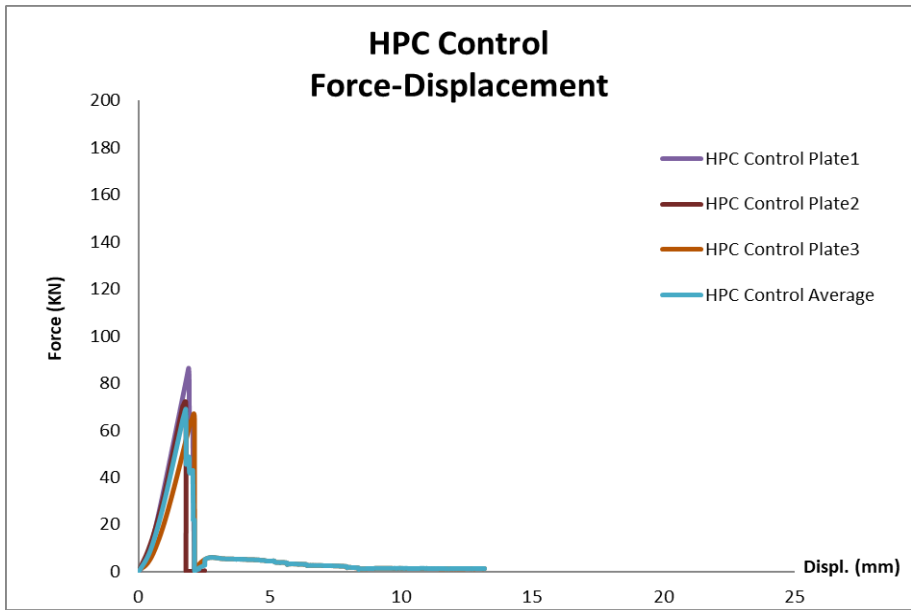


Figure A.8. Force Displacement Graphs of HPC Control

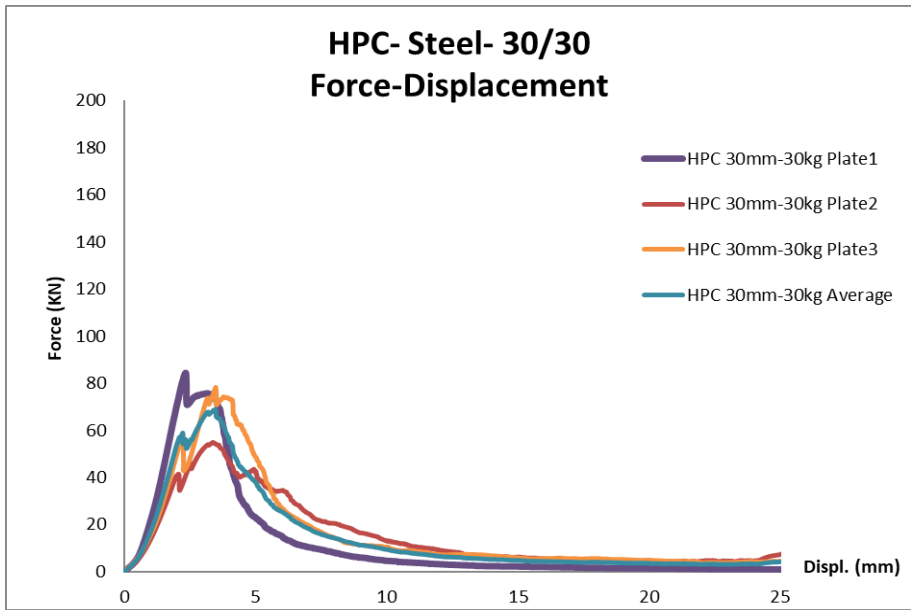


Figure A.9. Force Displacement Graphs of HPC Steel 30/30

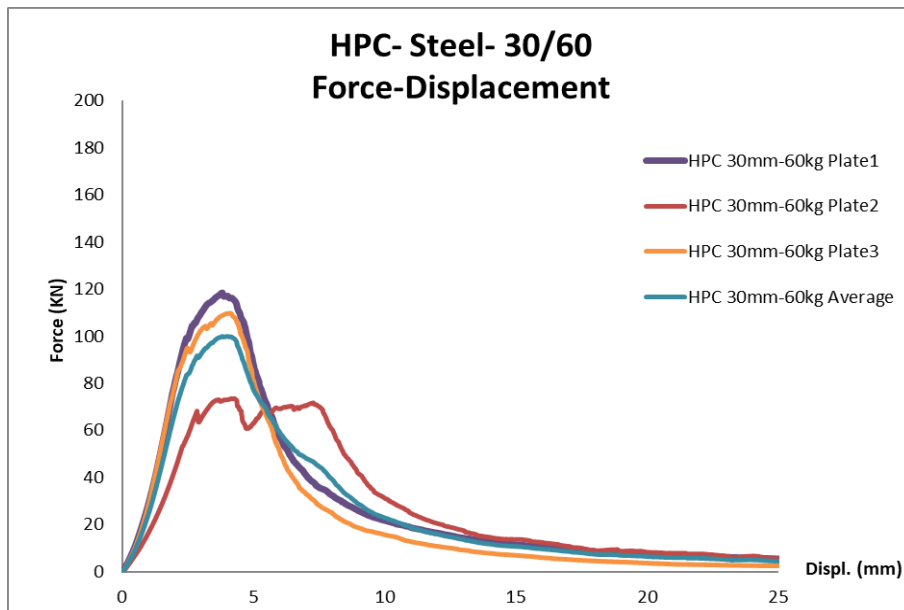


Figure A.10. Force Displacement Graphs of HPC Steel 30/60

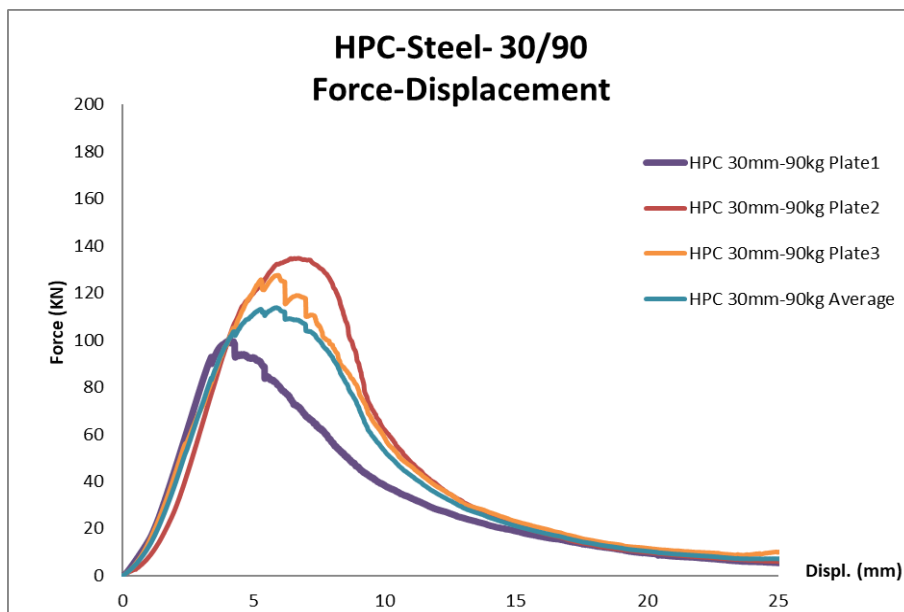


Figure A.11. Force Displacement Graphs of HPC Steel 30/90

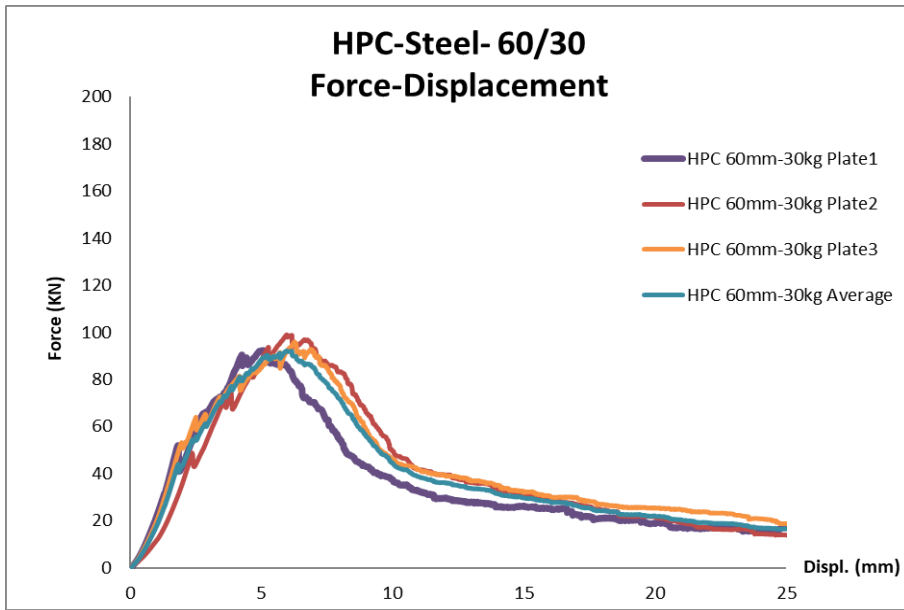


Figure A.12. Force Displacement Graphs of HPC Steel 60/30

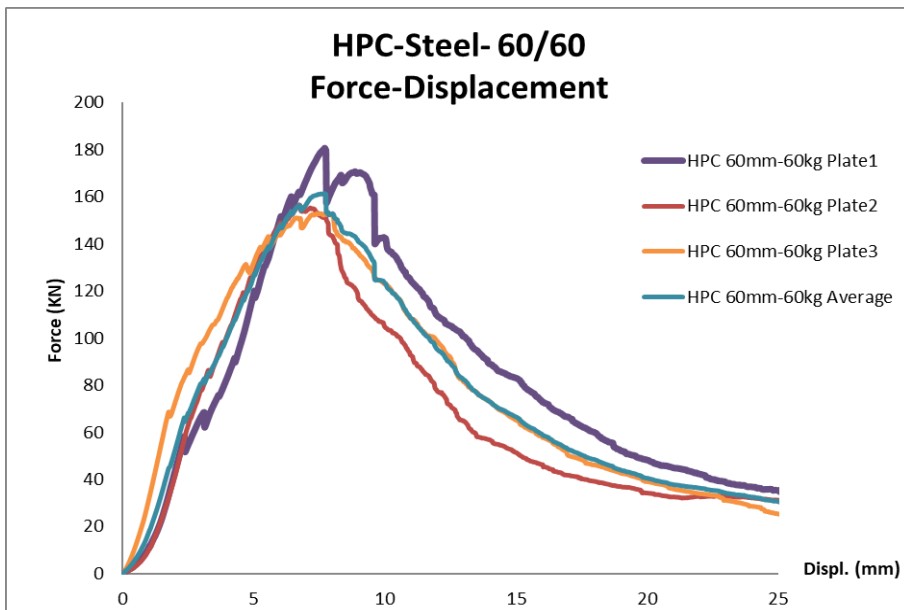


Figure A.13. Force Displacement Graphs of HPC Steel 60/60

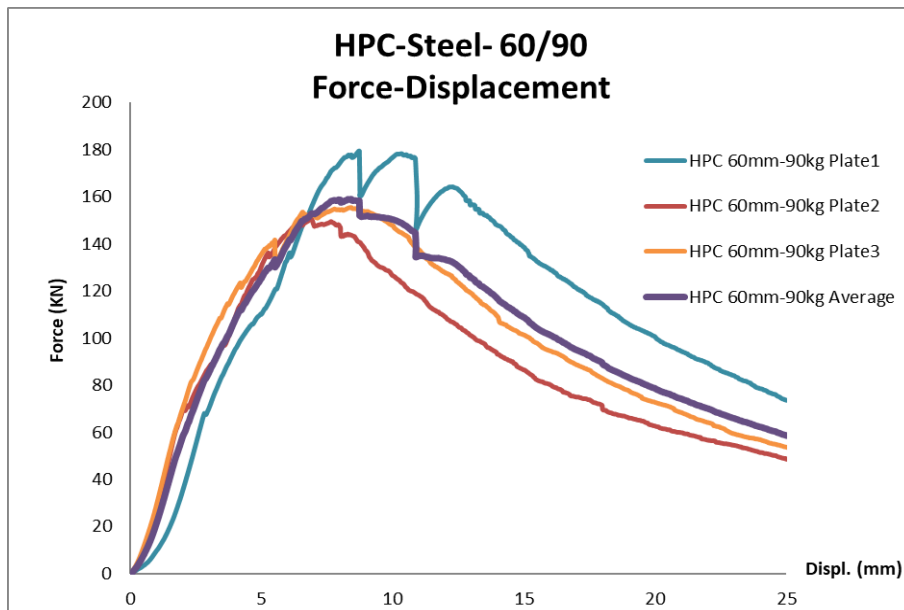


Figure A.14. Force Displacement Graphs of HPC Steel 60/90

Table A.2. Force Displacement Test Results of HPC Steel

		Max Force	Displacement At Max Force	Cracking Force	Displacement At Cracking Force
HPC Control	1	86.5	1.9	-	-
	2	72.1	1.8	-	-
	3	67.1	2.1	-	-
	Ave.	75.2	1.9	-	-
	St. Dev.	13.4	7.9	-	-
HPC 30-30	1	84.4	2.3	-	-
	2	54.9	3.4	41.0	2.0
	3	78.3	3.5	58.5	2.2
	Ave.	72.5	3.1	49.8	2.1
	St. Dev.	21.5	21.7	24.9	6.7
HPC 30-60	1	118.4	3.8	-	-
	2	73.5	4.3	68.2	2.9
	3	109.8	4.1	94.7	2.5
	Ave.	100.6	4.1	81.5	2.7
	St. Dev.	23.7	6.2	23.0	10.5
HPC 30-90	1	100.1	4.1	92.8	3.4
	2	134.8	6.7	-	-
	3	127.6	5.9	125.4	5.3
	Ave.	120.8	5.6	109.1	4.4
	St. Dev.	15.2	23.9	21.1	30.9
HPC 60-30	1	92.3	5.1	52.0	1.8
	2	99.0	6.0	48.6	2.3
	3	95.6	6.3	52.3	1.9
	Ave.	95.7	5.8	51.0	2.0
	St. Dev.	3.5	10.8	4.0	13.2
HPC 60-60	1	180.7	7.7	58.3	2.4
	2	156.6	6.7	86.3	3.2
	3	152.9	7.4	68.6	1.8
	Ave.	163.4	7.3	71.1	2.5
	St. Dev.	9.2	7.1	19.9	28.5
HPC 60-90	1	179.5	8.7	68.1	2.8
	2	150.7	6.9	69.3	2.0
	3	155.5	8.4	123.4	4.2
	Ave.	161.9	8.0	86.9	3.0
	St. Dev.	9.5	12.1	36.3	37.1

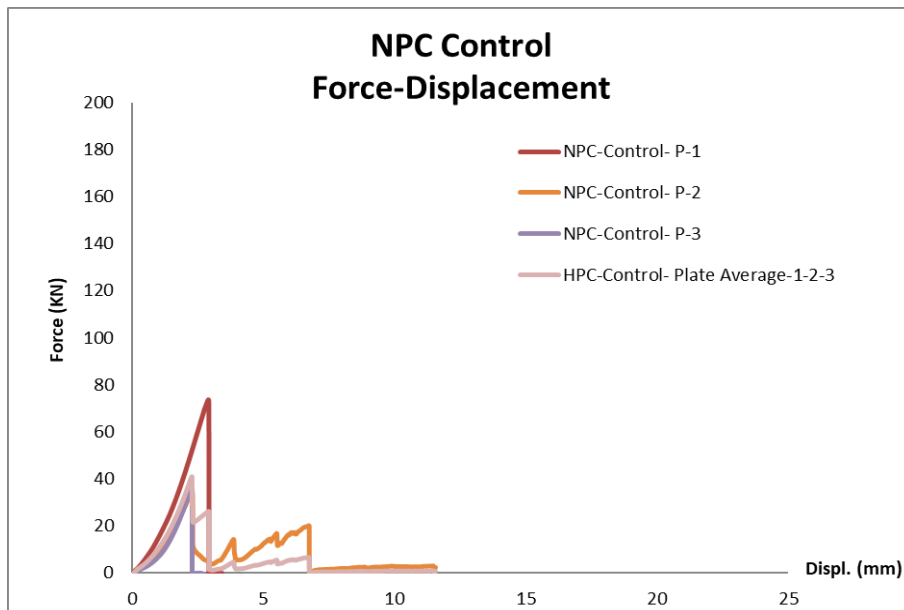


Figure A.15. Force Displacement Graphs of NPC Synthetic Control

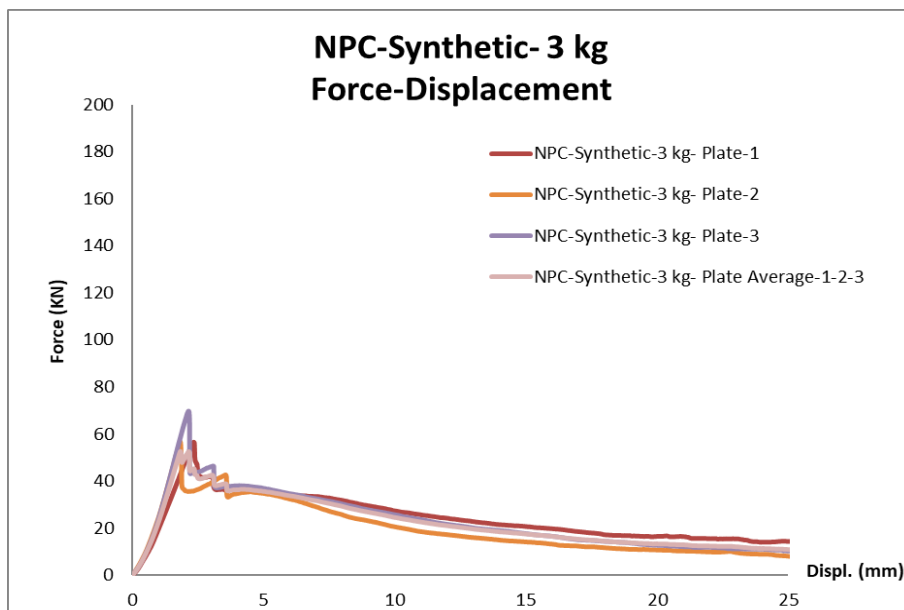


Figure A.16. Force Displacement Graphs of NPC Synthetic 3 kg

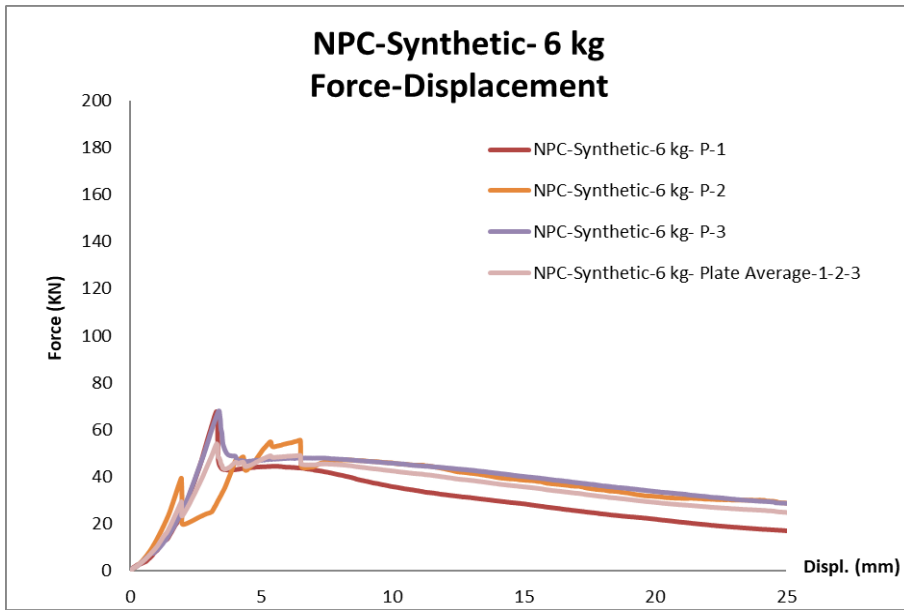


Figure A.17. Average Force Displacement Graphs of NPC Synthetic 6 kg

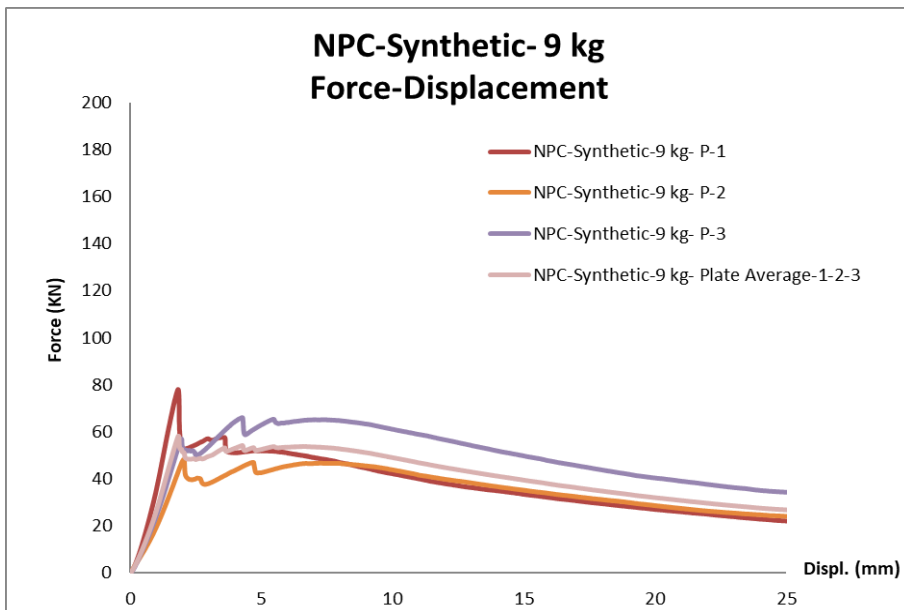


Figure A.18. Average Force Displacement Graphs of NPC Synthetic 9 kg

Table A.3. Force Displacement Test Values of NPC Synthetic

		Max Force	Displacement At Max Force	Cracking Force	Displacement At Cracking Force
NPC Control	1	73.6	2.9	73.6	2.9
	2	34.9	2.3	34.9	2.3
	3	36.1	2.3	36.1	2.3
	Ave.	48.2	2.5	48.2	2.5
	St. Dev.	45.7	15.0	45.7	15.0
NPC 3 kg	1	56.5	2.3	56.5	2.3
	2	56.7	1.8	56.7	1.8
	3	69.7	2.1	69.7	2.1
	Ave.	61.0	2.1	61.0	2.1
	St. Dev.	12.4	12.4	12.4	12.4
NPC 6 kg	1	67.8	3.3	12.9	1.3
	2	55.6	6.5	39.5	1.9
	3	68.1	3.4	5.8	0.8
	Ave.	63.8	4.4	19.4	1.3
	St. Dev.	11.2	41.5	91.7	41.3
NPC 9 kg	1	78.0	1.8	78.0	1.8
	2	48.3	2.0	48.3	2.0
	3	66.1	4.3	66.1	4.3
	Ave.	64.1	2.7	64.1	2.7
	St. Dev.	23.4	50.0	23.4	50.0

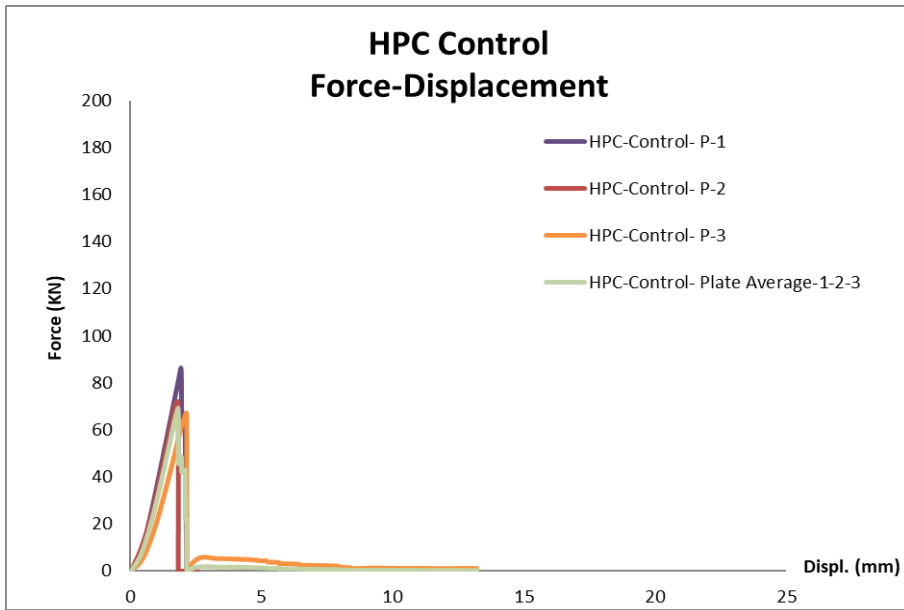


Figure A.19. Force Displacement Graphs of HPC Synthetic Control

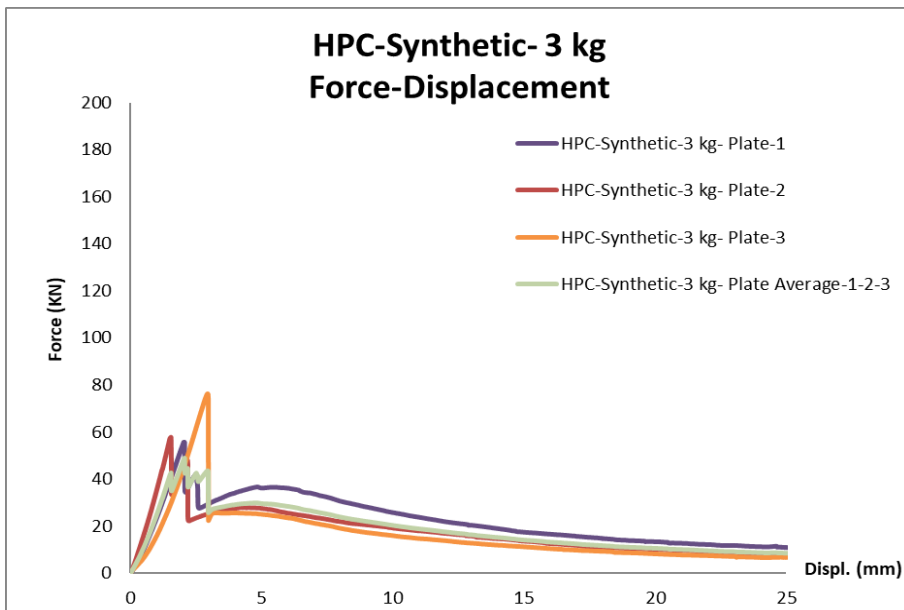


Figure A.20. Force Displacement Graphs of HPC Synthetic 3 kg

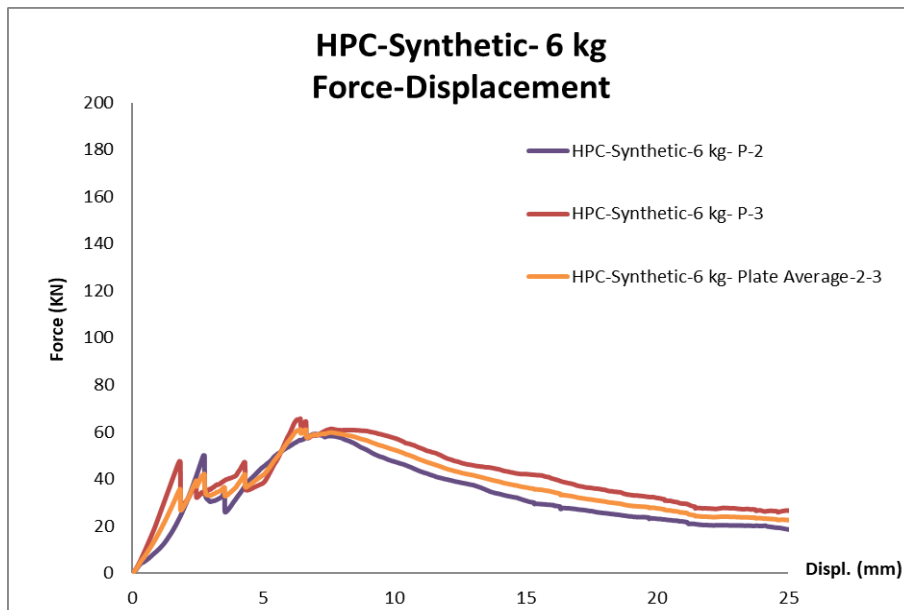


Figure A.21. Force Displacement Graphs of HPC Synthetic 6 kg

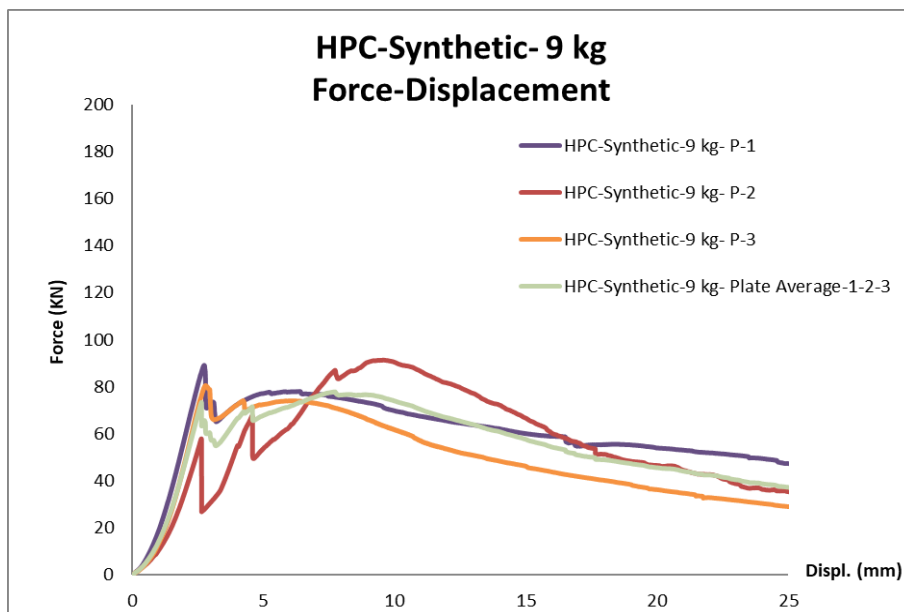


Figure A.22. Force Displacement Graphs of HPC Synthetic 9 kg

Table A.4. Force Displacement Test Values of HPC Synthetic

		Max Force	Displacement At Max Force	Cracking Force	Displacement At Cracking Force
HPC Control	1	86.5	1.9	-	-
	2	72.1	1.8	-	-
	3	67.1	2.1	-	-
	Ave.	75.2	1.9	-	-
	St. Dev.	13.4	7.9	-	-
HPC 3 kg	1	55.7	2.0	55.7	2.0
	2	57.8	1.5	57.8	1.5
	3	76.2	2.9	76.2	2.9
	Ave.	63.2	2.2	63.2	2.2
	St. Dev.	17.9	32.5	17.9	32.5
HPC 6 kg	1	-	-	-	-
	2	59.1	7.0	50.1	2.7
	3	65.7	6.4	47.1	1.8
	Ave.	62.4	6.7	48.6	2.3
	St. Dev.	7.4	5.9	4.3	27.9
HPC 9 kg	1	89.1	2.7	89.1	2.7
	2	91.4	9.6	57.2	2.6
	3	80.6	2.8	80.6	2.8
	Ave.	87.0	5.0	75.6	2.7
	St. Dev.	6.6	78.1	21.9	2.9

B. ENERGY-DISPLACEMENT TEST RESULTS

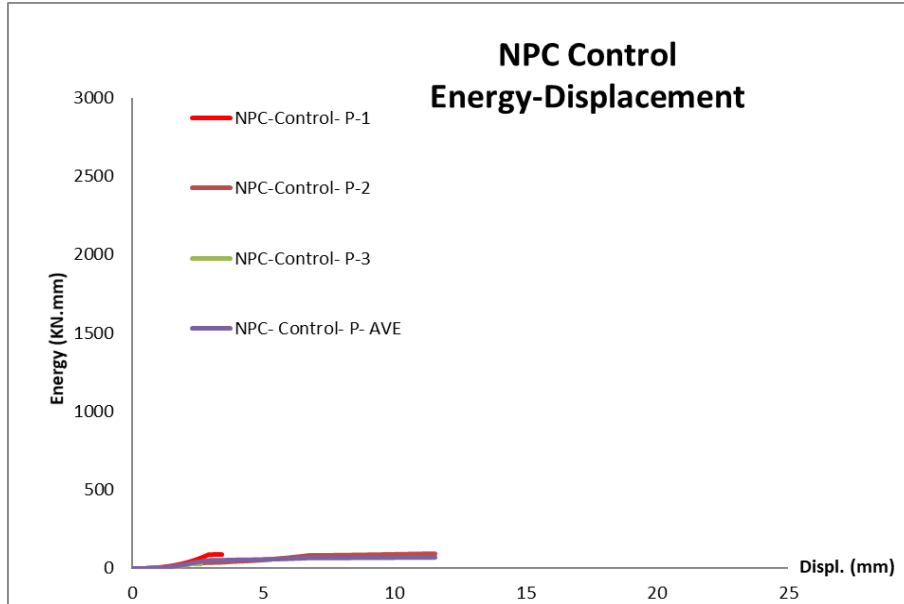


Figure B.23. Energy Displacement Graphs of NPC Control

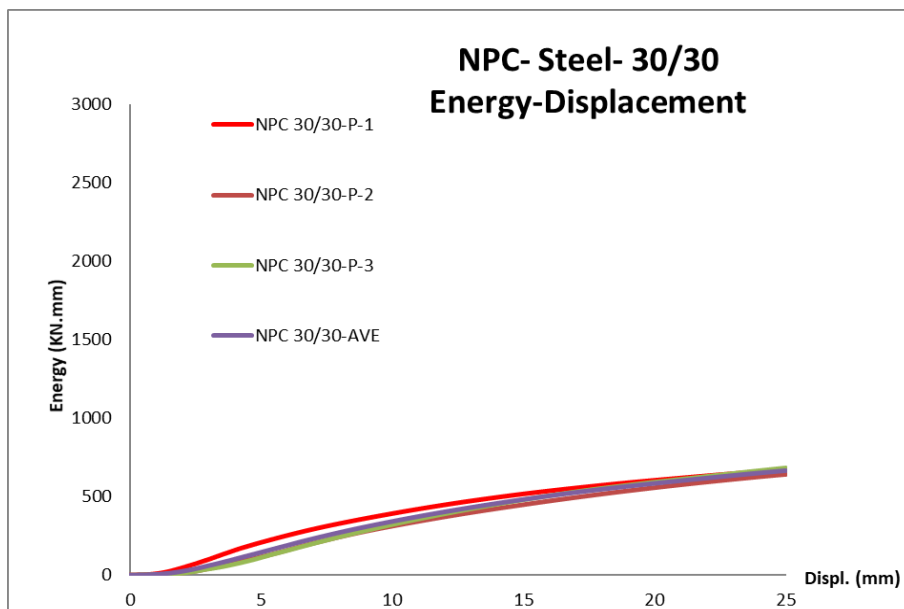


Figure B.24. Energy Displacement Graphs of NPC Steel 30/30

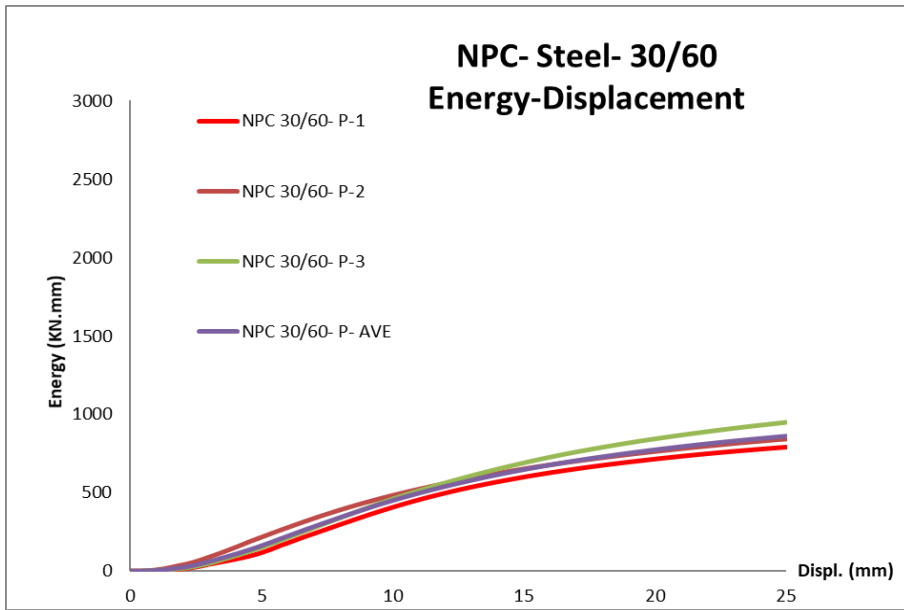


Figure B.25. Energy Displacement Graphs of NPC Steel 30/60

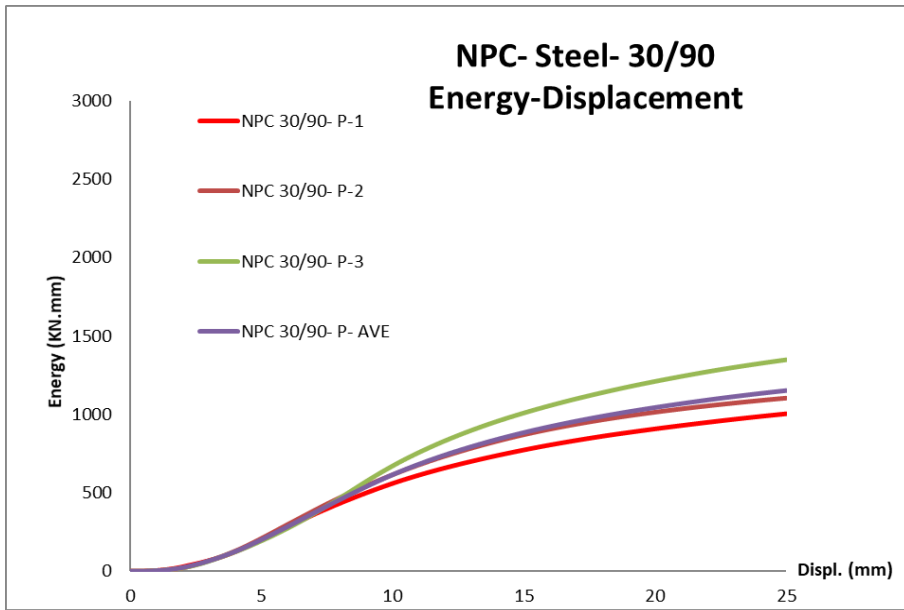


Figure B.26. Energy Displacement Graphs of NPC Steel 30/90

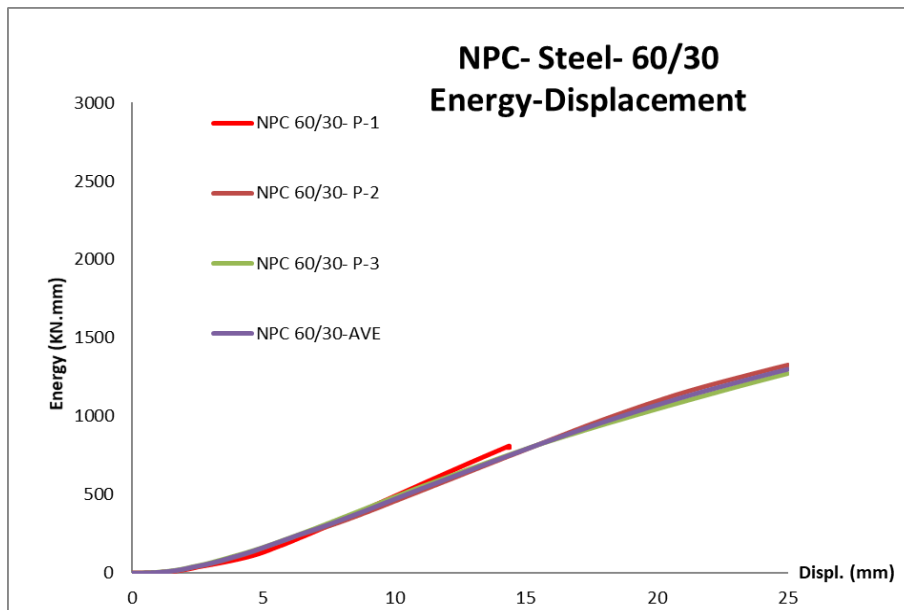


Figure B.27. Energy Displacement Graphs of NPC Steel 60/30

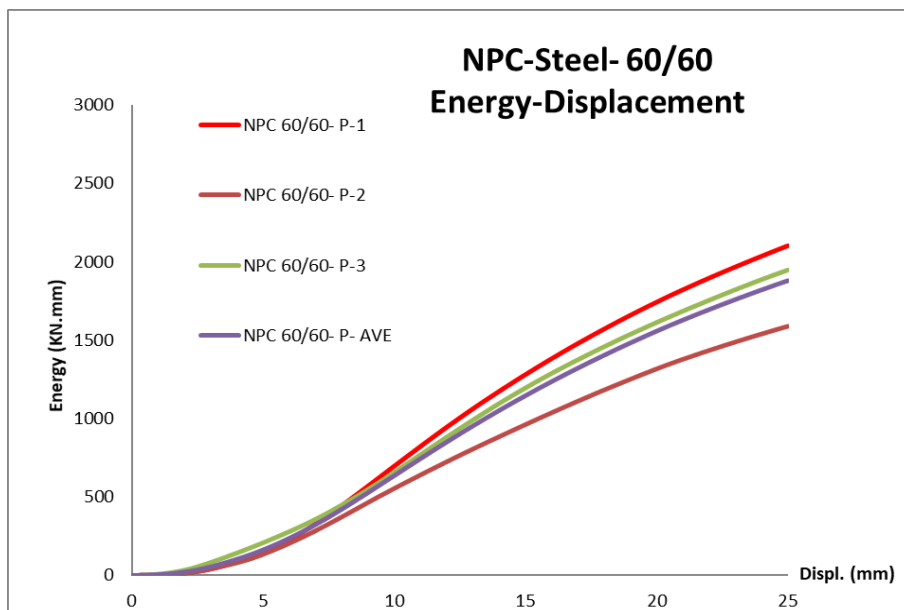


Figure B.28. Energy Displacement Graphs of NPC Steel 60/60

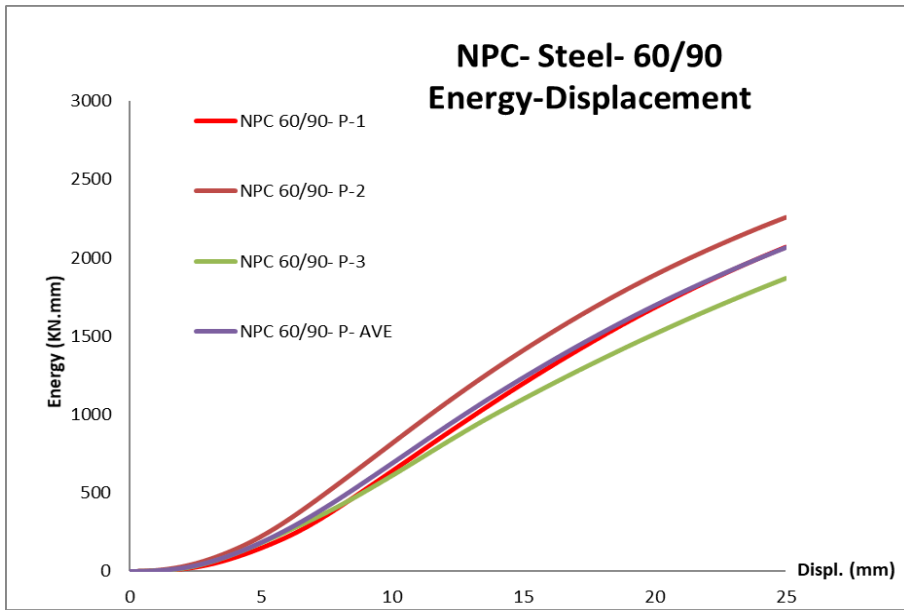


Figure B.29. Energy Displacement Graphs of NPC Steel 60/90

Table B.5. Energy Displacement Test Values of NPC Steel

		Energy at 5 mm Disp.	Energy at 10 mm Disp.	Energy at 15 mm Disp.	Energy at 20 mm Disp.	Energy at 25 mm Disp.
NPC Control	1	N/A				
	2	53.1	87.7	N/A		
	3	N/A				
	Ave.	53.1	87.7	N/A		
	St. Dev.	-	-	-	-	-
NPC 30-30	1	208.1	392.0	517.2	604.2	673.0
	2	116.0	311.9	448.6	557.0	641.9
	3	111.6	321.7	480.0	592.6	682.8
	Ave.	145.2	341.8	481.9	584.6	665.9
	St. Dev.	37.5	12.8	7.1	4.2	3.2
NPC 30-60	1	118.1	407.5	600.3	714.9	791.0
	2	217.1	483.7	652.6	763.2	842.8
	3	151.7	460.8	690.7	844.0	949.1
	Ave.	162.3	450.6	647.9	774.0	861.0
	St. Dev.	31.0	8.7	7.0	8.4	9.4
NPC 30-90	1	200.9	560.3	773.6	907.9	1004.4
	2	209.8	615.7	871.0	1014.4	1104.4
	3	194.2	672.0	1009.3	1210.7	1348.7
	Ave.	201.6	616.0	884.7	1044.4	1152.5
	St. Dev.	3.9	9.1	13.4	14.7	15.4
NPC 60-30	1	132.9	489.8	-	-	-
	2	160.9	458.0	787.6	1096.7	1327.1
	3	164.5	484.3	791.2	1046.0	1273.3
	Ave.	152.7	477.4	789.4	1071.4	1300.2
	St. Dev.	11.3	3.6	0.3	3.3	2.9
NPC 60-60	1	145.8	697.0	1281.1	1742.7	2102.2
	2	134.0	554.1	961.6	1316.8	1588.5
	3	68.3	111.2	96.1	1612.7	1949.1
	Ave.	208.0	657.3	1195.4	1612.9	1947.1
	St. Dev.	20.1	46.5	51.3	13.5	13.5
NPC 60-90	1	148.6	640.2	1199.2	1682.4	2068.3
	2	222.5	817.6	1410.7	1889.7	2257.5
	3	181.0	611.4	1099.7	1513.6	1869.1
	Ave.	184.0	689.8	1236.5	1695.2	2065.0
	St. Dev.	20.1	16.2	12.8	11.1	9.4

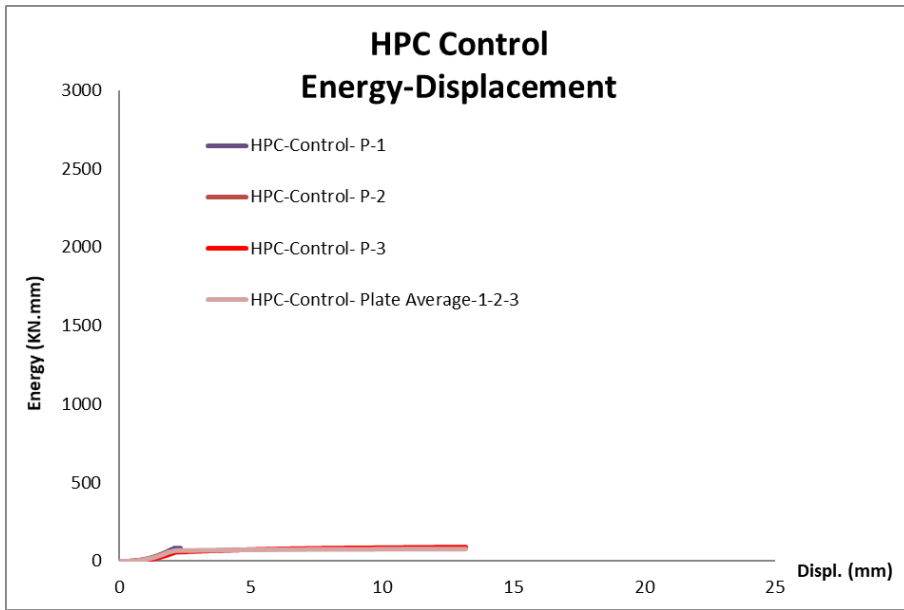


Figure B.30. Energy Displacement Graphs of HPC Control

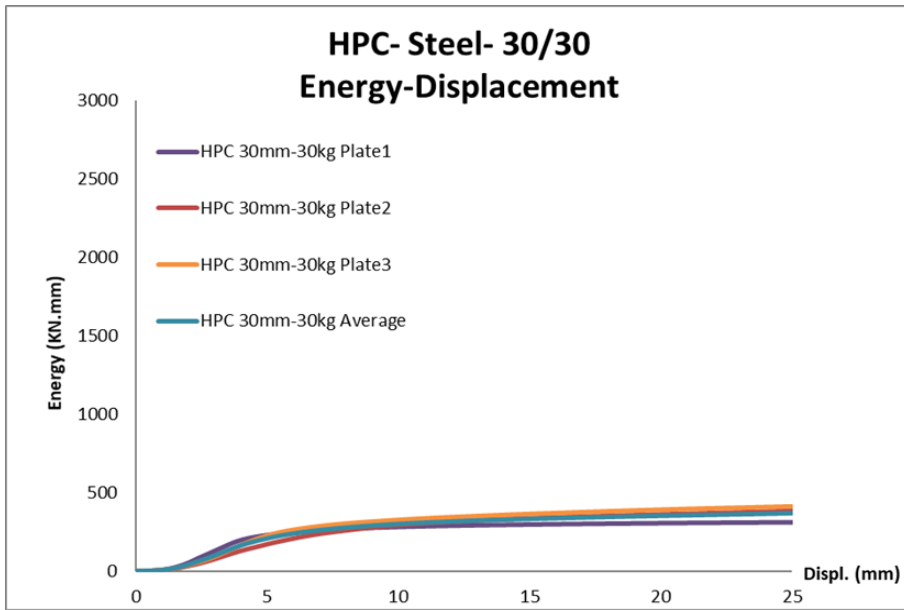


Figure B.31. Energy Displacement Graphs of HPC Steel 30/30

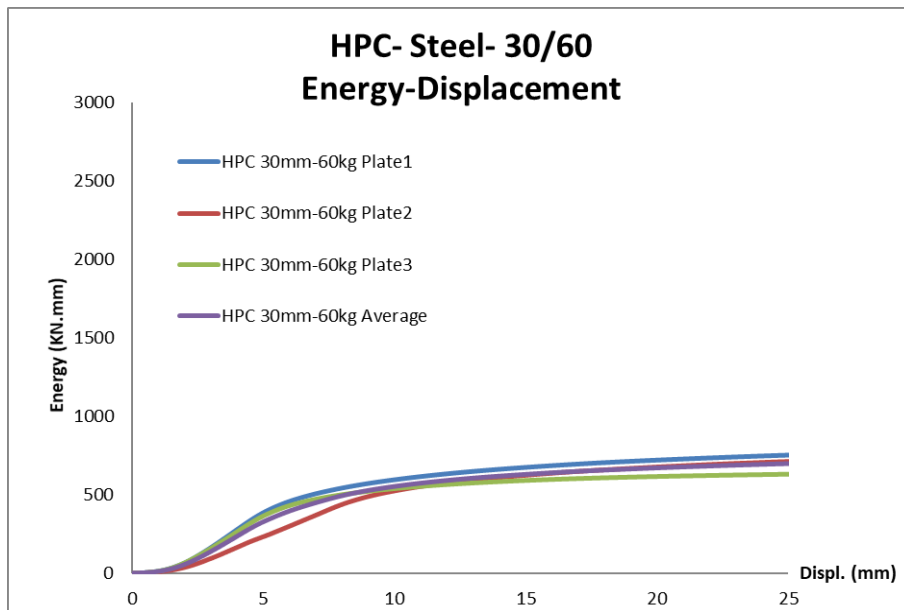


Figure B.32. Energy Displacement Graphs of HPC Steel 30/60

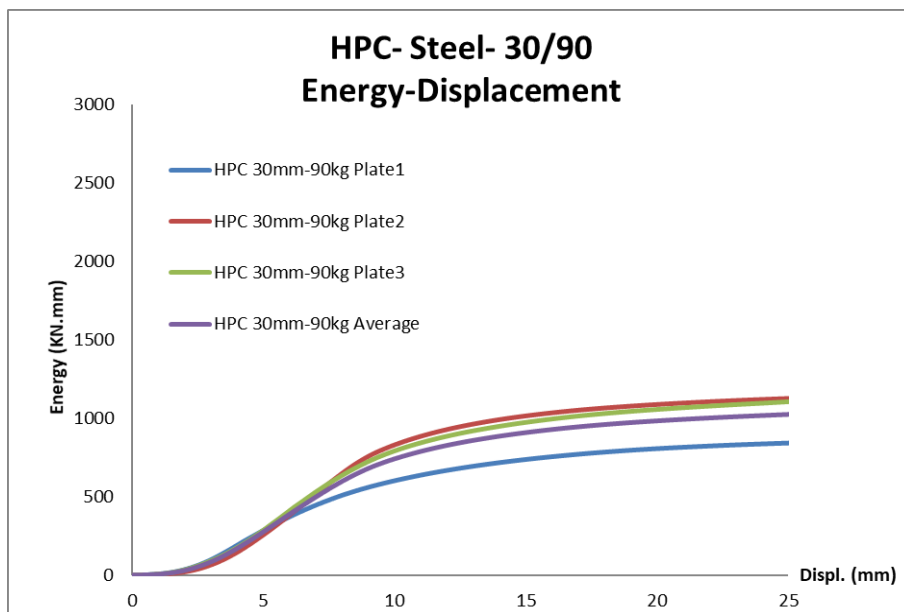


Figure B.33. Energy Displacement Graphs of HPC Steel 30/90

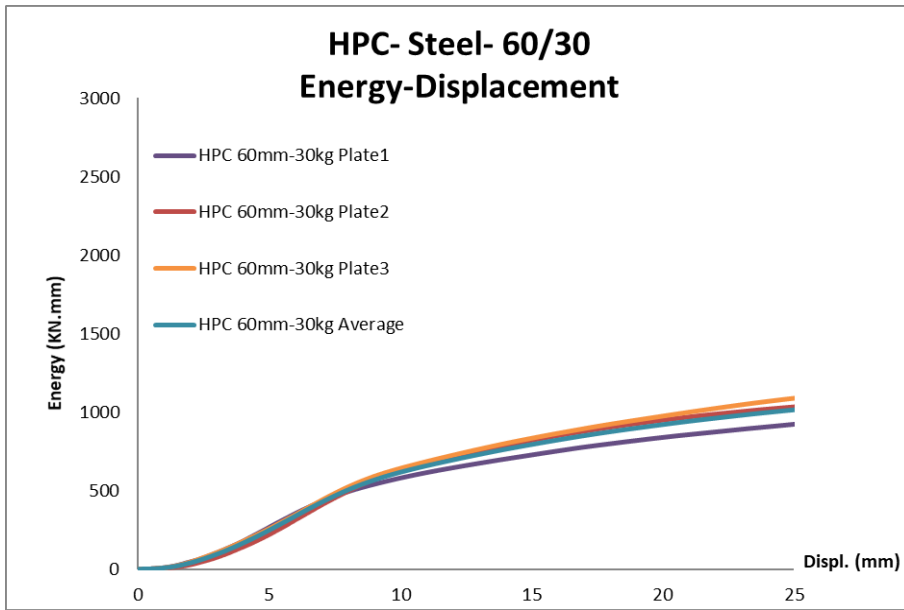


Figure B.34. Energy Displacement Graphs of HPC Steel 60/30

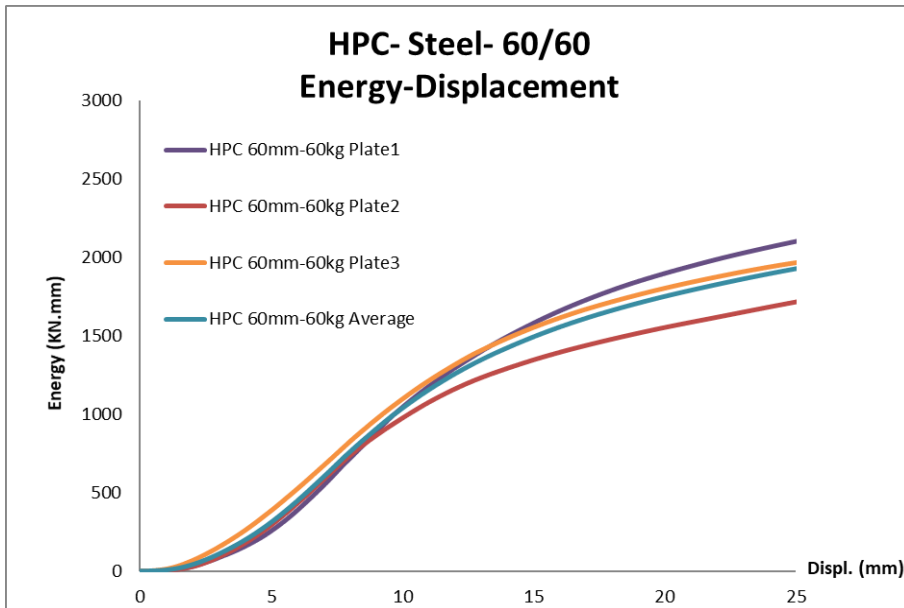


Figure B.35. Energy Displacement Graphs of HPC Steel 60/60

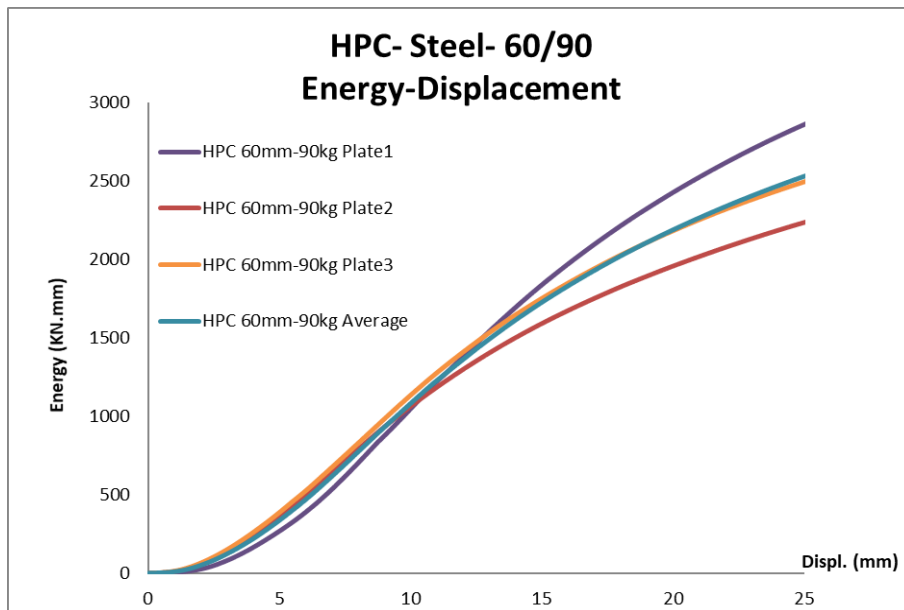


Figure B.36. Energy Displacement Graphs of HPC Steel 60/90

Table B.6. Energy Displacement Values of HPC Steel

		Energy at 5 mm Disp.	Energy at 10 mm Disp.	Energy at 15 mm Disp.	Energy at 20 mm Disp.	Energy at 25 mm Disp.
HPC Control	1	80.8	80.8	80.8	80.8	80.8
	2	59.2	59.2	59.2	59.2	59.2
	3	59.3	59.3	59.3	59.3	59.3
	Ave.	66.4	66.4	66.4	66.4	66.4
	St. Dev.	18.7	18.7	18.7	18.7	18.7
HPC 30-30	1	228.7	280.9	296.2	304.9	310.5
	2	170.8	292.2	335.7	360.5	384.1
	3	225.2	325.5	363.5	390.5	411.6
	Ave.	208.2	299.5	331.8	352.0	368.7
	St. Dev.	15.6	7.7	10.2	12.3	14.2
HPC 30-60	1	385.2	594.3	673.1	719.3	751.1
	2	231.6	523.4	622.8	675.3	710.5
	3	364.1	537.9	589.8	614.9	629.5
	Ave.	327.0	551.9	628.6	669.8	697.0
	St. Dev.	25.5	6.8	6.7	7.8	8.9
HPC 30-90	1	285.3	600.9	736.3	805.2	840.8
	2	256.7	829.1	1013.7	1086.4	1124.8
	3	286.3	790.9	972.7	1054.9	1104.2
	Ave.	276.1	740.3	907.6	982.2	1023.3
	St. Dev.	6.1	16.5	16.5	15.7	15.5
HPC 60-30	1	266.6	580.0	726.9	838.5	922.4
	2	219.9	629.2	820.4	948.6	1033.1
	3	257.8	641.6	833.3	974.5	1087.9
	Ave.	248.1	616.9	793.5	920.5	1014.5
	St. Dev.	10.0	5.3	7.3	7.8	8.3
HPC 60-60	1	255.8	1043.3	1579.8	1896.0	2100.1
	2	293.3	974.7	1345.4	1551.6	1714.2
	3	385.1	1096.0	1551.9	1801.8	1964.5
	Ave.	311.4	1038.0	1492.4	1749.8	1926.3
	St. Dev.	21.4	5.9	8.6	10.2	10.2
HPC 60-90	1	266.4	1045.2	1834.8	2424.1	2856.7
	2	353.6	1061.3	1588.7	1954.9	2233.1
	3	385.4	1132.3	1749.1	2179.8	2491.7
	Ave.	335.1	1079.6	1724.2	2186.3	2527.2
	St. Dev.	18.4	4.3	7.2	10.7	12.4

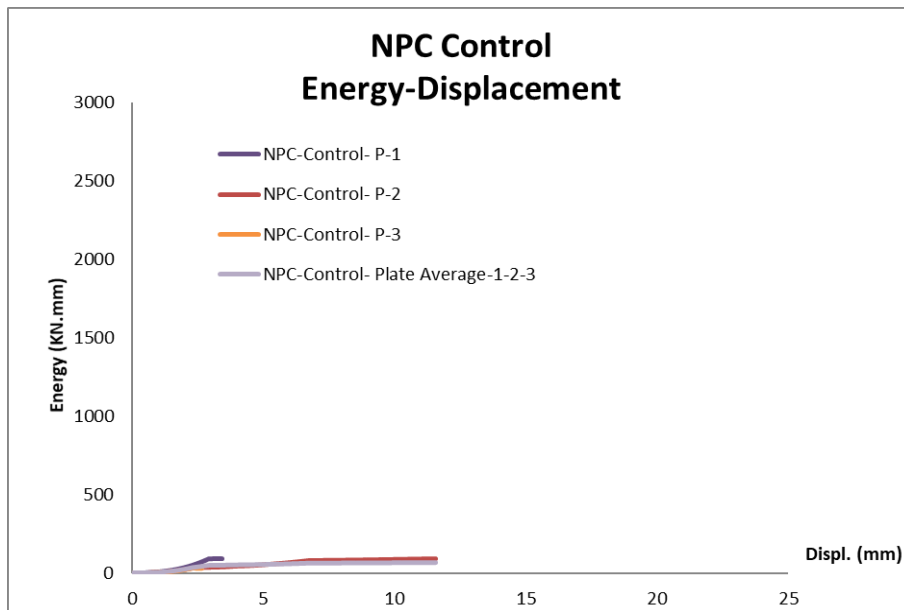


Figure B.37. Energy Displacement Graph of NPC Control

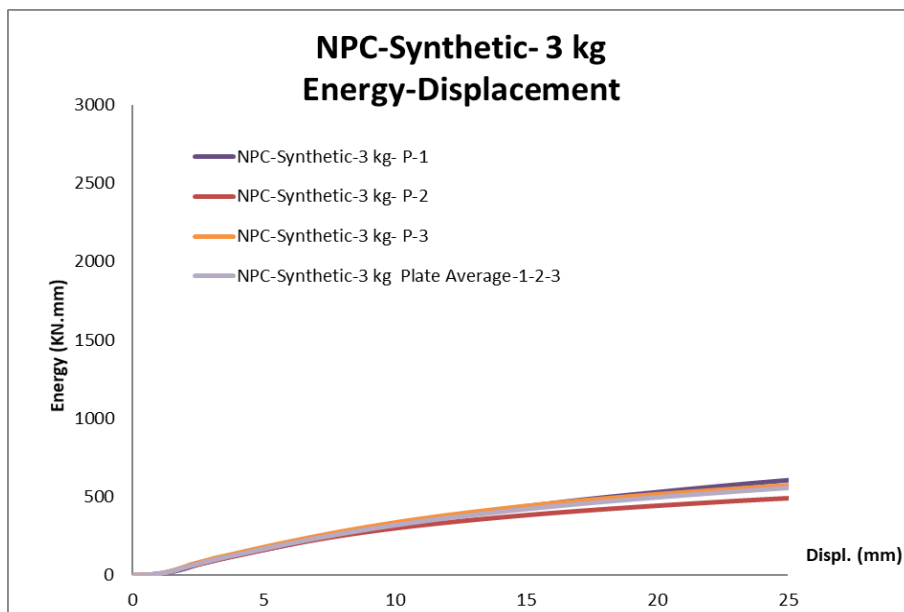


Figure B.38. Energy Displacement Graphs of NPC Synthetic 3 kg

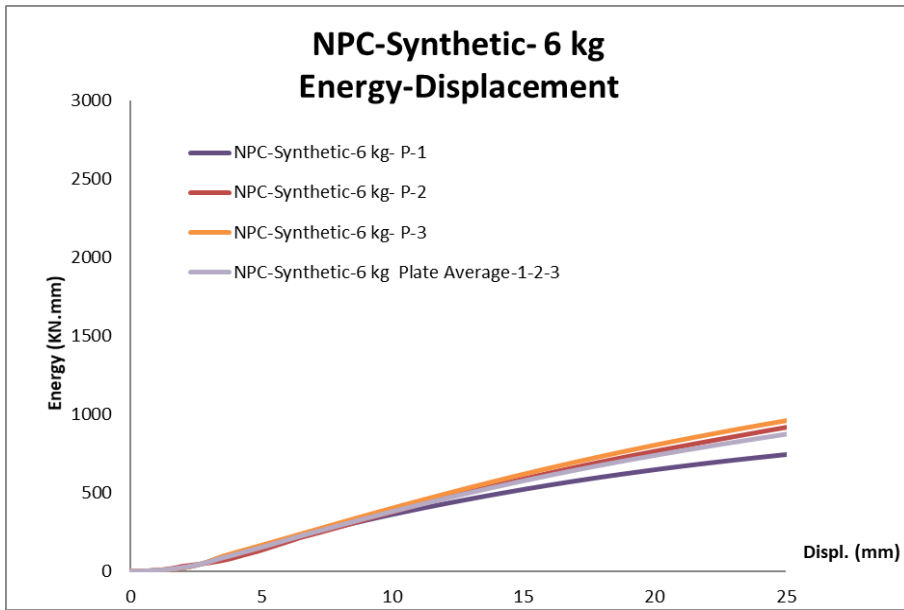


Figure B.39. Energy Displacement Graphs of NPC Synthetic 6 kg

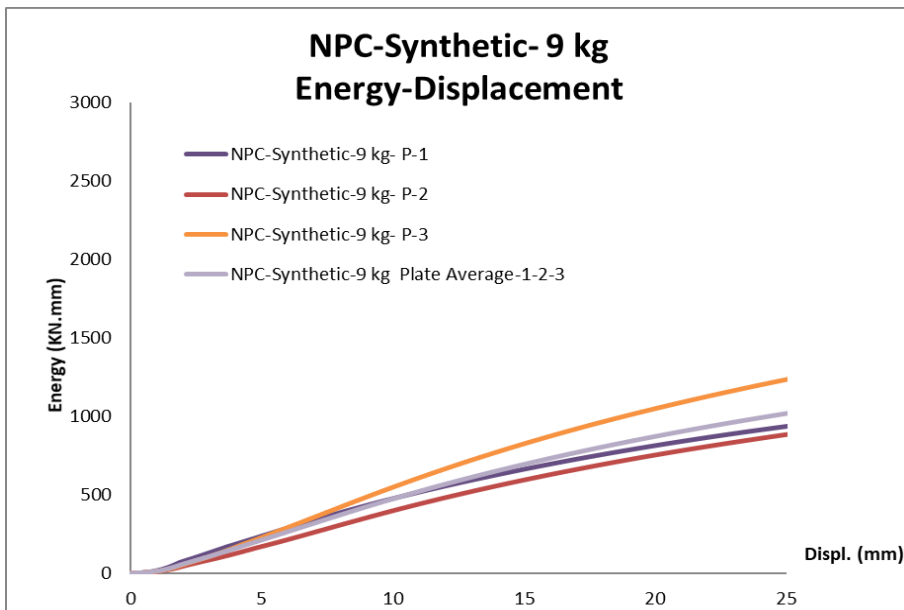


Figure B.40. Energy Displacement Graphs of NPC Synthetic 9 kg

Table B.7. Energy Displacement Values of NPC Synthetic

		Energy at 5 mm Disp.	Energy at 10 mm Disp.	Energy at 15 mm Disp.	Energy at 20 mm Disp.	Energy at 25 mm Disp.
NPC Control	1	N/A				
	2	53.1	87.7	N/A		
	3	N/A				
	Ave.	53.1	87.7	N/A		
	St. Dev.	-	-	-	-	-
NPC 3 kg	1	161.0	321.0	439.0	530.0	606.0
	2	161.0	299.0	383.0	443.0	491.0
	3	179.0	336.0	441.0	516.0	573.0
	Ave.	167.0	319.0	421.0	496.0	557.0
	St. Dev.	6.2	5.8	7.9	9.4	10.7
NPC 6 kg	1	155.0	361.0	521.0	646.0	742.0
	2	134.0	376.0	588.0	764.0	916.0
	3	165.0	402.0	618.0	802.0	958.0
	Ave.	151.0	380.0	575.0	737.0	872.0
	St. Dev.	10.6	5.4	8.6	11.1	13.1
NPC 9 kg	1	235.0	474.0	661.0	812.0	934.0
	2	169.0	397.0	593.0	752.0	882.0
	3	226.0	546.0	823.0	1047.0	1233.0
	Ave.	210.0	472.0	692.0	870.0	1016.0
	St. Dev.	17.1	15.8	17.1	17.9	18.6

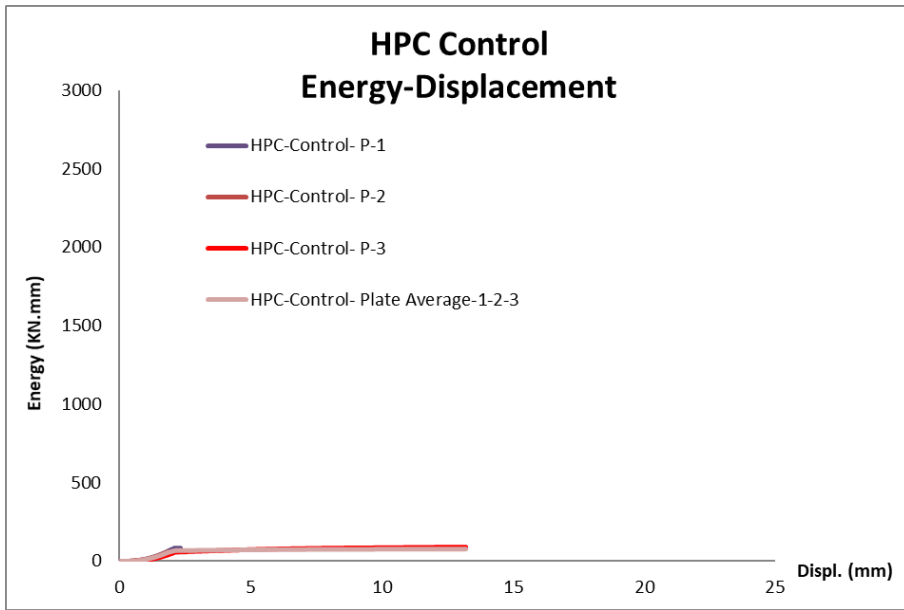


Figure B.41. Energy Displacement Graphs of HPC Control

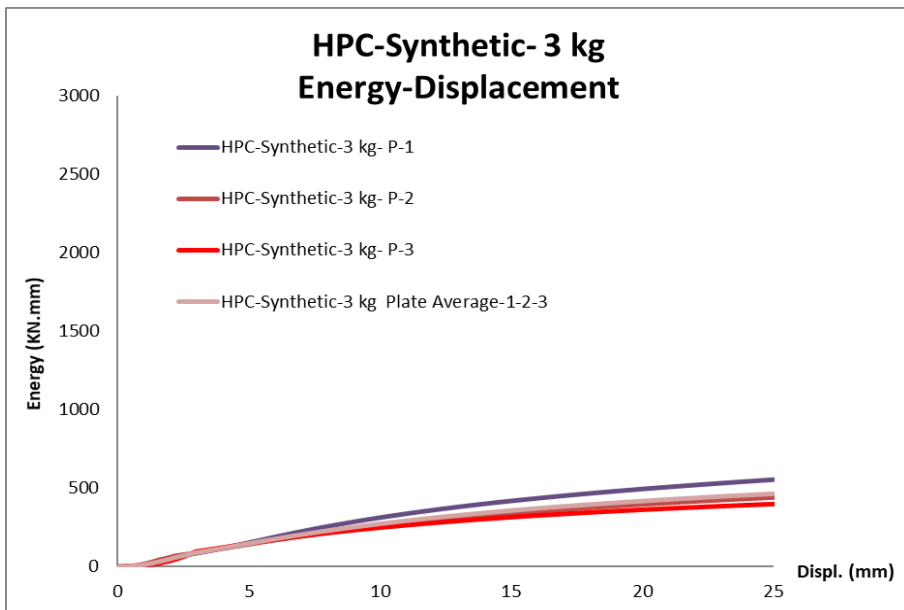


Figure B.42. Energy Displacement Graphs of HPC Synthetic 3 kg

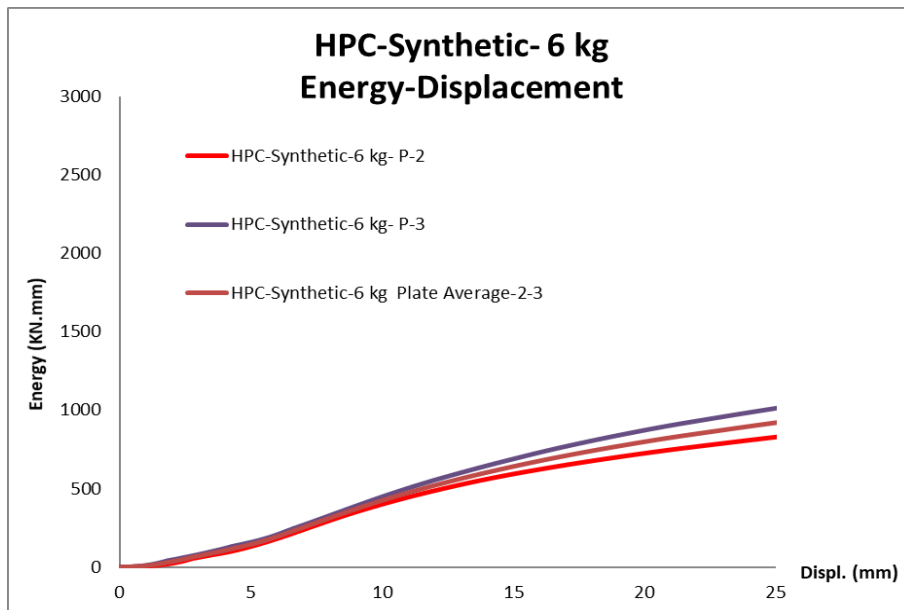


Figure B.43. Energy Displacement Graphs of HPC Synthetic 6 kg

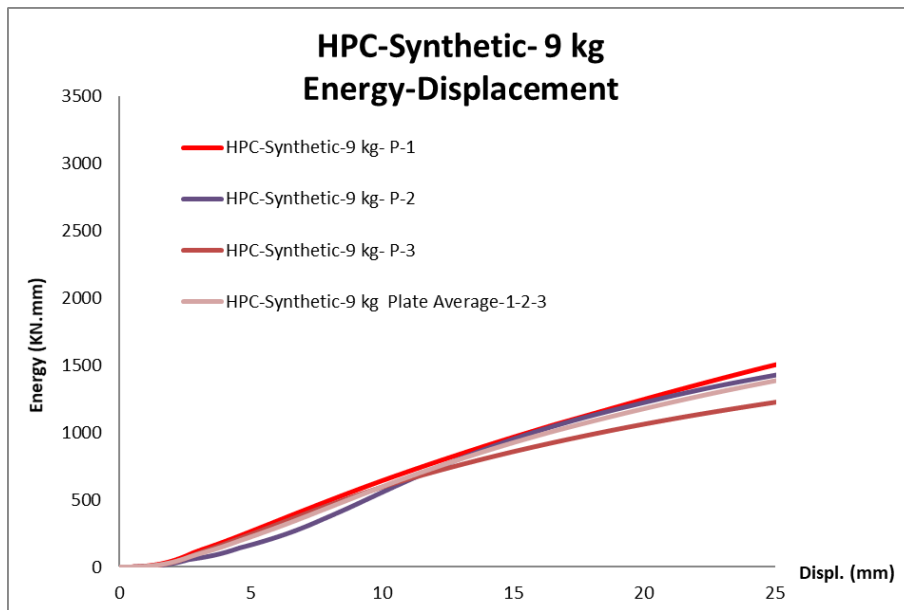


Figure B.44. Energy Displacement Graphs of HPC Synthetic 9 kg

Table B.8. Energy Displacement Test Values of HPC Synthetic

		Energy at 5 mm Disp.	Energy at 10 mm Disp.	Energy at 15 mm Disp.	Energy at 20 mm Disp.	Energy at 25 mm Disp.
HPC Control	1	80.8	80.8	80.8	80.8	80.8
	2	59.2	59.2	59.2	59.2	59.2
	3	59.3	59.3	59.3	59.3	59.3
	Ave.	66.4	66.4	66.4	66.4	66.4
	St. Dev.	18.7	18.7	18.7	18.7	18.7
HPC 3 kg	1	152.0	312.0	418.0	494.0	554.0
	2	142.0	257.0	338.0	396.0	440.0
	3	147.0	248.0	315.0	362.0	398.0
	Ave.	147.0	272.0	357.0	417.0	464.0
	St. Dev.	3.6	12.7	15.2	16.4	17.4
HPC 6 kg	1	-	-	-	-	-
	2	131.0	400.0	592.0	725.0	828.0
	3	158.0	447.0	688.0	872.0	1011.0
	Ave.	144.0	424.0	640.0	798.0	919.0
	St. Dev.	13.4	8.0	10.6	13.0	14.1
HPC 9 kg	1	264.0	641.0	965.0	1247.0	1503.0
	2	164.0	555.0	950.0	1223.0	1426.0
	3	243.0	593.0	857.0	1062.0	1225.0
	Ave.	224.0	596.0	924.0	1177.0	1385.0
	St. Dev.	23.6	7.3	6.3	8.5	10.4

C. CRACK PATTERNS

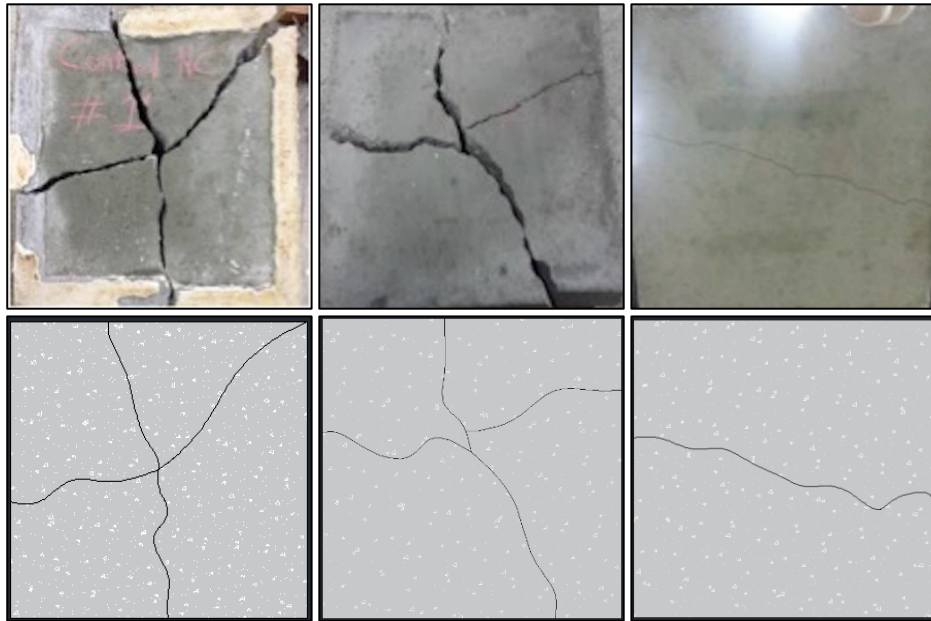


Figure C.45. Crack Patterns of NPC Control #1, #2 and #3

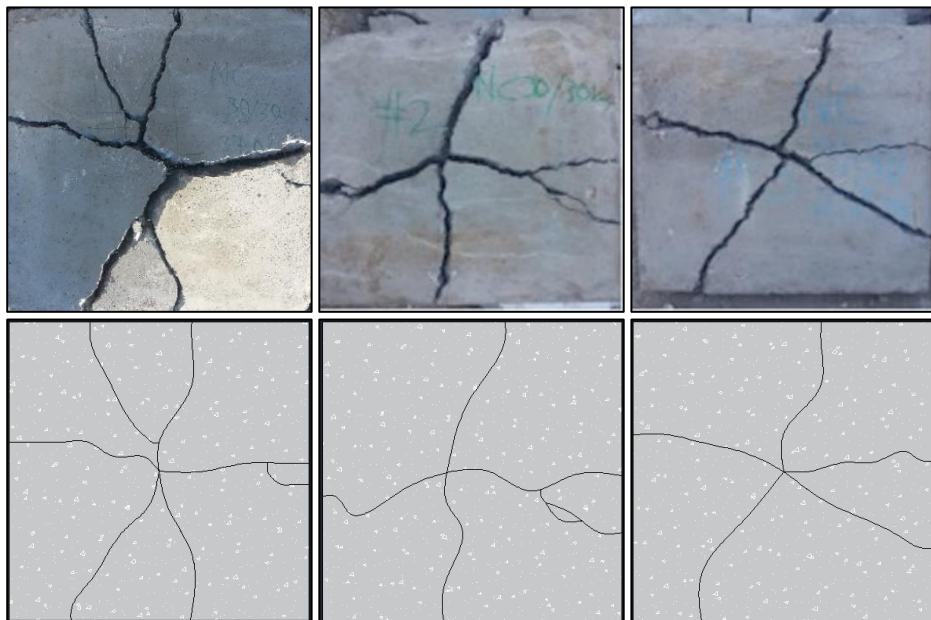


Figure C.46. Crack Patterns of NPC 30/30 #1, #2 and #3

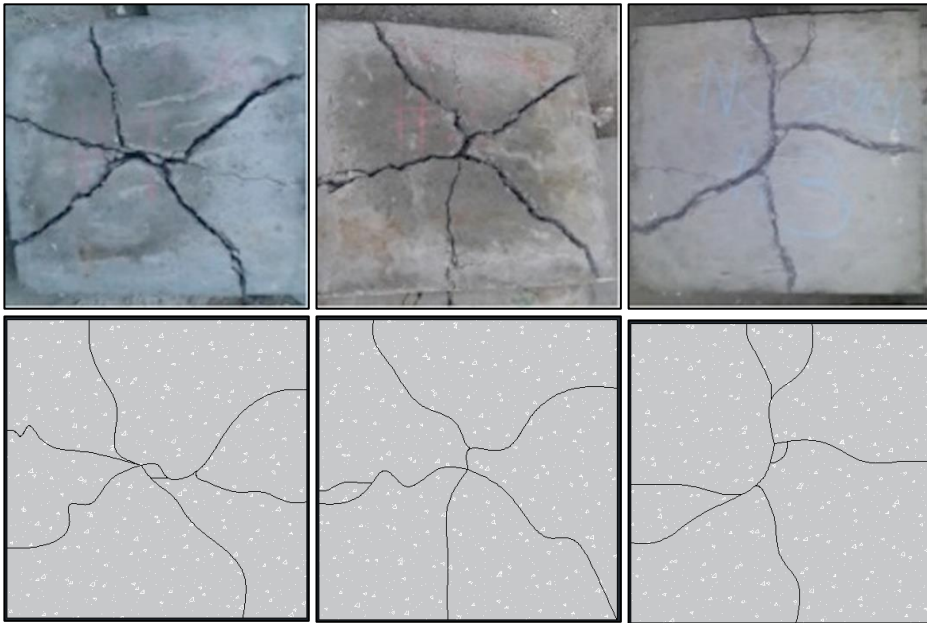


Figure C.47. Crack Patterns of NPC 30/60 #1, #2 and #3

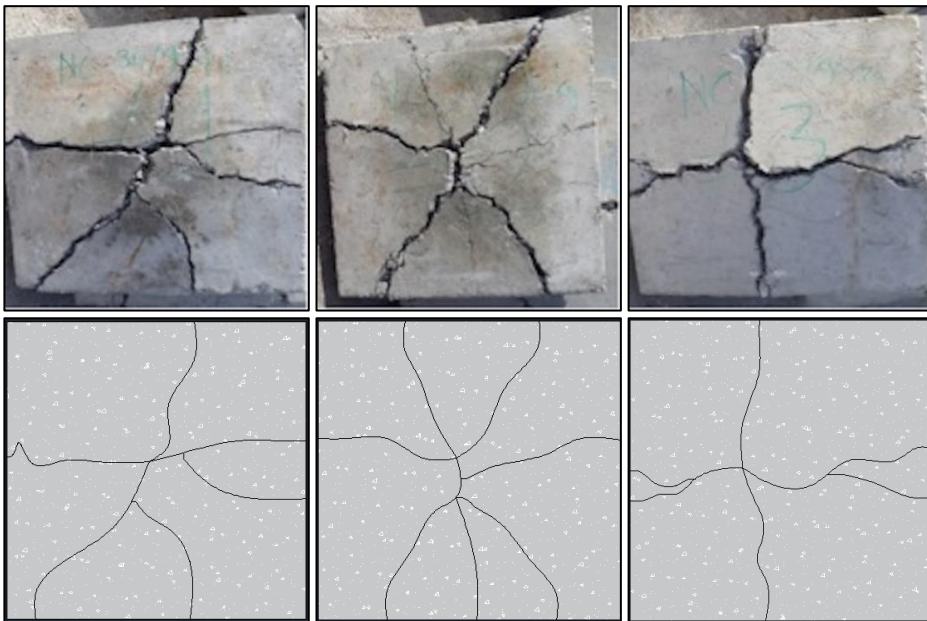


Figure C.48. Crack Patterns of NPC 30/90 #1, #2 and #3

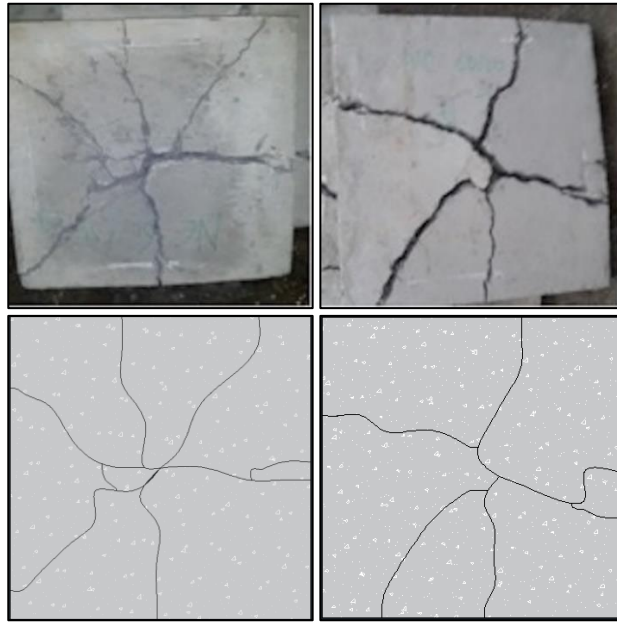


Figure C.49. Crack Patterns of NPC 60/30 #2 and #3

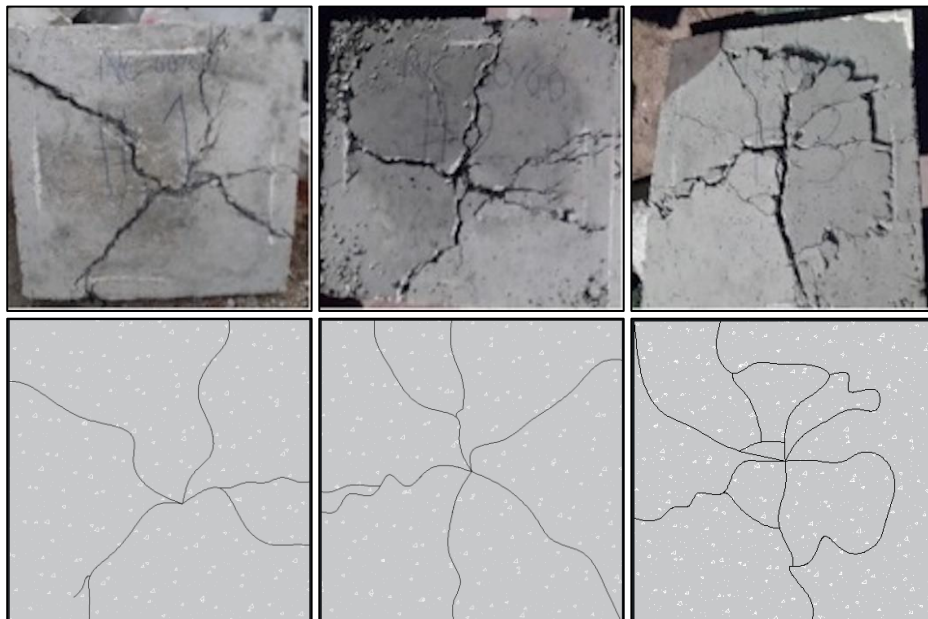


Figure C.50. Crack Patterns of NPC 60/60 #1, #2 and #3

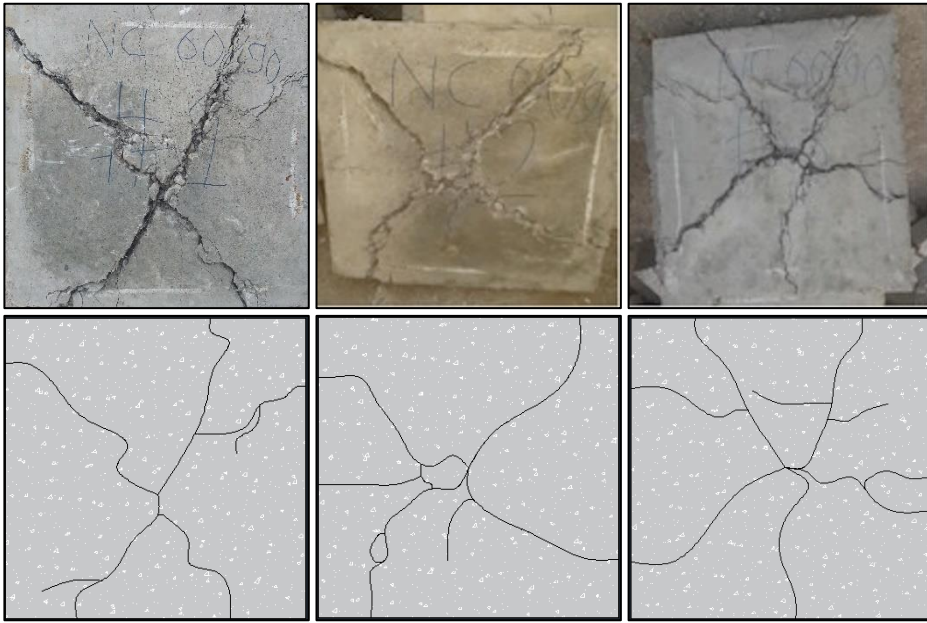


Figure C.51. Crack Patterns of NPC 60/90 #1, #2 and #3

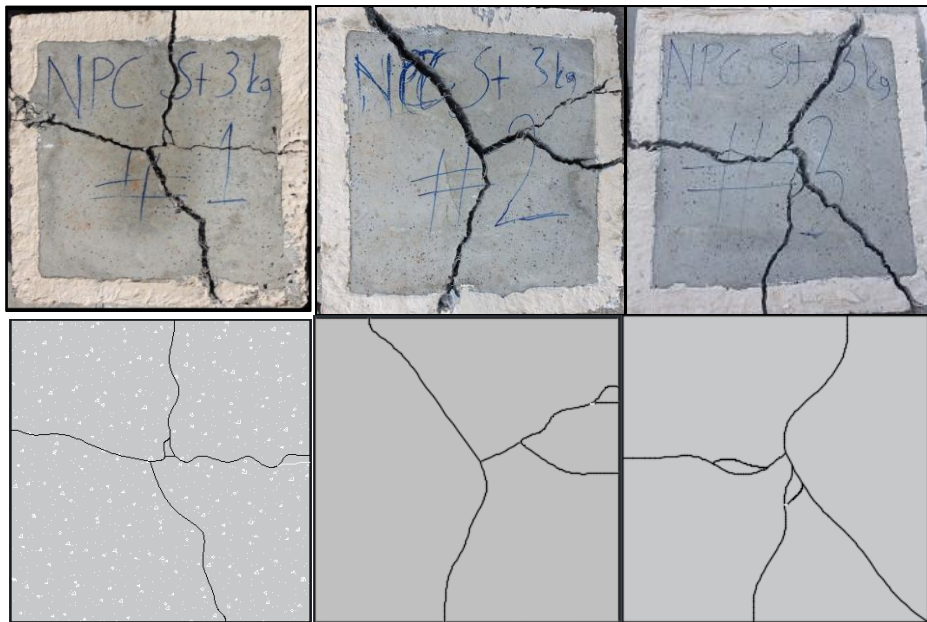


Figure C.52. Crack Patterns of NPC 3 kg #1, #2 and #3

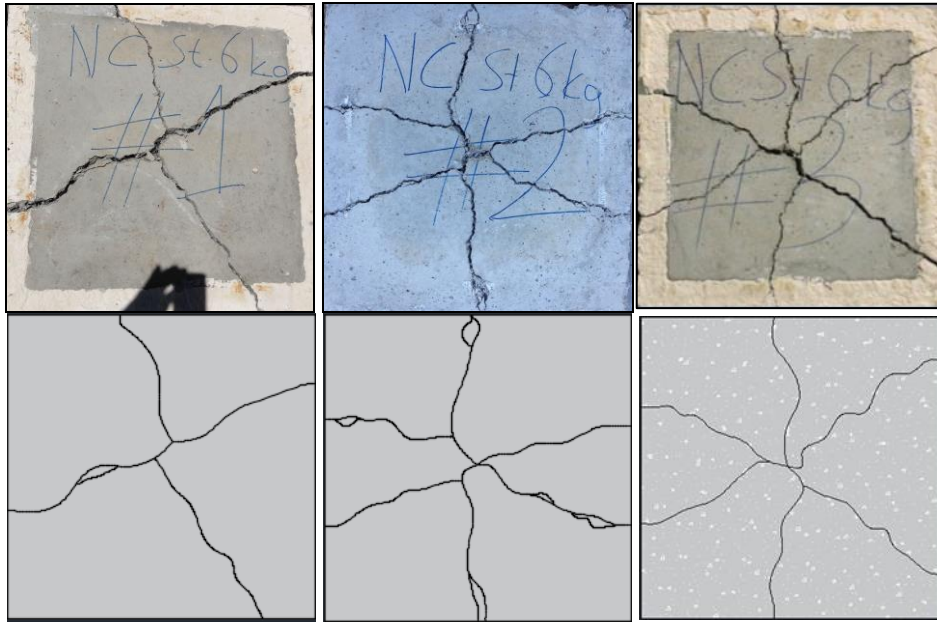


Figure C.53. Crack Patterns of NPC 6 kg #1, #2 and #3

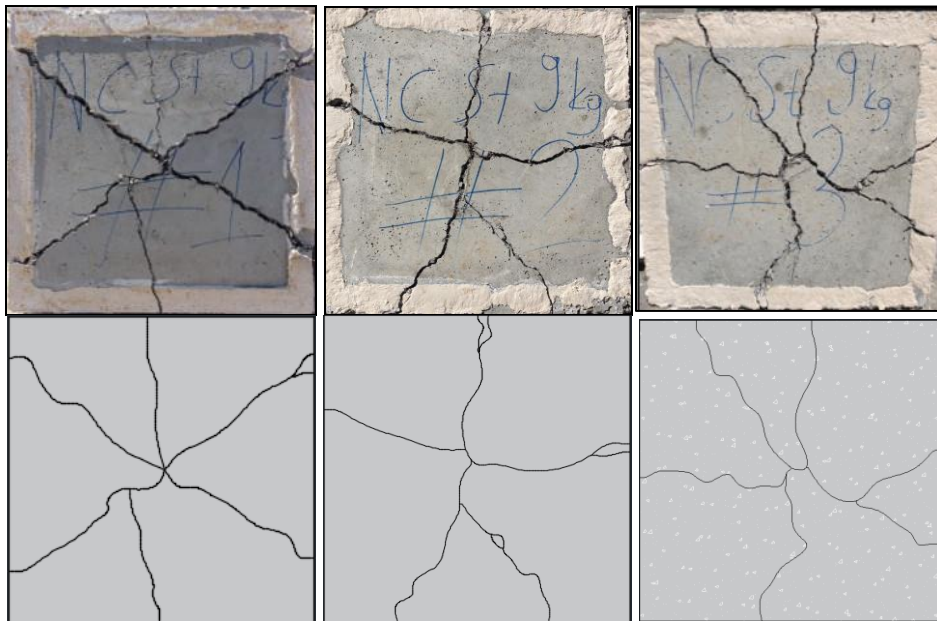


Figure C.54. Crack Patterns of NPC 9 kg #1, #2 and #3

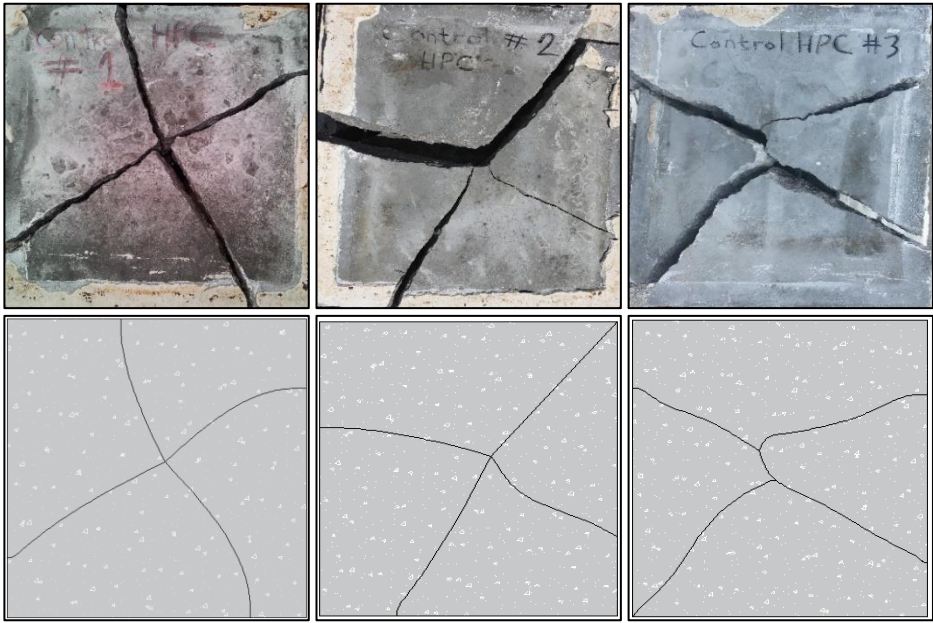


Figure C.55. Crack Patterns of HPC Control #1, #2 and #3

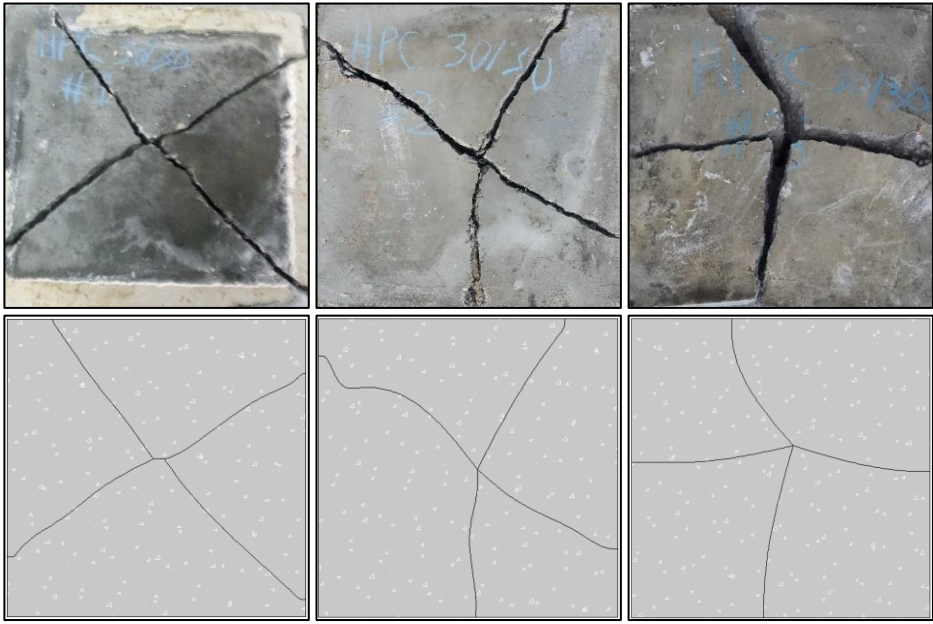


Figure C.56. Crack Patterns of HPC 30/30 #1, #2 and #3

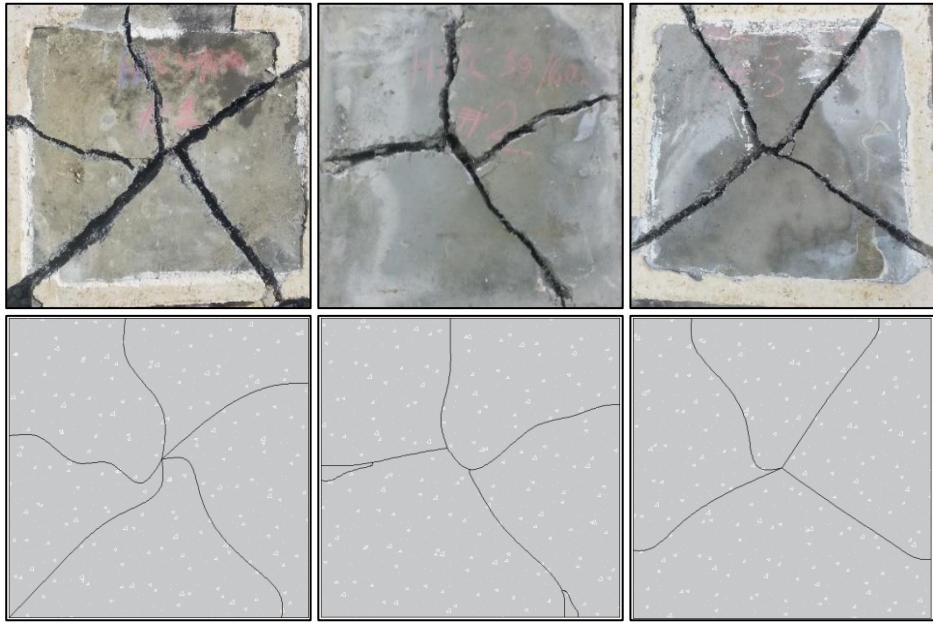


Figure C.57. Crack Patterns of HPC 30/60 #1, #2 and #3

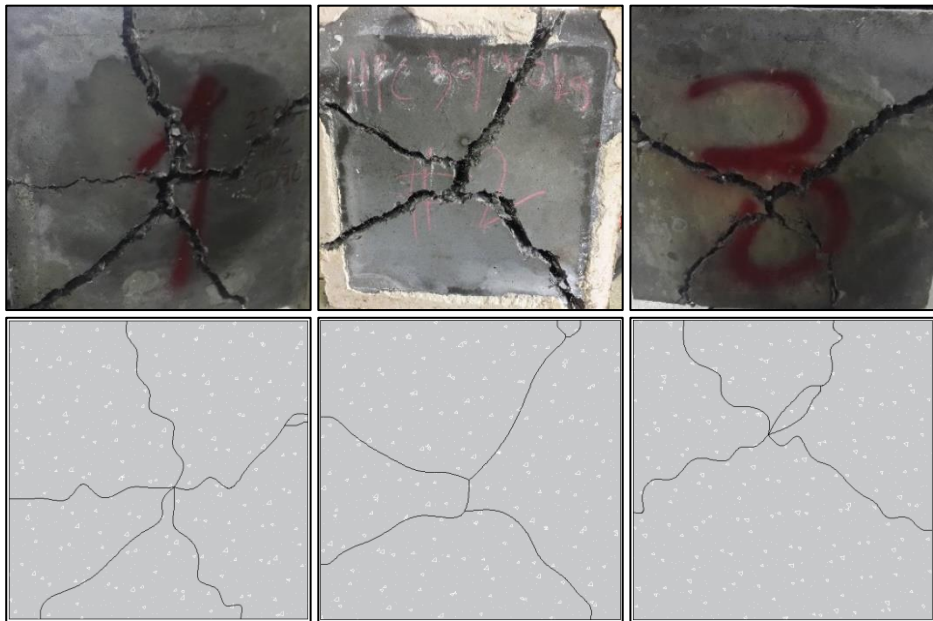


Figure C.58. Crack Patterns of HPC 30/90 #1, #2 and #3

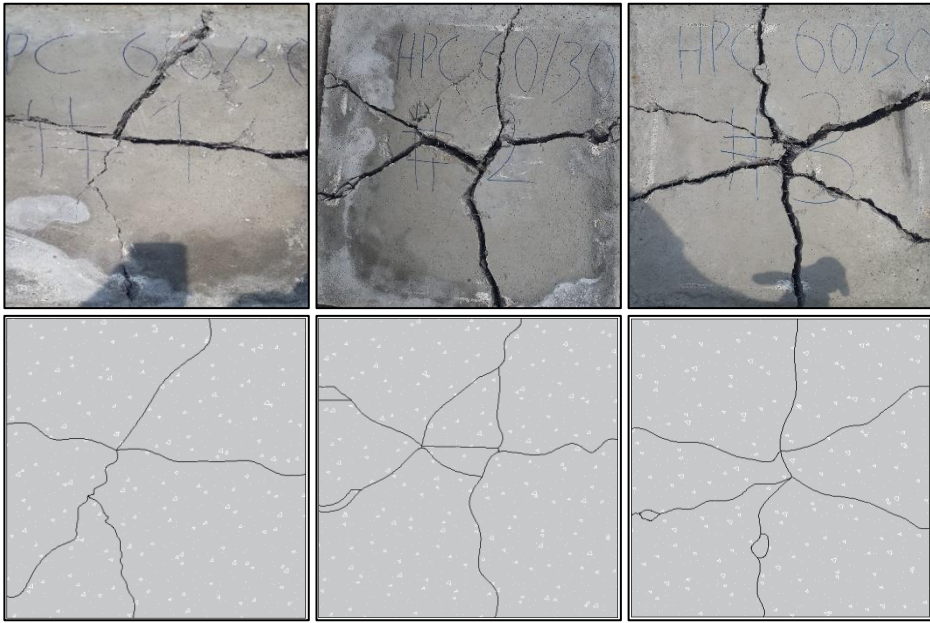


Figure C.59. Crack Patterns of HPC 60/30 #1, #2 and #3

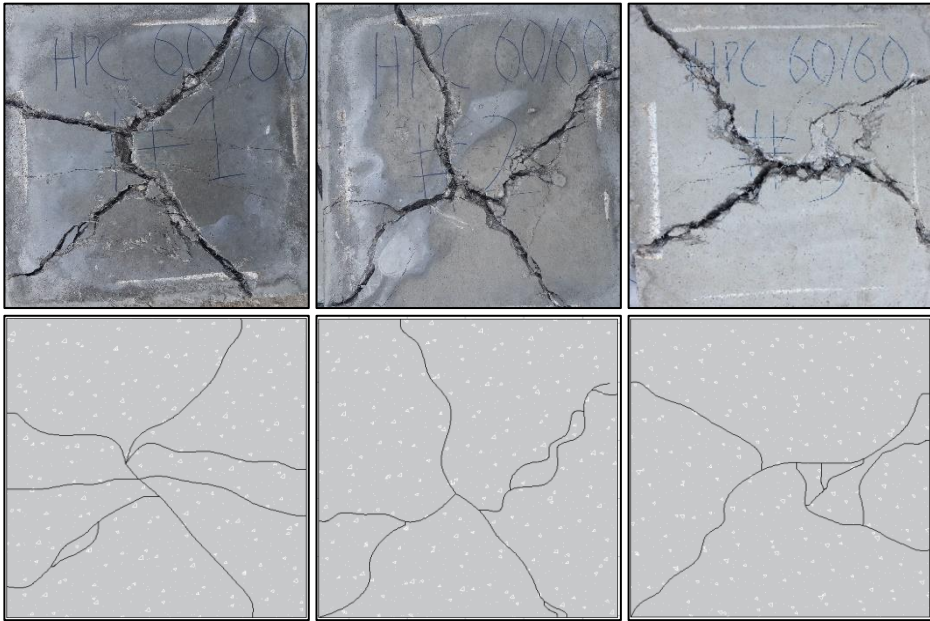


Figure C.60. Crack Patterns of HPC 60/60 #1, #2 and #3

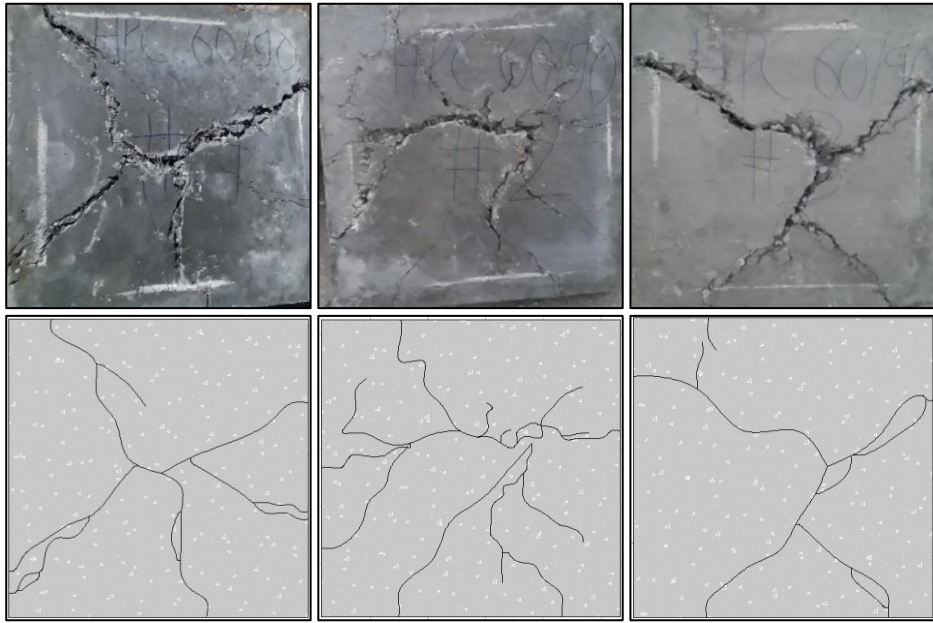


Figure C.61. Crack Patterns of HPC 60/90 #1, #2 and #3

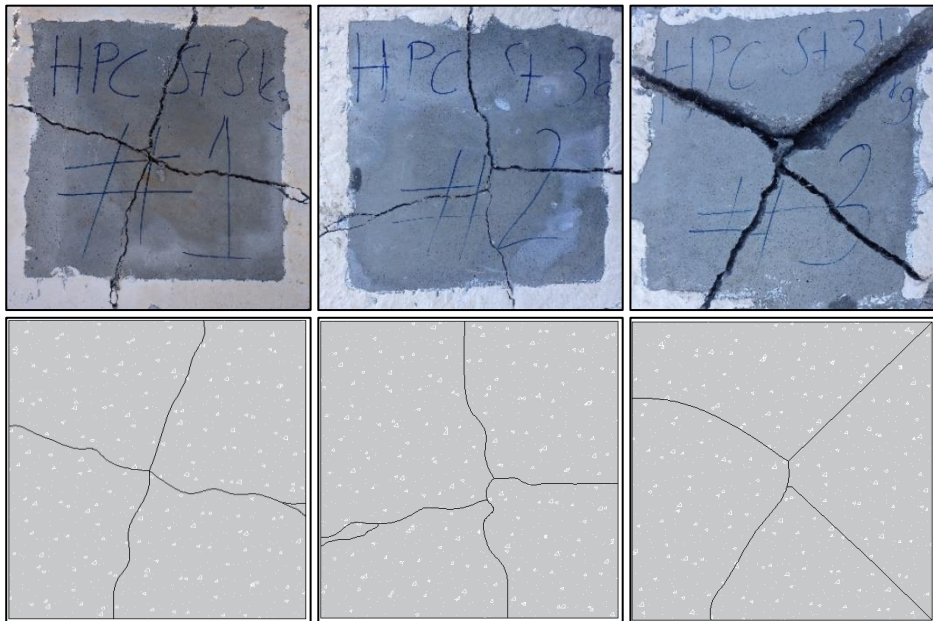


Figure C.62. Crack Patterns of HPC 3 kg #1, #2 and #3

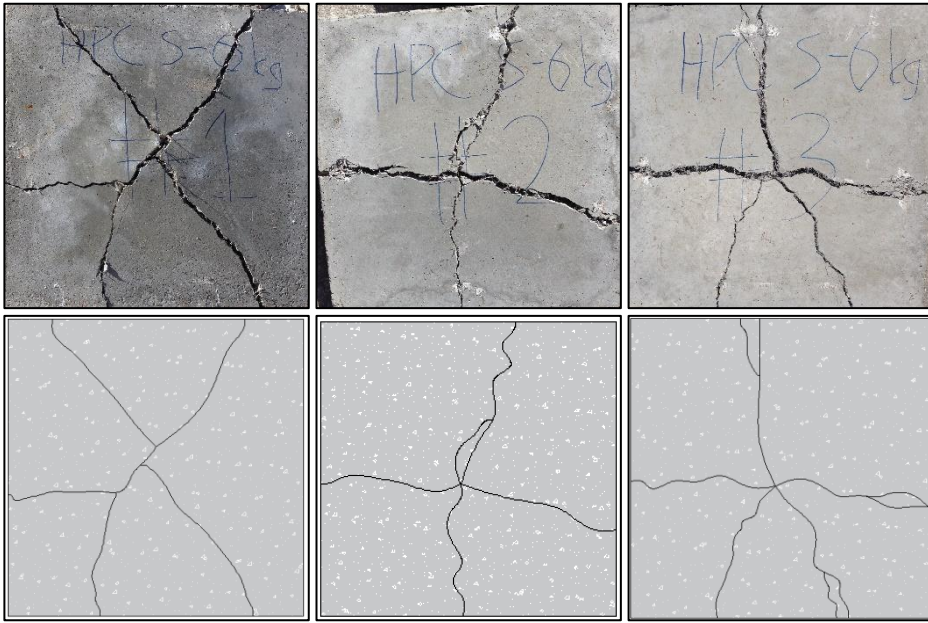


Figure C.63. Crack Patterns of HPC 6 kg #1, #2 and #3

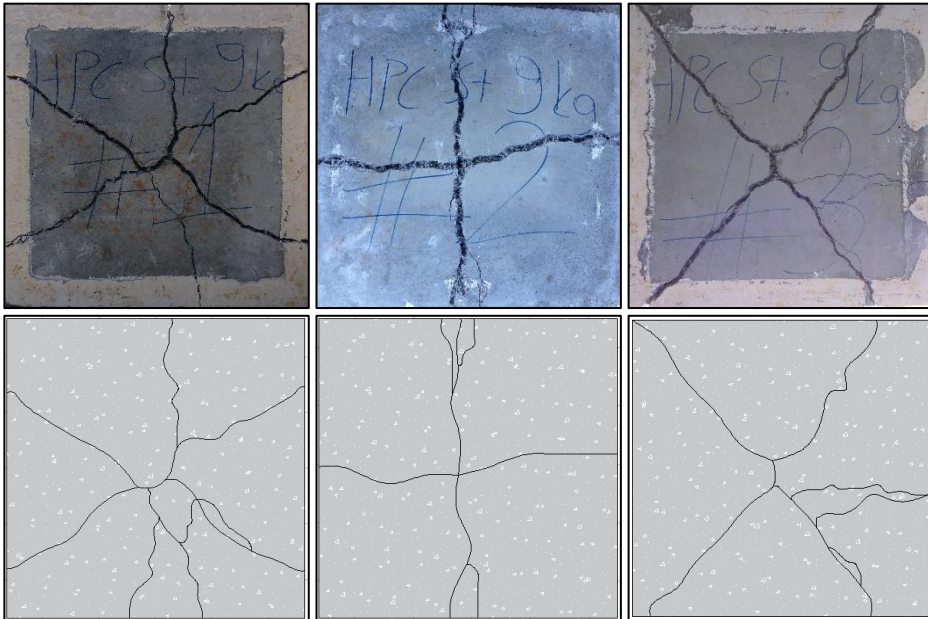


Figure C.64. Crack Patterns of HPC 9 kg #1, #2 and #3